UNIVERSITÀ DI PARMA

UNIVERSITA' DEGLI STUDI PARMA

DOTTORATO DI RICERCA IN
MEDICINA MOLECOLARE

CICLO XXXV

A REVERSED IMMUNO-GLYCOPROTEOMIC APPROACH FOR THE DISCOVERY OF NOVEL IMMUNOTHERAPEUTIC TARGETS

Coordinatore:

Chiar.mo Prof. Prisco Mirandola

Tutore:

Chiar.mo Prof. Roberto Perris

Dottorando:

Dott.ssa Naomi Borghini

Anno Accademico: 2019/2020-2022/2023

Al nonno Nelse

Table of content

ABSTRACT

A major challenge for the advancement of immunotherapeutic treatment of hematologic neoplastic conditions remains the identification of selective and fully targetable cell surface antigens. Transcriptomic and proteomic data, supported by computational analyses and propelled by experimentation at the single-cell level, are gradually becoming the mainstream approach to unveil novel immunotherapeutic targets. However, most of the discovered targets fail to pass the clinical, or even the advanced preclinical, experimental validation because of not being sufficiently cancer-specific and/or because of the lack of (or failure to produce) suitable immunological agents for their effective neutralization. Meanwhile, it is becoming increasingly clear that aberrant post-translational modifications of integral cell surface-associated/exposed proteins of neoplastic lymphocytes may delineate the outermost cancer-selective antigens for antibody-based therapeutic approaches.

Bearing this in mind, the present study has explored the potential to adopt an alternative drug discovery strategy having as a starting point unique monoclonal antibodies (mAbs) raised against highly glycosylated molecules of the cancer cell membrane, including proteoglycans, followed by structural-functional determination of the validity of the recognized antigen(s) as putative immunotherapeutic targets. The strategy that we have denominated "reversed immuno-glycoproteomics" was assayed using a follicular lymphoma cell line as model for the initial production of a panel of unique mAbs, which were generated through the conventional murine hybridoma technology. In parallel, a previously available battery of mAbs, originally produced against the human cartilage proteoglycan aggrecan, was investigated to confirm a previously proposed cross-recognition of antibodies raised against such proteoglycan with unidentified highly glycanated cell-associated molecules detected on lymphoma patient xenografts.

Immunization of mice with complex mixtures of enriched, heavily glycosylated proteins derived from the lymphoma cell line Sci-1 yielded a total of 25 hybridoma clones that were selected for their reactivity against Sci-1 cell extracts. This panel of mAbs was initially assayed against a panel of 98 lymphoma and leukemia cell lines by flow cytometry to select the ones reacting with native, surface-exposed antigens. The screen identified a subset of 14 antibodies which were differentially tested on healthy peripheral blood mononucleated cells and immortalized lymphocytes to discriminate their cancer cell-specificity. Four lead mAbs were derived from these tests and these were initially surveyed by flow cytometry, immunocytochemistry and immunoblotting against a panel of >100 cell

lines representing all major lymphoma and leukemia subtypes, such as to categorize and prioritize the pathologies of potentially highest clinical interest. Next, the same mAbs were assayed hematological cancer cells for their potential to influence primary cellular processes, with specific reference to regulated cell death and potentiation of drug sensitivity.

A parallel part of the study was focused on a screening of 17 previously generated anti-aggrecan mAbs on a subset of the hematological cancer cell lines. Flow cytometric analyses corroborated the previously proposed expression on lymphomas of highly glycosylated surface antigens cross-recognized by such anti-proteoglycan antibodies. A first effort to disclose the nature of the antigens recognized by mAbs raised against the plasma membrane-associated macro-complexes of Sci-1 cells was pursued by conventional immunoprecipitation (IP)/shot-gun, label-free mass spectrometry and screening of protein arrays spotted with >20,000 recombinant human proteins. While refinement of the sample preparation and IP procedures are still needed to yield trustable and reproducible information on the nature of the recognized antigen, surprisingly, the protein array screening identified as a primary candidate protein believed to be transiently exposed on the outer cancer cell surface. Treatment of model cell lines of diverse pathological origin with the four lead mAbs was found to induce cell aggregation, interfere with proliferation and induce regulated cell death, in an antibody versus cell phenotype-specific manner, suggesting that the recognized surface antigens are functionally linked to cell survival pathways. Accordingly, combined treatment of model cells with low doses of doxorubicin and the most effective pro-cytotoxic antibody strongly accentuated the cell death-inducing effect exerted by each of the agents alone. While a full structural-functional characterization of the antigens recognized by the unique antibodies investigated in this study awaits to be completed, several of these immunological agents seem to possess the proper attributes to be further explored preclinically as putative immunotherapeutic drugs.

1 - INTRODUCTION

1.1 Main features of *leukemia* and *lymphomas*

Depending on the type of cell involved in cancerous transformation, the clinical manifestation of hematological malignancies could be leukemia, myeloma, or lymphoma. Leukemia are comprised of a wide spectrum of pathologies differentiated by the types and maturation stadium of cells involved in malignant transformation and the speed of tumor growth. Based on the involved cell lineage, leukemia could be classified as myeloid or lymphoid, as acute or chronic depending on the maturation stage of the cells affected by the neoplastic transformation, and the speed of cancer progression. Normally, the malignant transformation initiates in the bone marrow and then extends to primary and secondary lymphoid organs through the bloodstream.

Acute myeloid leukemia (AML) are heterogenous hematological malignancies characterized by the abnormal proliferation of undifferentiated myeloid blasts and progranulocytes with a deleterious impact on patients, who often suffer poor outcomes. AML consists of different subtypes, depending on the stage of maturation of the cells involved in the neoplastic transformation, and one of the most studied of them is probably acute promyelocytic leukemia (APL), typical of children and young adults and characterized by the gene translocation PML-RARα [t(15;17)]. Risk factors for AML development are manyfold, including genetic predisposition and environmental exposures to cancerous agents, while the previous development of other hematological disorders or chemotherapy could be the first step for the development of secondary AML and treatment-related AML (1). Based on the United States Cancer Statistics (USCS) of 2022, AML cover 13% of the rare hematological malignancies and represents an elderly pathology with an incidence rate (IR) of close to 20 cases per 100,000/year in those aged 55-64 years, 4-5 per 100,000/year in those aged 20-44 and <1 per 100,000 in children (0-14 years old). The survival rate (SR) is better in APL than in AML cases after 1 versus 5 years post diagnosis because of the effectiveness of all-trans retinoic acid (ATRA) and arsenic trioxide (ATO). By contrast, the lack of promising therapeutic approaches for AML are responsible for the associated poor outcome (2).

Until 2017, the first-line therapeutic strategy for AML was the combination of cytarabine with an anthracycline (daunorubicin or idarubicin). The success rate of this intervention has been strongly related to the age of the patients (60-85% of full recovery for the children and young adult and 5-

15% for the adult over 65 years old). In recent years the introduction of lower-intensity treatments, which strategically work on several specific targets, has increased the rate of success in cases with poor outcomes. Some of these new agents are hypomethylating compounds (azacitidine and decitabine), Bcl-2 (Venetoclax) and FLT3 inhibitors (midostaurin and gilteritinib) or hedgehog pathways inhibitors (Glasdegib). Other more advanced strategies are based on immunotherapy and cell therapy (stem cell transplantation and CAR-T cells; (1,3).

Chronic myeloid leukemia (CML) is a type of leukemia involving myeloid cells in different maturation stages and which tends to develop slowly in the first phases of the disease until the final blast crisis ensues. The starter event is the formation of the fusion gene BCR-ABL that encodes for a tyrosine-kinase dislocated in the cytoplasm, able of activating different anti-apoptotic and pro-proliferative pathways (5). The IR rate is 7-8 cases per 100,000/year in individuals aged 55-64 years, 2-3 per 100,000/year in those aged 20-44 years and <1 per 100,000 in children (0-14 years old). The SR at 5 years after the diagnosis reaches 65% and depends on the availability of a gold standard therapy based on the successful use of tyrosine-kinase inhibitors (TKI) (2,5).

The leukemic transformation may alternatively involve the lymphoid lineage and the clinical manifestations are acute lymphoblastic leukemia (ALL) and chronic lymphoblastic leukemia (CLL). ALL is a type of cancer characterized by the neoplastic transformation of lymphocytes (B or T cells) present in the bone marrow or blood and by a high speed of development. This pathology is reported more frequently in children and with a male-to-female ratio of 1:2 (6). The ALL IR for the US is 4 per 100,000 yearly and the SR after 5 years from the diagnosis is 69%, with a better prognosis if the pathology is diagnosticated at an early stage (2). The chemotherapy adopted for this malignancy reckons on the use in different stages of the treatment of the following drugs: glucocorticoids, vincristine, L-asparaginase, anthracycline, prednisone, and dexamethasone. Novel emerging therapies are those involving anti-CD19, anti-CD20, anti-CD22 monoclonal antibodies and next-generation CAR-T cell strategies (6).

CLL leukemia involving either B and T cells are indolent neoplastic transformations characterized by a slow progression. They are considered pathologies of the elderly because, in most cases, the peak incidence is around 70 years old. In rare cases, neoplastic manifestation appears in patients below 45 years, while men seem to be more affected than women, with a ratio of 1.9:1 (2,7). The outcome depends on many factors and the personalized therapeutic regimens consists of the use

of Bruton kinases inhibitors (BKIs), Bcl-2, and PI3K inhibitors. Novel drugs, therapeutic antibodies and cell-based approaches involving CAR-NK cells or CAR-T cells, alongside bispecific antibodies, are in clinical experimentation (7,8).

The term lymphoma describes a type of cancer that involves the neoplastic transformation of B and T cells started prevalently in the bone marrow and lymphoid organs and it is a heterogeneous group of malignancies divided for convenience into two large subtypes: non-Hodgkin's lymphoma or NHL (90% of the lymphoma diagnoses) and Hodgkin's lymphoma or HL. NHL includes a series of pathologies (nearly 50 different disease variants) with variable incidence and outcomes, classified by the World Health Organization (WHO) on the basis of the location and cellular phenotype of the primary tumor (9). The specific chemotherapy, named CHOP, is a combination of different drugs, such as cyclophosphamide, doxorubicin, vincristine, and prednisone, which sometimes is combined with rituximab (R-CHOP). CAR-T cells and drug-conjugated antibodies represent novel strategies in clinical trials that could overcome problems related to chemoresistance and side effects (10). The IR rate is nearly 88 cases per 100,000/year in individuals aged 55-64 years, 24-25 per 100,000/year in those aged 20-44, and 1 case per 100,000 in children. The 5-year relative survival rate for this pathology is 72% (2).

HL has a simpler classification due to the lower phenotypic heterogeneity, and the peculiarity of this malignancy is the presence of CD30-expressing Reed-Sternberg cells alongside an extensive inflammatory microenvironment. Primary forms are classic-Hodgkin lymphoma (cHL) and nodular lymphocyte-predominant Hodgkin Lymphoma (NLPHL), which differ from each other because the malignant cells in NLPHL are termed lymphocyte-predominant cells (LP), lack CD30 expression and score positively for CD20 (11). The IR rate is 3-4 cases per 100000 per year in those aged 55-64, 4-5 per 100000 per year in those aged 20-44, and <1 per 100,000 in children and SR is up to 80% at 5 years after diagnosis (2). The adopted therapeutic regimen depends on the disease state at diagnosis and consistently involving a combination of drugs including bleomycin, etoposide, doxorubicin, cyclophosphamide, vincristine, procarbazine, prednisone (eBEACOPP). Rituximab in combination with CHOP seems to be successful for better outcomes in advance NLPHL (11).

1.2 Cancer treatment by immunotherapy

In the last two decades, the increasing failure of chemotherapy (the gold standard cancer therapy), accounted by both chemoresistance and immune escape, has incited the search for therapeutic

alternatives and has fueled the advent of immunotherapy. The National Cancer Institute (NCI) reports that immunotherapy is *a therapy that uses substances to stimulate or suppress the immune system to help the body fight cancer, infection, and other diseases.* This immunomodulatory effect can be carried out by cytokines, vaccines, adoptive transfer of ex vivo activated T (CAR-T) and natural killer cells (NK CAR-T), oncolytic viruses, and monoclonal antibodies (4,12). Immunotherapeutic approaches may be divided in two separate categories, passive or active (Figure 1), depending on the mode through which the procedure should reach its therapeutic effectiveness, i.e., by (re)activating the immune system's anti-cancer response or electively directing the treatment towards a specific target on tumor cells.

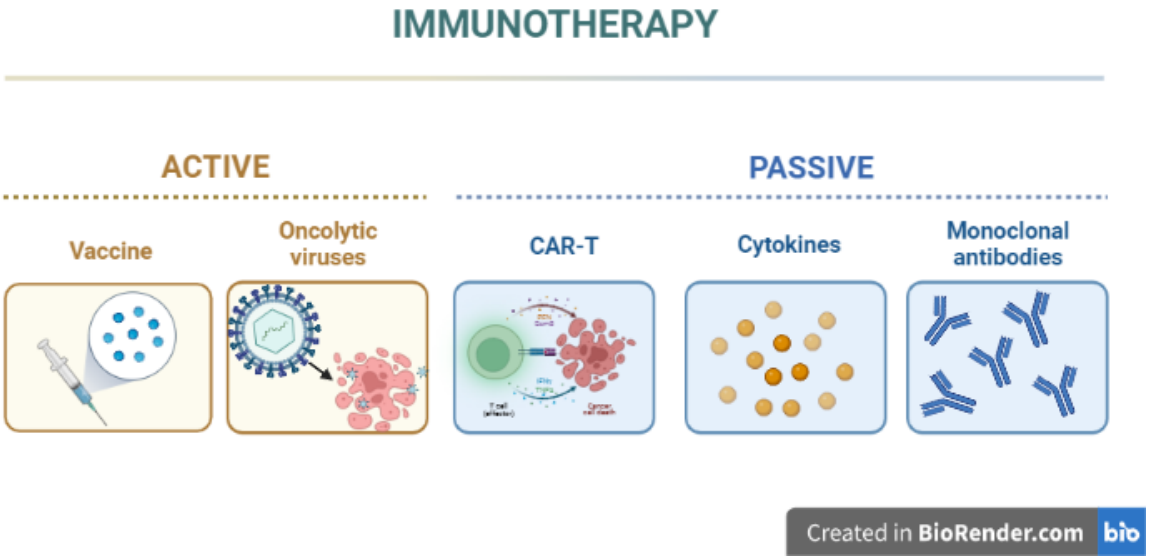

Figure 1. *Classification of immunotherapy based on the mechanism of action*

This thesis focuses on monoclonal antibodies (mAbs) that are exploitable for both active and passive immunotherapy, are rapidly becoming the most represented anti-cancer medicinal in the clinics and are by far the currently most experimented (considering all ongoing Phase I-III trials) therapeutic drugs in oncology, as well as for several other pathologies, including infectious, autoimmune, degenerative and neurological diseases.

1.3 Therapeutic antibodies for hematological malignancies

The highly potentiated clinical use of antibodies (of different origin and format) for treatment of cancer during and the associated successful outcomes of their exploitation recorded during the last two decades have pushed investments in this research area and have brought more than 500 therapeutic antibodies to be considered for clinical trials (13). The US Antibody Society has recently stilled out a comprehensive list of therapeutic antibodies approved and in regulatory review in the

European Union (EU) and the United States (14,15) between the years 1997 and 2021 for cancer and non-cancer treatment purposes (Figure 2).

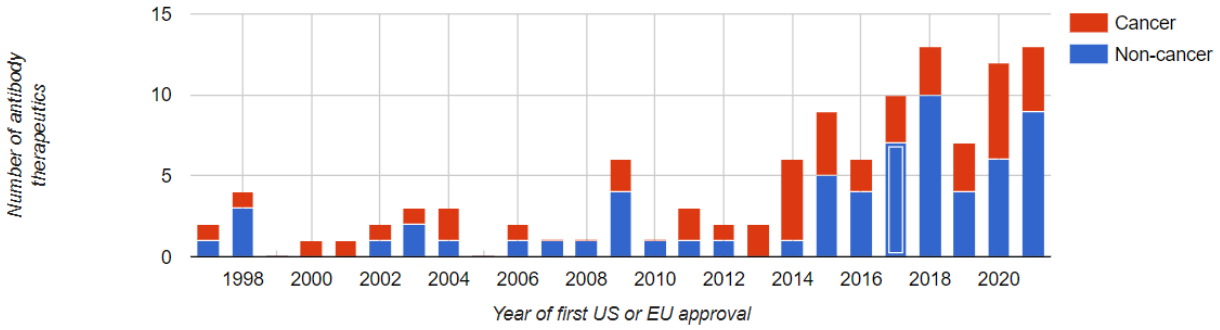

Figure 2. *US Antibody Society's representation of the number of antibodies approved by the EU and the US between 1997 and 2021*

Most of the antibodies approved for standard-of-care patient treatment or in clinical trials are indicated for solid tumors, while less than 20% are intended uniquely applied to hematological malignancies (13). The individuated targets for hematological tumors are mainly CD38, CD138, B-cell maturation antigen and SLAMF7 are contemplated for multiple myeloma, while CD3, CD19, CD20, CD22, CD30, CD33, CD52 and CD79 are applied and/or investigated for different types of leukemia and lymphoma. A concise listing of the approved and in-review antibodies for hematological malignancies (in human, humanized bispecific configurations) is reported below (Table 1).

Table 1. *Monoclonal antibodies approved or in review by the EU and/or US authorities for approval for clinical use on hematological malignancies*

International non-proprietary name	*Brand name*	*Target*	*Indicated pathology*	*First EU approval year*	*First US approval year*
Rituximab	MabThera, Rituxan	CD20	Non-Hodgkin lymphoma	**1998**	**1997**
Ibritumomab tiuxetan	Zevalin	CD20	Non-Hodgkin lymphoma	**2004**	**2002**
Tositumomab-I131	Bexxar	CD20	Non-Hodgkin lymphoma	**Not approved**	**2003 (Discontinued)**
Ofatumumab	Arzerra	CD20	Chronic lymphocytic leukemia	**2010**	**2009**
Brentuximab vedotin	Adcetris	CD30	Hodgkin lymphoma, systemic anaplastic large cell lymphoma	**2012**	**2011**

Obinutuzumab	Gazyva, Gazyvaro	CD20	Chronic lymphocytic leukemia	**2014**	**2013**
Blinatumomab	Blincyto	CD19, CD3	Acute lymphoblastic leukemia	**2015**	**2014**
Alemtuzumab	Lemtrada; MabCampath	CD52	Chronic myeloid leukemia	**2001 (Discontinued)**	**2001 (Discontinued)**
Daratumumab	Darzalex	CD38	Multiple myeloma	**2016**	**2015**
Elotuzumab	Empliciti	SLAMF7	Multiple myeloma	**2016**	**2015**
Inotuzumab ozogamicin	BESPONSA	CD22	Acute lymphoblastic leukemia	**2017**	**2017**
Gemtuzumab ozogamicin	Mylotarg	CD33	Acute myeloid leukemia	**2018**	**2017**
Moxetumomab pasudotox	Lumoxiti	CD22	Hairy cell leukemia	**2021**	**2018**
Polatuzumab vedotin	Polivy	CD79b	Diffuse large B-cell lymphoma	**2020**	**2019**
Isatuximab	Sarclisa	CD38	Multiple myeloma	**2020**	**2020**
Belantamab mafodotin	BLENREP	B-cell maturation antigen	Multiple myeloma	**2020**	**2020**
Tafasitamab	Monjuvi	CD19	Diffuse large B-cell lymphoma	**2021**	**2020**
Loncastuximab tesirine	Zynlonta	CD19	Diffuse large B-cell lymphoma	**In review**	**2021**
Mosunetuzumab	Lunsumio	CD20, CD3	Follicular lymphoma	**2022**	**In review**
Teclistamab	TECVAYLI®	B-cell maturation antigen, CD3;	Multiple myeloma	**2022**	**In review**
Glofitamab	(Pending)	CD20, CD3e	Diffuse large B-cell lymphoma	**In review**	**Not approved**

A recent article by Kaplon and colleagues summarizes the global state of the art of the ongoing research in the field of antibody-based immunotherapy and, interestingly, it emerges that the majority of the data on new products is related to cancer therapy (45%), while only minor percentages are concerning treatments of immune-mediated disorders, infectious diseases, cardiovascular/hemostasis disorders and other pathologies (16). Again, the prevalent number of clinical trials are exploring

agents intended for the treatment of solid tumors and only a few for therapy of hematological cancers. Below is reported a grouping of the most recent information on late-phase clinical trials (Table 2).

Table 2. *Monoclonal antibodies in ongoing clinical trials for treatment of hematological malignancies*

International non-proprietary name	***Drug code***	***Target***	***Indicated pathology***	***Phase of clinical development***
Zilovertamab vedotin	MK-2140	ROR1	Diffuse large B cell Lymphoma	Phase 2/3
Zilovertamab	UC-961	ROR1	Diffuse large B cell lymphoma, mantle cell lymphoma	Phase 3
Talquetamab	JNJ-64407564	G protein-coupled receptor 5D, CD3	Multiple myeloma	Phase 2
Sabatolimab	MBG453	TIM-3	Myelodisplastic syndromes, chronic myeloid leukemia	Phase 3
Odronextamab	REGN1979	CD20, CD3	Non-Hodgkin lymphoma	Phase 2
Magrolimab	ONO-7913, Hu5F9-G4	CD47	Myelodisplastic syndromes, acute myeloid leukemia	Phase 3
Linvoseltamab	REGN5458	BCMA, CD3	Multiple myeloma	Phase 2
Felzartamab	TJ202, MOR202, MOR03087	CD38	Multiple myeloma	Phase 3
Epcoritamab	GEN3013, DuoBody-CD-3x-CD20	CD20, CD3	Diffuse large B cell lymphoma	Phase 3
Elranatamab	PF-06863135	BCMA, CD3	Multiple myeloma	Phase 3
Cetrelimab	JNJ-63723283	PD-1	Multiple myeloma	Phase 2/3
Camidanlumab tesirine	ADCT-301	CD25	Hodgkin Lymphoma	Phase 2
Apamistamab-Iodine (131I)	I-131-BC8, Iomab-B	CD45	Acute myeloid leukemia	Phase 3
(Pending)	AFM13	CD30, CD16A	Peripheral T-cell lymphoma or transformed mycosis fungoides	Phase 2

(Pending)	MIL62	CD20	Follicular lymphoma and marginal zone lymphoma	Phase 3
(Pending)	GLS-010	PD-1	Hodgkin lymphoma	Phase 3

1.4 Characteristics of monoclonal antibodies

Monoclonal antibodies are composed of immunoglobulins, which are dimeric or pentameric glycoproteins comprised of two heavy chains of a mass of 50 kDa each and two light chains measuring 25 kDa each, such as to reach a total of 150 kDa (plus the weight of glycosylation moieties) for the predominant bivalent form. In man and most mammalian species the constant region is a product of five different genes defining five different immunoglobulin classes or isotypes, IgA, IgD, IgE, IgG and IgM. The structural traits of immunoglobulins are extremely well-defined and the primary features are the crystallizable constant region (Fc), which may bind to the dedicated cell surface receptors and is implicated in mediating biological processes involving antibodies bound to their cognate antigen, such as interactions with immune system cells and complement, and the antigen-binding domain (Fab) responsible antigen recognition. The antigen binding site, so called paratope, is structured as a V-site, which is formed by the complementarity determining regions (CDR) of each variable domain that come together after the protein folding (Figure 3).

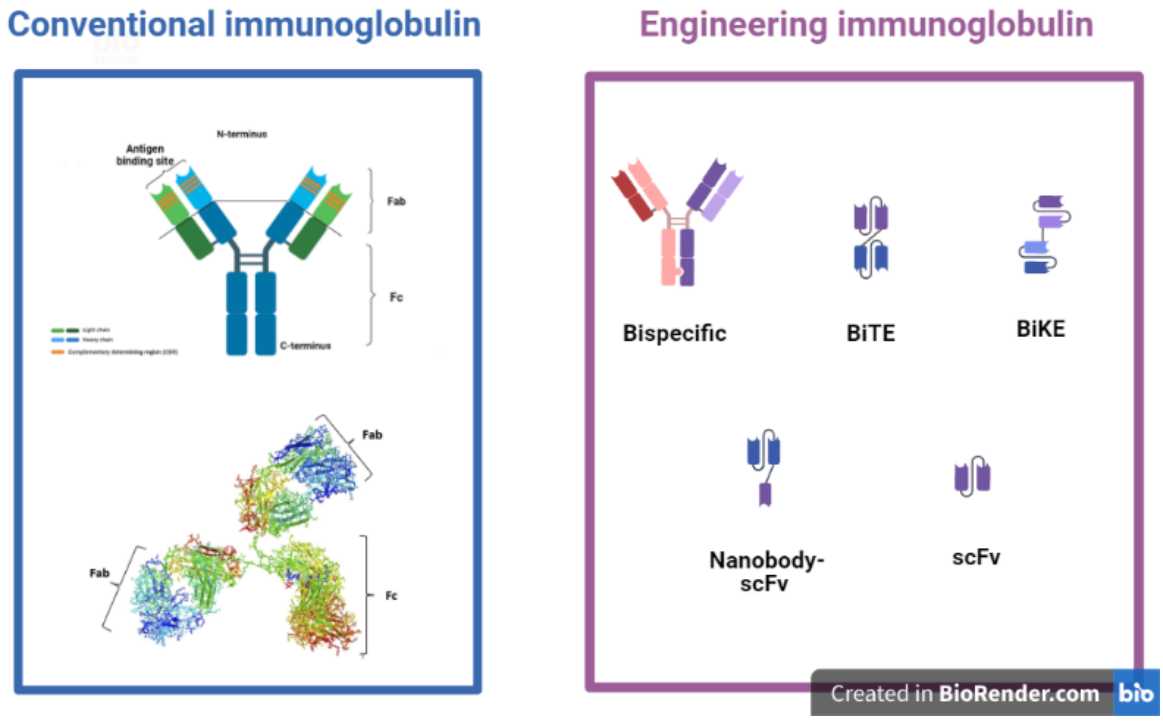

Figure 3. *Schematic representation of conventional and engineering immunoglobulin*

The milestone event for the large-scale production of novel monoclonal antibodies was the development of the hybridoma technique introduced by Milstein and Köhler (1975), which is based on immunization of a model animal (typical mouse or rat, but more lately also rabbits and larger mammals as lama and camels) with an immunogen and the following fusion of the immunized spleen plasma cells with human myeloma cells to obtain immortal antibody producing clones (Figure 4).

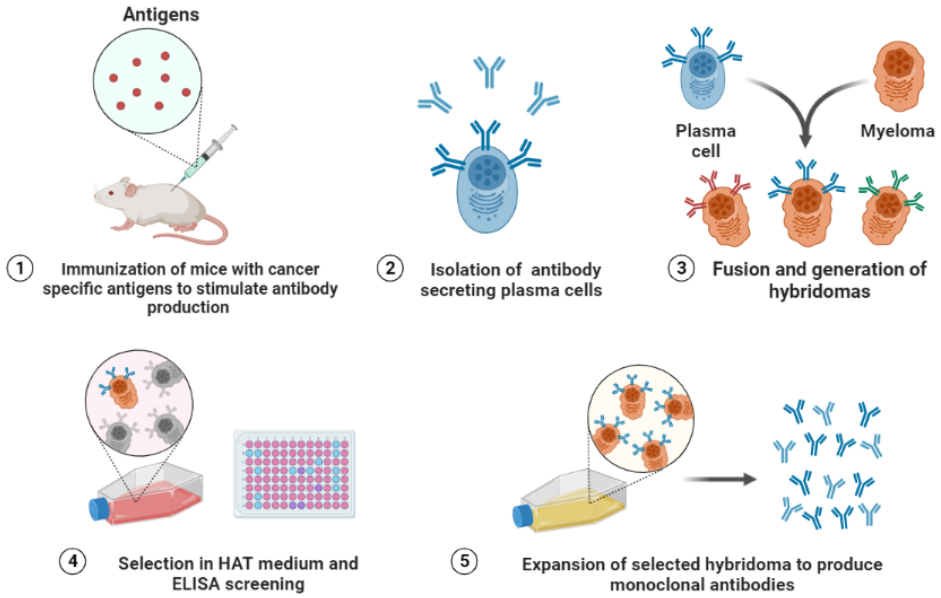

Figure 4. *Schematic outline of the main steps involved in the production of monoclonal antibodies according to the conventional Kohler and Milstein hybridoma technology*

With the expansion of recombinant DNA procedures, it has been possible to device systems to obtain monoclonal antibodies through alternative methods and the pioneering technology in this field is phage-display, developed by McCafferty and Winter at the beginning of 1990s, which allows the isolation of high-affinity antigen-binding sequences lacking eukaryotic post-translational modifications and derived from any type of species including man (17-20). Another display technology is yeast surface display (YSD), which is based on the expression of antibody fragments on yeast cell membranes and the subsequent selection of targets through rounds of mutagenesis and fluorescent-activated cell sorting (FACS) (17, 21-24). An important aspect of the YSD technology is the presence of eukaryotic post-translation modifications in the secreted proteins (25). An emerging technique, not established yet, is virus/mammalian cell display in which the antibodies are displayed, based on the systems adopted. With this approach, the FACS step has an important role in distinguishing antibodies selected on the basis of their binding affinity (17, 26-30). As reviewed by Kennedy and collaborators, some systems for antibody production have omitted the cells and display antibodies on ribosome or mRNA in translation

systems such bacteria, wheat germ, rabbit or insect cell lysates (17, 31-37). The scheme reported below illustrates the chronology of the development of protocols and methods for antibody production and some of their applications (Figure 5).

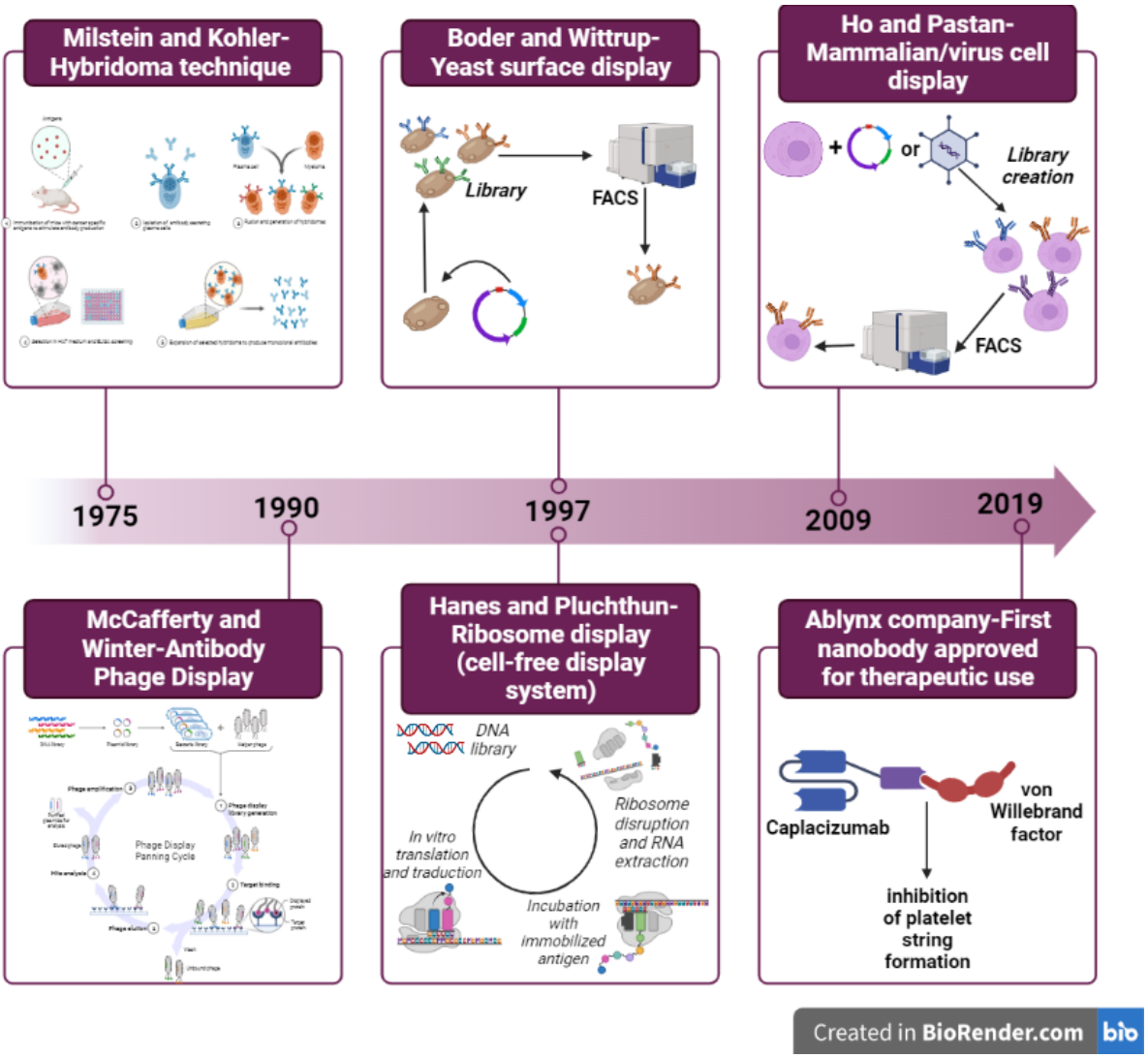

Figure 5. *Temporal outline of milestones reached in the evolution of antibody production protocols*

Most of the monoclonal antibodies used in clinics for treatment of neoplastic pathologies are directed against specific components the tumor cell surface and their interaction with the antigen may induces directly or indirectly modulation of signaling pathways. These include those associated with regulated cell death, or those that engage extracellular molecular interactions involving immune system components and cells. Alternatively, tumor cell death could be induced by the delivery in the tumor site of an antibody conjugated to a drug, radionuclide, nanoparticles, or cytotoxic agents (Figure 6). All these mechanisms of action represent the direct way of tumor cell killing mediated by antibodies, which is a highly preferred way to approach the engineering

of therapeutic antibodies for treatment of hematological malignancies (12). As highlighted above monoclonal antibodies may also indirectly induce cell death through the recruitment and activation of elements of the immune system (e.g., natural killer cells, macrophages, and complement) to react with neoplastic cells and cause cellular lysis or induced phagocytic elimination of the cells. These mechanisms are classified as antibody-dependent cellular cytotoxicity (ADCC) and complement-dependent cytotoxicity (CDC) (4, 12, 13, 38) (Figure 6).

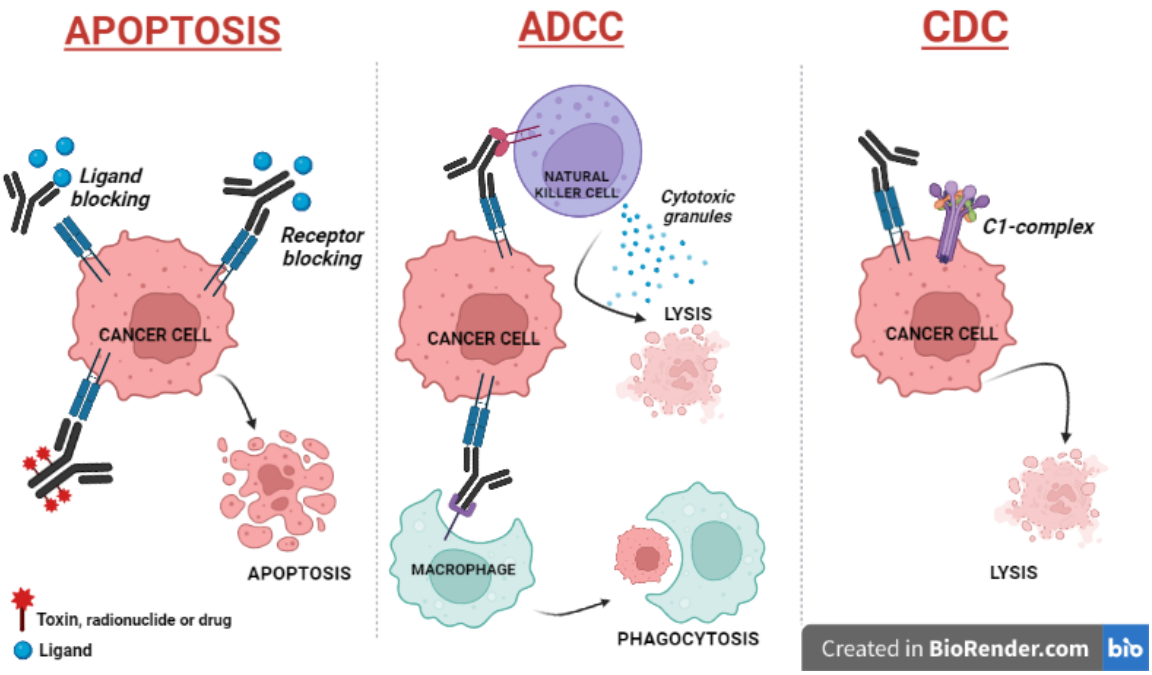

Figure 6. *Schematization of antibody-induced cell death.*

Anti-neoplastic effects exerted by antibodies may be mitigated *in vivo* by their size (150kDa), which could cause a reduction in the capacity of the antibodies to transverse blood vessel walls, penetrate and disseminate through tissues to effectively reach to the tumor lesions. This impacts on both their pharmacodynamics and their pharmacokinetics. Protocols for miniaturization of full-length immunoglobulins have been developed to counteract this problem and the primordial such strategy is to generate scFv fragments of the antibodies retaining their full antigen binding properties. However, "small size" harbors intrinsic complications, such as lower stability of the molecule, exhibit a lower affinity for the antigen because of the omitted contribution by the constant region to the antigen binding dynamics, and the difficulties encountered in large-scale production (38). A possible solution emerged in early 1990 with the discovery of nanobodies, small antigen-binding fragments (~15 kDa) derived from camelid naturally occurring antibodies composed solely of the light chains. The nanobody structure consists of three CDR, which represents the antigen binding site, and four frame regions (FR) responsible for its functional

characteristics such as stability, reduced aggregation ability, high-affinity binding, and antigen recognition (39), in addition of reducing the cross-species immunogenic properties. All these features highlight their usefulness as diagnostic or therapeutic agents, but their future use is challenged by issues that limit their clinic applications, such as the expensive cost of production, the more rapid elimination through glomerular-kidney filtration, and their impact of their non-immediate degradation (i.e., altered pharmacokinetics).

Another step forward in fighting cancer though antibody-based drugs is represented by the development of bispecific antibodies, which differ from the single target ones for their capacity of binding two different targets or two different epitopes of the same target, enhancing binding affinity, activating ADCC or CDC by bridging tumor cells and immune cells and modulating simultaneously dual cellular pathways, overcoming immune escape (40,41). Bispecific antibodies are produced through various molecular platforms and they could be divided into two wide groups: IgG-like and non-IgG-like (Fc-deficient). In the first case, the backbone is the same as IgG immunoglobulins, with the Fc domain indispensable for ADCC or CDC response. The non-IgG-like bispecific antibodies lack the Fc portion, leading to rapid and effective clearance in vivo (41,42).

Based on their origin and molecular format, currently approved monoclonal antibodies for clinical applications or antibodies under experimentation on man, are referred to as (Figure 7): (1) *murine* (or the species from which derived, rat, rabbit, etc), when they are used in their native, original full-length form (in such case their scientific denomination contains the suffix "-mab"); (3) *human,* when the antibody is entirely based on human amino acid sequences (denominated with the suffix "-umab"); (4) *chimeric,* when the constant region of the original antibody is substituted by the human counterpart to reduce the cross-species antigenic properties (denominated with the suffix "-ximab"); and (5) *humanized,* when the entire structure of the antibody is of human nature with the exception of the variable antigen-binding region which preserved in its original format (denominated with the suffix "-zumab"). The molecular engineering processes that allow to the generation of chimeric or humanized antibodies are the primary measures to overcome unwanted immunogenicity-related side effects of the antibody drugs of animal origin administered to human beings (17).

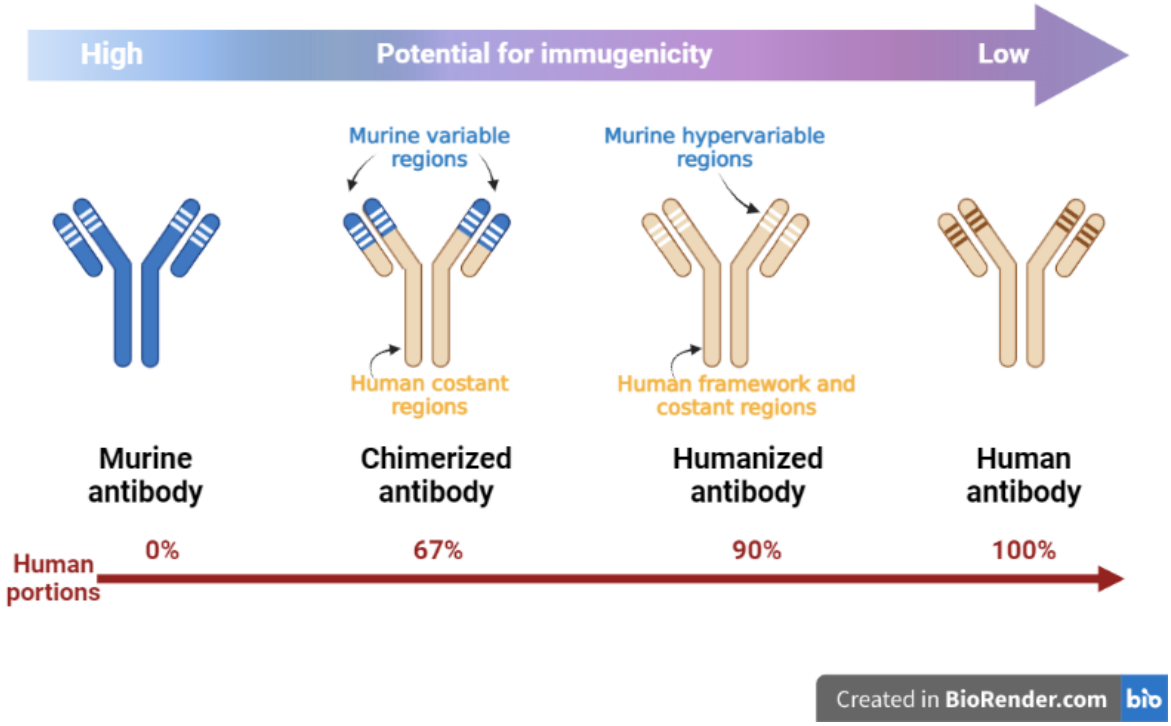

Figure 7. *Schematic representation of the different engineering processes to create species-compatible antibodies, including those to be used on man*

1.5 Identifying targets for immunotherapy

There are obviously numerous ways of identifying novel immunotherapeutic targets and to establish their potential usefulness. Notably, however, identifying truly tumor-elective targets (not expressed by any of the healthy cell types/tissue of the human body, remains a major and in some cases insurmountable challenge. Therefore, a compromise is normally accepted in the selection of tumor markers as targets that may correspond to molecules strongly upregulated by the tumor cells in comparison to their healthy counterparts, or molecules that show a scanty and restricted distribution being localized in specific tissues. It is also considered that a valid immunotherapeutic target should preferably play a primary role in the pathophysiology of the disease and/or being a disease-modifying component and be readily accessible by systemically delivered antibodies (43).

De novo immunotherapeutic target identification strategies may grossly follow two antithetic ways, as schematically depicted in Figure 8. Experimental and/or computational data may lead to the discovery of alluring immunotherapeutic target molecules and the challenge is then to generate suitable immunological agents directed against that target for which not only the proper specificity and affinity would need to be determined, but also the effective tumor selectivity and potential functional effects would need to be firmly established. The reversed approach would be to generate panels of highly reactive immunological reagents against “unknown” target molecules, determine

their tumor selectivity and their functional properties and then define the nature of the recognized antigens. This latter approach is compatible with the concept of phenotype-based drug discovery, which emphasis the study of a potential drug substance and the observation of its effect on the biological system assayed, bringing a deconvolutional approach to target discovery, in which the target identity is determined after the identification of the drug that provokes the observed phenotypic effects (44,45).

With the improvement of molecular biological and proteomic procedure, particularly whole-genome sequencing global protein profiling, target discovery has largely shifted from a deconvolutional to a molecular approach (target discovery) based on the genomic study of potential drug targets, while the identification of possible drugs and the observation of the effects on biological models are evaluated at a later stage. Many are the methods that lead to target deconvolution, such as affinity chromatography, expression-cloning by function, screening of protein microarrays or 'reverse transfected' cell microarrays, and biochemical suppression approaches (45). The most relevant advantage of the target deconvolution approach, as Lansdowne underscored in her article, is its ability to demonstrate the efficacy of a drug in the context of a cellular environment and the recent possibility to miniaturize the biological assays or to work with 3D systems, improving scalability physiological relevance, could represent a start point for the increasing adoption of this method. On the other hand, the molecular approach to target discovery is easy to carry out, less expensive and the process is faster than the phenotypic one. The methods applicable to this approach are crystallography, computational modeling, genomics, biochemistry, and binding kinetics to understand how drugs could interact with the potential target (46). The important point in target validation remains the process of demonstrating the functional role of the identified target in the disease phenotype (47, 48).

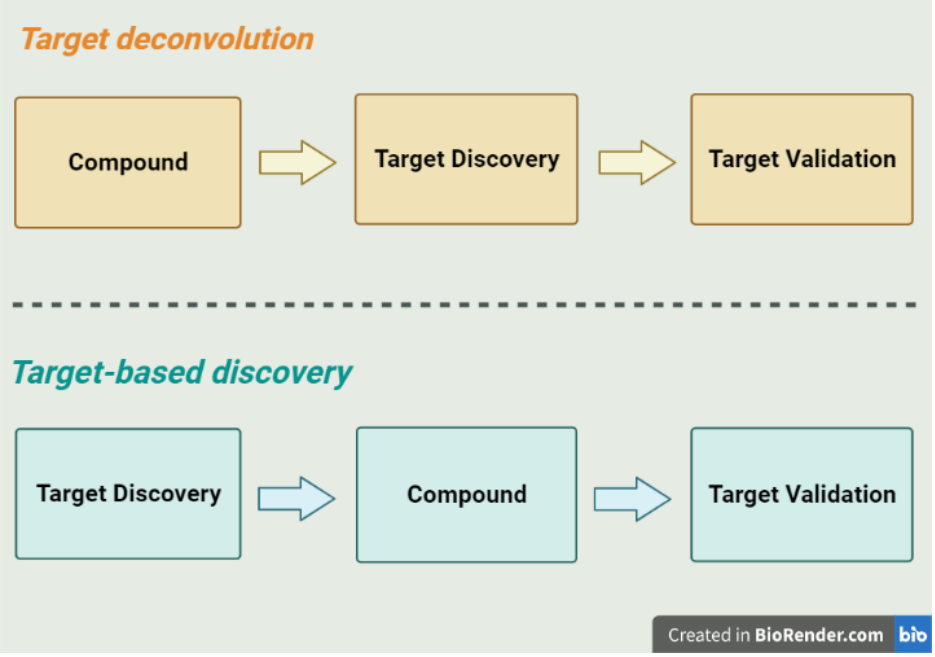

Figure 8. *Schematic representation of two primary conceptual approaches for immunotarget discovery*

In recent years huge signs of progress are being evident in every cancer area of research and numerous attractive targets are being studied and validated for different tumor types. The field of post-translation modifications (PTMs), with more than 500 PTMs identified, is becoming a new area to explore in the context of immunotarget discovery, as a wealth of parallel studies have unveiled dramatic differences in PTM in the proteins produced by cancer cells. PTMs of key molecules are known to influence cell behavior in healthy and neoplastic conditions, controlling important processes like growth, metabolism, or cell death, and, lately, approaches to their regulation for therapeutic purposes are spreading (49,50). PTMs are classified into the following classes: protein acylation modification, lipid-related protein modification, metabolite-related protein modification, and ubiquitin-like small-molecule protein modification (51) (Figure 9). PTMs may affect positively or negatively chromatin organization and gene transcription (influencing gene expression and DNA repair), protein-protein interaction, cancer signal cascade, metabolic reprogramming, epithelial-mesenchymal transition (EMT) regulation, and immune-escaping (49-51).

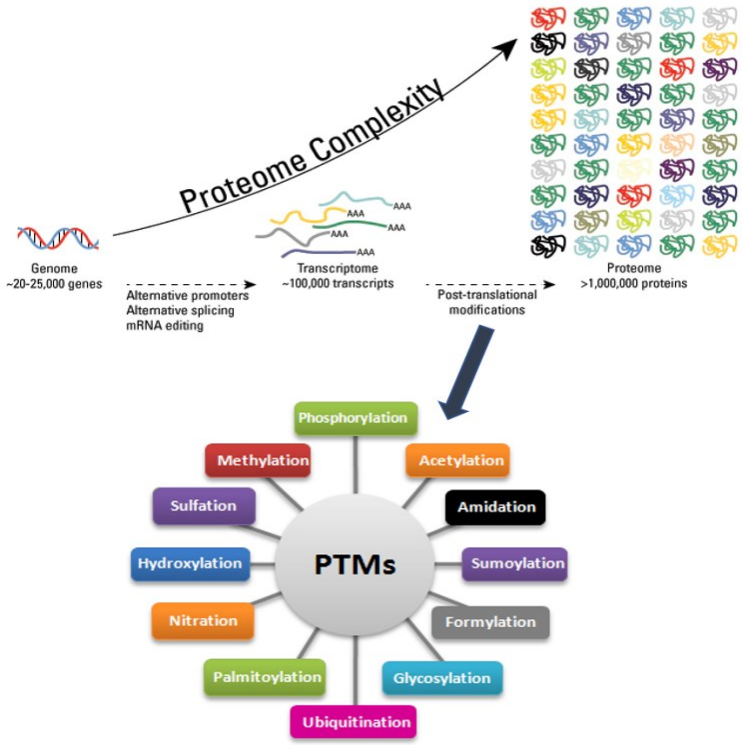

Figure 9. *Upper scheme shows highlights how post-translational modifications (PTMs) contribute to the dramatic increase in number of protein variants of the human proteome compared to those generated through linear translation of the transcriptome. Lower scheme summarizes the known types of PTMs occurring in the human proteome*

Strongly connected to the targets represented by heavily post-translationally modified proteins are other potential targets for hematological malignancies belonging to the class of proteoglycans (PGs) - complex macromolecules highly glycosylated, which are involved in most cellular functions (52). PGs expression influences normal hematopoiesis as they are constitutively expressed by numerous hematopietic cells and their precursors at different stages of development, while becoming aberrantly up- or down-regulated upon (ref. Borghini et al., in preparation) (55-62). The family of PGs is large and embodies highly diversified members for which the consensus classification and nomenclature have recently established (Figure 10; 54).

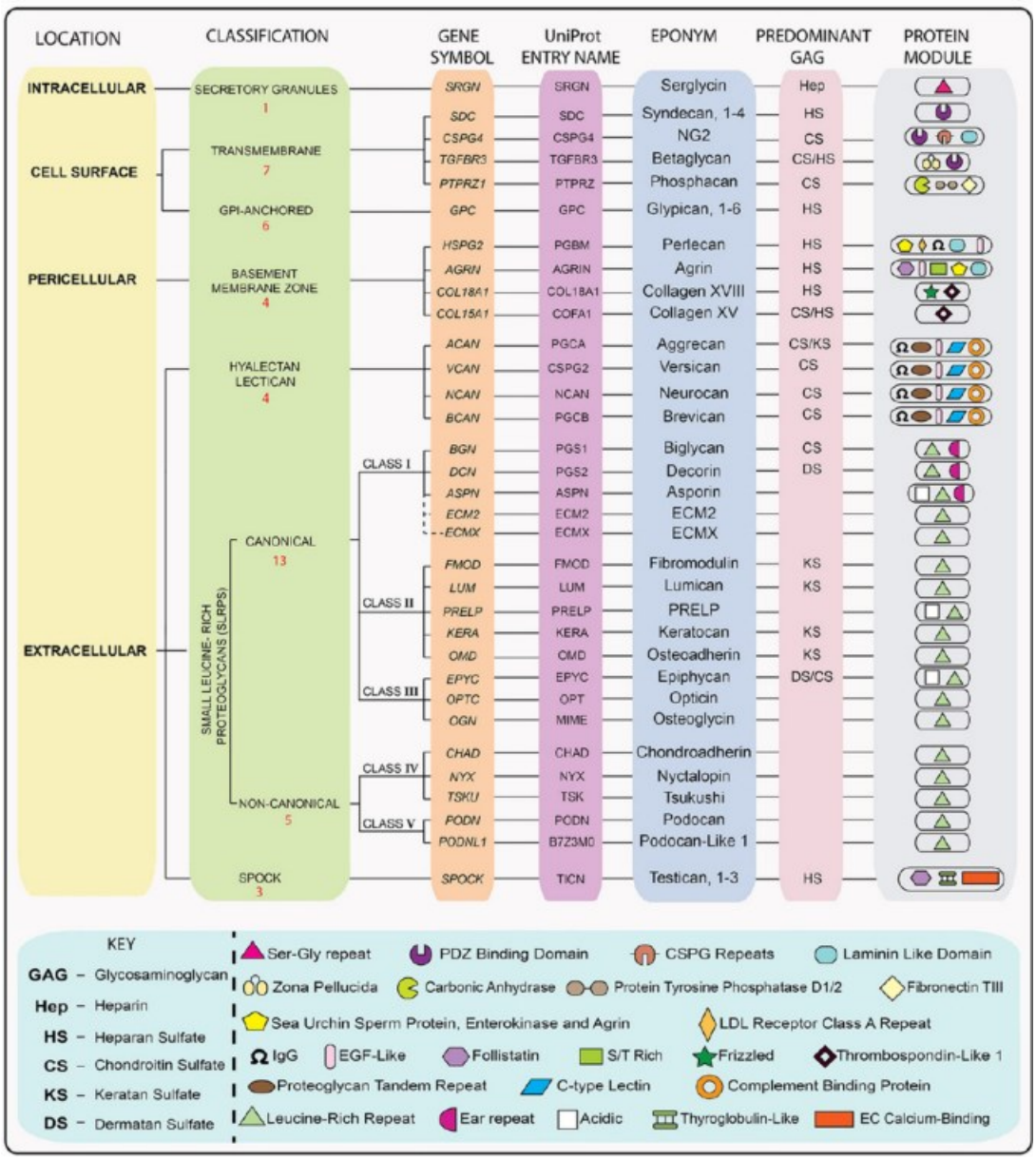

Figure 10. *Comprehensive classification and nomenclature of PGs*

Aberrant or de novo expression of PGs is frequently found to be the basis of malignant transformation, which implicitly makes them suitable targets for new therapeutic approaches, as well as for diagnostic tests. If summarizing the available data for CLL, AML, and B/T-ALL, primary PGs of interest for hematological malignancies are CD44, Syndecan-1/CD138, Syndecan-2/CD362, Endoglycan, Glypican-2, Endocan, NG2/CSPG4, Versican, Perlecan, and Fibromodulin, with several of these macromolecules being involved in different cellular processes, such as an overall promotion of malignancy, enhanced bone marrow-infiltration capabilities, favoring of an increased tumor burden, and induced drug resistance (63-79). Due to the role of these macromolecules in neoplastic transformation and tumor progression in the different types of hematological malignancies, they represent attractive targets for direct or indirect immunotherapy.

2 MATERIALS AND METHODS

2.1 Monoclonal antibody production

The production and partial characterization of monoclonal antibodies (mAbs) against the PG aggrecan is described in Virgintino et al. (79). To generate mAbs against unique, post-translationally modified cell surface components of neoplastic lymphocytes, we performed sequential cell surface biotinylations (80) of the follicular lymphoma cell line, Sci-1 arbitrary selected as lymphoma model, using conventional protocols (more effective procedures have been proposed more recently). Cells (three rounds with 10-15x10^6 cells/each) were washed with PBS and surface labeled with EZ-Link Sulfo-NHS-LC-Desthiobiotin dissolved in DMSO, essentially following the manufacturer's protocol. Cells were extensively washed with PBS, lysed on ice with 50 mM Tris HCl buffer, pH 7.4, with 150 mM NaCl, 0.5% deoxycholate, 1% CHAPS, 0.3% N-Octyl-β-D-glucoside, 5 mM EDTA and a protease inhibitor cocktail (Millipore-Merck). Solubilized material was separated by affinity chromatography on Pierce High-Capacity Streptavidin Agarose columns through elution with excess biotin (25 mM) in 50 mM Tris HCl buffer, pH 7.4, with 1 M NaCl, 1% n-Dodecyl-β-D-maltoside, 0.3% N-Octyl-β-D-glucoside, 5 mM EDTA and the protease inhibitor cocktail (modified protocol of Grun et al. (81) and Cheah and Yamada (82)). The eluted material was concentrated, pelleted by centrifugation, resolubilized in elution buffer and incubated with an excess of NeutrAvidin (50 mM) for 1 hour at room temperature to saturate all free biotin. The material was extensively washed to remove all non-bound NeutrAvidin and re-biotinylated with Biotin-LC-hydrazide (4.6mg/12 mmol), dissolved in DMSO in the presence glacial acetic acid, for 1 hour at 65°C, to specifically tag glycan-bearing molecules. Female Bulb/c mice were immunized with according to standard protocols involving repeated intraperitoneal and intravenous injection of the immunogen preparation dissolved in complete Freund's adjuvant. Spleen cells were fused with NS1 myeloma cells and the resulting hybridoma clones were screened by ELISA against the biotinylated immunogen immobilized.

2.2. Hybridoma culturing

Hybridomas were cultured as suspension cells using RPMI 1640 (Euroclone SPA-Milano ITA) 2mM L-glutamine (Euroclone SPA-Milano ITA), 2mM Penicillin/Streptomycin (Euroclone SPA-Milano ITA) and 10% of fetal bovine serum (ThermoFisher Scientific-Waltham, MA USA). The cell lines are maintained in the cell incubator at 37° C and 5% partial pressure of CO2. The hybridoma cells release the antibodies in the culture medium and are collected by clarification process, which consists of centrifugation at high speed (11000 rpm) for 20 minutes at 4° C (Centrifuge 5810R Eppendorf-

Hamburg, DE). The clones are initially cultured with Hybridoma Serum Free Medium (HSFM-ThermoFisher Scientific-Waltham, MA USA), or alternative with addition of FBS a medium supplement (Capricorn Scientific-Germany) to implement antibody production, but the effect of increasing antibody production resulted better with solely FBS. We identify through ELISA for several clones mixed population of IgG and IgM cells.

2.3 Cell lines and their culturing

Type, characteristic traits, and source of cell lines used for the study are summarized in Table 3. Cell lines included 53 lymphomas, 45 leukemia, one cell representing a myeloproliferative disorder, one cell type representing multiple myeloma, and immortalized lymphocytes. Cells were cultured according to established, specific protocols reported in the literature and/or indicated by the provider. Thus, they were grown in RPMI 1640 medium, IMDM or DMEM with low glucose, 2mM L-glutamine, 2mM Penicillin/Streptomycin (Euroclone S.p.A., Milan, Italy) and 10-20% of fetal bovine serum (ThermoFisher Scientific-Waltham, MA USA), depending on the specific requirement of the given cell line.

Table 3. *Phenotypic traits and derivation of model cell lines used in this study*

Pathology	Cell line	Subtype	Characteristics	Number of positive antibodies	Source
Non-Hodgkin lymphoma (NHL)	**DOH-H2**	**Follicular lymphoma**	**t(14;18) BCL-2 expression**	**5**	**Prof. Carmelo Carlo-Stella IRCSS-Humanitas-Milano**
Non-Hodgkin lymphoma (NHL)	**SCI-1**	**Follicular lymphoma**	**t(14;18) co-expression BCL-2 and MYC**	**13**	**ATCC**
Non-Hodgkin lymphoma (NHL)	**GRANTA-519**	**Mantle cell lymphoma**	**t(11;14) rearrangement at 9p22 associated with CCND1 (cyclin D1) activation**	**3**	**Prof. Carmelo Carlo-Stella IRCSS-Humanitas-Milano**
Non-Hodgkin lymphoma (NHL)	**JEKO-1**	**Mantle cell lymphoma**	**carries cryptic rearrangements of CCND1 and IGH (IGH)**	**2**	**Prof. Carmelo Carlo-Stella IRCSS-Humanitas-Milano**
Non-Hodgkin lymphoma (NHL)	**JVM-2**	**Mantle cell lymphoma**	**t(11;14) leading to IGH-CCND1 (BCL1) fusion gene and CCND1 activation**	**7**	**ATCC**
Non-Hodgkin lymphoma (NHL)	**MINO**	**Mantle cell lymphoma**	**t(11;14)(q13;q32) leading to CCND1-**	**6**	**Dr. Giorgia Simonetti IRST**

			IGH (BCL1-IGH) fusion gene		"Dino Amadori"-Meldola-Meldola-Meldola
Non Hodgkin lymphoma (NHL)	Z-138	Mantle cell lymphoma	t(11;14)	7	Dr. Giovanna Roncador Centro Nacional de Investigaciones Oncológicas-Madrid
Non Hodgkin lymphoma (NHL)	UPN-2	Mantle cell lymphoma	t(11;14)	4	Dr. Giovanna Roncador Centro Nacional de Investigaciones Oncológicas-Madrid
Non Hodgkin lymphoma (NHL)	IRM-2	Mantle cell lymphoma		3	Dr. Giovanna Roncador Centro Nacional de Investigaciones Oncológicas-Madrid
Non Hodgkin lymphoma (NHL)	SU-DHL-2	Diffuse large B cell lymphoma	Activated B cell-like diffuse large B cell lymphoma (ABC-DLBCL)	2	Prof. Carmelo Carlo-Stella IRCSS-Humanitas-Milano
Non-Hodgkin lymphoma (NHL)	SU-DHL-5	Diffuse large B cell lymphoma	Germinal center B cell-like lymphoma (GCB-like)	6	Prof. Carmelo Carlo-Stella IRCSS-Humanitas-Milano
Non-Hodgkin lymphoma (NHL)	SU-DHL-6	Diffuse large B cell lymphoma	Germinal center B cell-like lymphoma (GCB-like)	5	Prof. Carmelo Carlo-Stella IRCSS-Humanitas-Milano
Non-Hodgkin lymphoma (NHL)	MHH-PREB	Diffuse large B cell lymphoma	Germinal center B cell-like lymphoma (GCB-like)	3	Dr. Giovanna Roncador Centro Nacional de Investigaciones Oncológicas-Madrid
Non Hodgkin lymphoma (NHL)	OCI-LY-1	Diffuse large B cell lymphoma	t(14;18)	3	DSMZ
Non Hodgkin lymphoma (NHL)	OCI-LY-3	Diffuse large B cell lymphoma	t(14;19) t(4;18)	9	DSMZ
Non Hodgkin lymphoma (NHL)	OCI-LY-19	Diffuse large B cell lymphoma	t(14;18)	12	Prof. Carmelo Carlo-Stella IRCSS-Humanitas-Milano
Non Hodgkin lymphoma (NHL)	RC-19	Diffuse large B cell lymphoma	t(14;18) effecting rearrangement of	6	Prof. Carmelo Carlo-Stella

			BCL2 with IGH (IGH)		IRCSS-Humanitas-Milano
Non Hodgkin lymphoma (NHL)	HT	Diffuse large B cell lymphoma	assigned to GCB-like lymphoma subtype	9	Prof. Carmelo Carlo-Stella IRCSS-Humanitas-Milano
Non Hodgkin lymphoma (NHL)	BC-2	Diffuse large B cell lymphoma	effusion samples of a 31-year-old man at diagnosis of AIDS-related primary effusion lymphoma (PEL)	3	ATCC
Non Hodgkin lymphoma (NHL)	Karpas-422	Diffuse large B cell lymphoma	t(14;18) IGH-BCL2 fusion gene	1	Prof. Carmelo Carlo-Stella IRCSS-Humanitas-Milano
Non Hodgkin lymphoma (NHL)	Riva	Diffuse large B cell lymphoma	t(4;8) and der(18) effecting MYC rearrangement and amplification of BCL2	3	CRO-Aviano
Non Hodgkin lymphoma (NHL)	DB	Diffuse large B cell lymphoma	t(14;18)	4	Prof. Carmelo Carlo-Stella IRCSS-Humanitas-Milano
Non Hodgkin lymphoma (NHL)	TOLEDO	Diffuse large B cell lymphoma	cells resemble Burkitt's lymphoma, but lack the typical chromosomal translocations of Burkitt's lymphoma	8	Dr. Giovanna Roncador Centro Nacional de Investigaciones Oncológicas-Madrid
Non Hodgkin lymphoma (NHL)	U-2932	Diffuse large B cell lymphoma	overexpress of BCL2, BCL6 and p53	4	Prof. Carmelo Carlo-Stella IRCSS-Humanitas-Milano
Non Hodgkin lymphoma (NHL)	BCBL-1	Diffuse large B cell lymphoma	carries IGH rearrangements and genomic MYC amplification	0	ATCC
Non-Hodgkin lymphoma (NHL)	SU-DHL-8	Histiocytic lymphoma	t(8;22)	8	Prof. Carmelo Carlo-Stella IRCSS-Humanitas-Milano
Non-Hodgkin lymphoma (NHL)	SU-DHL-10	Histiocytic lymphoma	EZH2 Y641F mutation	11	Prof. Carmelo Carlo-Stella IRCSS-Humanitas-Milano
Non-Hodgkin lymphoma (NHL)	SU-DHL-16	Histiocytic lymphoma	t(14;18)	8	Prof. Carmelo Carlo-Stella

					IRCSS-Humanitas-Milano
Non-Hodgkin lymphoma (NHL)	**RC-K8**	**Histiocytic lymphoma**	**BCL6 translocation**	**4**	**Prof. Carmelo Carlo-Stella IRCSS-Humanitas-Milano**
Non-Hodgkin lymphoma (NHL)	**U937**	**Histiocytic lymphoma**	**carries t(10;11) (seen in AML M5) t(1;5) resembles variant of t(2;5) (histiocytic lymphoma)**	**0**	**ATCC**
Non Hodgkin lymphoma (NHL)	**SUP-M2**	**Anaplastic large B cell lymphoma**	**t(2;5)(p23;q35) leading to the NPM1-ALK (NPM-ALK) fusion gene and to express CD30**	**6**	**Prof. Carmelo Carlo-Stella IRCSS-Humanitas-Milano**
Non Hodgkin lymphoma (NHL)	**SU-DHL-1**	**Anaplastic large B cell lymphoma**	**t(2;5)(p23;q35)**	**1**	**DSMZ**
Non Hodgkin lymphoma (NHL)	**Karpas-299**	**T cell lymphoma**	**CD30+ cells carry the NPM-ALK fusion gene**	**4**	**Prof. Carmelo Carlo-Stella IRCSS-Humanitas-Milano**
Non Hodgkin lymphoma (NHL)	**SUP-T1**	**T cell lymphoma**	**inv(2)(p22q11)x2, t(2;20)(p13;p11), del(4)(q31q35), del(6)(q25)x2, add(7)(q32), add(9)(q34)x2, inv(14)(q11q32)x2**	**1**	**Prof. Carmelo Carlo-Stella IRCSS-Humanitas-Milano**
Non Hodgkin lymphoma (NHL)	**SR-786**	**T cell lymphoma**	**NPM1-ALK (NPM-ALK) fusion gene**	**7**	**Prof. Carmelo Carlo-Stella IRCSS-Humanitas-Milano**
Non Hodgkin lymphoma (NHL)	**HUT-78**	**T cell lymphoma**	**Sezary syndrome**	**0**	**ATCC**
Non Hodgkin lymphoma (NHL)	**HUT-102**	**T cell lymphoma**	**Sezary syndrome**	**0**	**ATCC**
Non Hodgkin lymphoma (NHL)	**HH**	**T cell lymphoma**	**Aggressive lymphoma**	**0**	**Prof. Carmelo Carlo-Stella IRCSS-Humanitas-Milano**
Burkitt's lymphoma (BL)	**RAMOS**		**t(8;14) p53 mutation**	**1**	**Prof. Carmelo Carlo-Stella IRCSS-Humanitas-Milano**
Burkitt's lymphoma (BL)	**BJAB**		**no IG/MYC translocation detected**	**3**	**Prof. Carmelo Carlo-Stella IRCSS-Humanitas-Milano**

Burkitt's lymphoma (BL)	**DAUDI**		**BCL-2 expression**	**5**	**ATCC**
Burkitt's lymphoma (BL)	**RAJI**		**t(8;14 ki8)**	**4**	**ATCC**
Burkitt's lymphoma (BL)	**NAMALWA**		**carries sequences of the squirrel monkey retrovirus (SMRV)**	**15**	**Prof. Carmelo Carlo-Stella IRCSS-Humanitas-Milano**
Burkitt's lymphoma (BL)	**P3H-R1**		**clonally derived subline of Jiyoye**	**2**	**ATCC**
Burkitt's lymphoma (BL)	**BL-2**		**t(8;22) effecting juxtaposition of MYC with IGL**	**1**	**ATCC**
Burkitt's lymphoma (BL)	**W133**			**2**	**Dr. Giovanna Roncador Centro Nacional de Investigaciones Oncológicas-Madrid**
Burkitt's lymphoma (BL)	**Rj 2/2.5 β5/B1**			**3**	**Dr. Giorgio Malpeli-University of Verona**
Burkitt's lymphoma (BL)	**AKATA**		**Mutation; HGNC, p53**	**5**	**Dr. Giovanna Roncador Centro Nacional de Investigaciones Oncológicas-Madrid**
Hodgkin Lymphoma (HL)	**HD-MY-Z**	**ns-cHL**	**CD30-**	**3**	**Prof. Carmelo Carlo-Stella IRCSS-Humanitas-Milano**
Hodgkin Lymphoma (HL)	**L-428**	**ns-cHL**	**expression of fusion gene ELMO1-SLCO3A1**	**3**	**Prof. Carmelo Carlo-Stella IRCSS-Humanitas-Milano**
Hodgkin Lymphoma (HL)	**KM-H2**	**cHL**	**expression of fusion genes PRRC2B-MGMT (BAT2L1-MGMT) and CIITA-BX648577**	**4**	**Prof. Carmelo Carlo-Stella IRCSS-Humanitas-Milano**
Hodgkin Lymphoma (HL)	**L-1236**	**cHL**		**8**	**Prof. Carmelo Carlo-Stella IRCSS-Humanitas-Milano**
Hodgkin Lymphoma (HL)	**DEV**	**Nodular-lymphocyte predominant HL (NLPHL)**		**10**	**Dr. Giovanna Roncador Centro Nacional de Investigaciones**

					Oncológicas-Madrid
Acute lymphoblastic leukemia (ALL)	**RS 4-11**	**B-cell leukemia**	**t(4;11)(q21;q23)**	**1**	**ATCC**
Acute lymphoblastic leukemia (ALL)	**697**	**B-cell leukemia**	**fusion gene TCF3-PBX (E2A-PBX) t(1;19)(q23;p13), del(6)(q21)**	**2**	**IZSLER-Brescia**
Acute lymphoblastic leukemia (ALL)	**JURKAT**	**B-cell leukemia**		**2**	**ATCC**
Acute lymphoblastic leukemia (ALL)	**REH**	**B-cell leukemia**	**t(12;21) leading to ETV6-RUNX1 (TEL-AML1) fusion gene**	**3**	**IRST "Dino Amadori'- Meldola**
Acute lymphoblastic leukemia (ALL)	**KOPN-8**	**B-cell leukemia**	**t(11;19)(q23;p13) leading to the KMT2A-MLLT1**	**1**	**Dr. Giorgia Simonetti IRST "Dino Amadori"-Meldola-Meldola-Meldola**
Acute lymphoblastic leukemia (ALL)	**CCRF-SB**	**B-cell leukemia**		**2**	**IZSLER-Brescia**
Acute lymphoblastic leukemia (ALL)	**CCRF-HSB**	**B-cell leukemia**		**3**	**IZSLER-Brescia**
Acute lymphoblastic leukemia (ALL)	**SD-1**	**B-cell leukemia**	**BCR-ABL1 fusion gene**	**6**	**Dr. Giovanna Roncador Centro Nacional de Investigaciones Oncológicas-Madrid**
Acute lymphoblastic leukemia (ALL)	**HAL-01**	**B-cell leukemia**	**t(17;19)(q22;p13) TCF3-HLF (E2A-HLF) fusion gene**	**4**	**Dr. Giorgia Simonetti IRST "Dino Amadori"-Meldola-Meldola-Meldola**
Acute lymphoblastic leukemia (ALL)	**SUP-B15**	**B-cell leukemia**	**BCR-ABL1 fusion gene**	**3**	**Dr. Giorgia Simonetti IRST "Dino Amadori"-Meldola-Meldola-Meldola**
Acute lymphoblastic leukemia (ALL)	**TOM-1**	**B-cell leukemia**	**BCR-ABL1 fusion gene**	**6**	**Dr. Giorgia Simonetti IRST "Dino Amadori"-Meldola-Meldola-Meldola**
Acute lymphoblastic leukemia (ALL)	**NALM-6**	**B-cell leukemia**	**t(5;12)(q33.2;p13.2)**	**1**	**Prof. P. Lunghi-SCVSA Department-University of Parma**
Acute lymphoblastic leukemia (ALL)	**ALL-PO**	**B-cell leukemia**	**t(4;11)**	**1**	**ATCC**

Acute lymphoblastic leukemia (ALL)	**CEM/C1**	**T-cell leukemia**	**Altered Topoisomerase I**	**2**	**IZSLER-Brescia**
Acute lymphoblastic leukemia (ALL)	**MOLT-3**	**T-cell leukemia**		**5**	**Dr. Giorgio Malpeli-University of Verona**
Acute lymphoblastic leukemia (ALL)	**MOLT-4**	**T-cell leukemia**	**Closely related to MOLT-3**	**2**	**CRO-Aviano**
Acute lymphoblastic leukemia (ALL)	**RPMI-8402**	**T-cell leukemia**	**STIL-TAL1 (SIL-TAL1) fusion gene**	**5**	**Dr. Giorgia Simonetti IRST "Dino Amadori"-Meldola-Meldola-Meldola**
Acute lymphoblastic leukemia (ALL)	**PF-382**	**T-cell leukemia**		**0**	**Centre for biological resources-Ospedale San Martino-Genova**
Acute lymphoblastic leukemia (ALL)	**PEER**	**T-cell leukemia**		**1**	**Prof. Carmelo Carlo-Stella IRCSS-Humanitas-Milano**
Acute lymphoblastic leukemia (ALL)	**CCRF-CEM**	**T-cell leukemia**	**expression of NKX2-5**	**0**	**IZSLER-Brescia**
Acute lymphoblastic leukemia (ALL)	**BE-13**	**T-cell leukemia**	**Subclone of PEER**	**0**	**Dr. Giovanna Roncador Centro Nacional de Investigaciones Oncológicas-Madrid**
Chronic lymphoblastic leukemia (CLL)	**MEC-1**			**6**	**Dr. Giovanna Roncador Centro Nacional de Investigaciones Oncológicas-Madrid**
Chronic lymphoblastic leukemia (CLL)	**PGA-1**		**trisomy 12 associated with CLL**	**7**	**Dr. Giovanna Roncador Centro Nacional de Investigaciones Oncológicas-Madrid**
Chronic lymphoblastic leukemia (CLL)	**HG-3**		**del(13) associated with CLL**	**5**	**Dr. Giovanna Roncador Centro Nacional de Investigaciones Oncológicas-Madrid**
Acute myeloid leukemia (AML)	**MOLM-16**	**AML-M0**		**5**	**Dr. Giorgia Simonetti IRST "Dino Amadori"-**

					Meldola-Meldola-Meldola
Acute myeloid leukemia (AML)	**NOMO-1**	**AML-M5**	**t(9;11)(p22;q23) KMT2A-MLLT3 (MLL-MLLT3; MLL-AF9) alteration**	**5**	**Dr. Giorgia Simonetti IRST "Dino Amadori"-Meldola-Meldola-Meldola**
Acute myeloid leukemia (AML)	**FLG 29.1**	**AML-M5**		**4**	**ATCC**
Acute myeloid leukemia (AML)	**MONOMAC-6**	**AML-M5**	**t(9;11)(p22;q23) leading to KMT2A-MLLT3 (MLL-MLLT3; MLL-AF9) fusion gene**	**2**	**Centre for biological resources-Ospedale San Martino-Genova**
Acute myeloid leukemia (AML)	**OCI/AML-2**	**AML-M4**	**DNMT3A R635W mutation**	**2**	**ATCC**
Acute myeloid leukemia (AML)	**OCI/AML-3**	**AML-M4**	**DNMT3A R882C mutation**	**10**	**Prof. P. Lunghi-SCVSA Department-University of Parma**
Acute myeloid leukemia (AML)	**GF-D8**	**AML-M1**		**0**	**Centre for biological resources-Ospedale San Martino-Genova**
Acute myeloid leukemia (AML)	**KASUMI-1**	**AML-M2**	**t(8;21) leading to RUNX1-RUNX1T1 (AML1-ETO) fusion gene**	**0**	**Dr. Giorgio Malpeli-University of Verona**
Acute myeloid leukemia (AML)	**KG-1**	**AML-M0**	**FGFR1OP2-FGFR1 (OP2-FGFR1) fusion gene**	**0**	**ATCC**
Acute myeloid leukemia (AML)	**HL-60**	**AML-M2**	**MYC amplification**	**1**	**Prof. P. Lunghi-SCVSA Department-University of Parma**
Acute myeloid leukemia (AML)	**NB4**	**AML-M3**	**t(15;17) PML-RARA fusion gene**	**6**	**Prof. P. Lunghi-SCVSA Department-University of Parma**
Acute myeloid leukemia (AML)	**THP-1**	**AML-M5**	**t(9;11)(p21;q23) leading to KMT2A-MLLT3 (MLL-MLLT3; MLL-AF9) fusion gene**	**2**	**Prof. P. Lunghi-SCVSA Department-University of Parma**
Acute myeloid leukemia (AML)	**MV-4-11**	**AML-M5**	**t(4;11) FLT3-ITD mutation**	**4**	**ATCC**

Acute myeloid leukemia (AML)	**MOLM-13**	**AML-M5**	**KMT2A-MLLT3 (MLL-MLLT3; MLL-AF9) fusion gene**	**0**	**Prof. P. Lunghi-SCVSA Department-University of Parma**
Acute myeloid leukemia (AML)	**HEL**	**AML-M6**	**JAK2 V617F mutation**	**4**	**Dr. Giorgia Simonetti IRST "Dino Amadori"-Meldola-Meldola-Meldola**
Chronic myeloid leukemia (CML)	**BV-173**		**BCR-ABL-1 fusion gene**	**1**	**ATCC**
Chronic myeloid leukemia (CML)	**LAMA-84**		**BCR-ABL-1 fusion gene**	**1**	**Prof. P. Lunghi-SCVSA Department-University of Parma**
Chronic myeloid leukemia (CML)	**CML-T1**		**BCR-ABL-1 fusion gene**	**2**	**Dr. Giovanna Roncador Centro Nacional de Investigaciones Oncológicas-Madrid**
Chronic myeloid leukemia (CML)	**MEG-01**		**BCR-ABL-1 fusion gene**	**4**	**Centre for biological resources-Ospedale San Martino-Genova**
Chronic myeloid leukemia (CML)	**KCL-22**		**BCR-ABL-1 fusion gene p53 mutation**	**1**	**Prof. P. Lunghi-SCVSA Department-University of Parma**
Chronic myeloid leukemia (CML)	**K562**		**BCR-ABL-1 fusion gene**	**1**	**Prof. P. Lunghi-SCVSA Department-University of Parma**
Myeloproliferative disorder	**SET-2**	**Essential thrombocythemia**	**JAK2 V617F mutation DNMT3A R882H mutation**	**2**	**Dr. Giovanna Roncador Centro Nacional de Investigaciones Oncológicas-Madrid**
Multiple myeloma (MM)	**IM-9**			**5**	**Prof. P. Lunghi-SCVSA Department-University of Parma**

Immortalized lymphocytes					**ATCC**

2.4 Antibody purification

The purification of immunoglobulins from hybridoma supernants were performed through affinity chromatography on Protein-G matrix columns (HiTrap® ProteinG High Performance-Cytiva, Washington DC, USA) in the case of IgG isotypes and columns with a thiophilic adsorption medium, 2-merCaptopyridine coupled to Sepharose (HiTrap® IGM High Performance-Cytiva, Washington DC, USA) in the case of IgM isotypes.

2.5 Isolation of peripheral blood mononucleated cells

Peripheral blood mononucleated cells (PBMC) were collected from whole blood of six healthy donors, after informed consent, and processed as conventionally by gradient separation on a Ficoll-Pacque matrix (Euroclone S.p.A., Milan, Italy). Briefly, heparinized peripheral blood samples were diluted 1:2 in PBS and supplemented addition of 3ml of Ficoll for every 8ml of diluted blood. Samples were centrifuged at 1,400 rpm for 15 minutes and lymphocytes were collected from the interface re-diluted in PBS, spin down by centrifugation at 1,000 rpm for 7 minutes and washed in PBS to remove traces of Ficoll and other unwanted blood components.

2.6 Flow cytometry

For flow cytometry, 10^5-10^6 cells were thoroughly washed in PBS with 1% FBS and resuspended 200ml of hybridoma culture supernatant or 2-20mg/ml of purified Igs for 30 min on ice, followed by washing in PBS with 1% FBS and incubation with isotype-specific anti-Ig secondary antibodies conjugated to FITC or PE (Southern-Biotech, Birmingham, USA) diluted 1:100 for 30 min at room temperature. Cells were further washes with PBS with 1%FBS and analyzed with a NovoCyte cytometer (ACEA-San Diego, CA USA) using the Novoexpress software program (ACEA-San Diego, CA USA) for data analysis. Flow cytometry analyses for cell viability/apoptosis were performed with Annexin V-FITC/PI kit (ThermoFisher Scientific, Waltham, MA USA), following the manufacturer's protocol.

2.7 Immunocytochemistry

For microscopic analysis of the patterns of antibody binding to cell surfaces, we used the Cytospin (ThermoFisher- Waltham, MA USA) approach. Cells (0.125 ml suspension of 10^5 cells/ml) were pipetted into the cyto-funnel connected to the glass slide (~300ml) and centrifuged at 1,000 rpm for 5 minutes. Glass slides with attached cells were then incubated with 200ml 4% PFA for 10 min at room temperature, followed by extensive rinsing with PBS. Cells were then incubated with antibodies hybridoma culture supernatants containing 5% of Block-Aid blocking solution (LifeSciences Tech-Carlsbad, CA USA) overnight at 4°C. Glass slides were then rinsed with PBS and incubated for 1hr with the secondary Alexa555 labelled anti-mouse IgG or IgM antibodies (Southern-Biotech-Birmingham, AL USA), at 1:400 dilution with 5% Block-aid, followed by nuclear counterstain with Hoescht for 20 min added at 1:1,000 dilution. Stained slides were then dried, covered with a coverslip with FluorGuard Mounting Medium (Hysto-Line Laboratories Srl, Milan, Italy) and viewed with a Axio Observer.ZI (Zeiss) fluorescence microscope.

2.8 Western blotting

Cells were lysed with RIPA buffer (ThermoFisher Scientific-Waltham, MA USA) and 1% of protease inhibitors cocktail (PIC, ThermoFisher Scientific-Waltham, MA USA), following a standard protocol for WB provided by reagent suppliers. Solubilized material was separated by SDS-PAGE on precast 4-15% gradient gels (BioRad-Hercules, CA USA) and transferred onto nitrocellulose membrane through the Transblot System (Biorad-Hercules, CA USA). Primary antibodies were used at a dilution of 1:10,000 and secondary goat anti-mouse HRP-conjugated antibodies (Southern-Biotech-Birmingham, AL USA) and 1:4,000 dilution. As a loading control we used β-actin which was simultaneously revealed through an anti-human β-actin antibody directly conjugated to HRP (ThermoFisher Scientific-Waltham, MA USA). For chemiluminescent detection we used a dedicated kit, Westar-One provided by Cyanagen Srl (Bologna, Italy).

2.9 Cell proliferation assays

Assessment of cell proliferation was carried out with the AlamarBlue™ Cell Viability Reagent (Invitrogen™, Waltham, MA USA), according to the protocol provided by the manufacturer. Here below is a graphic representation of the assay operation published by Ligasova et al. (83) (Figure 11).

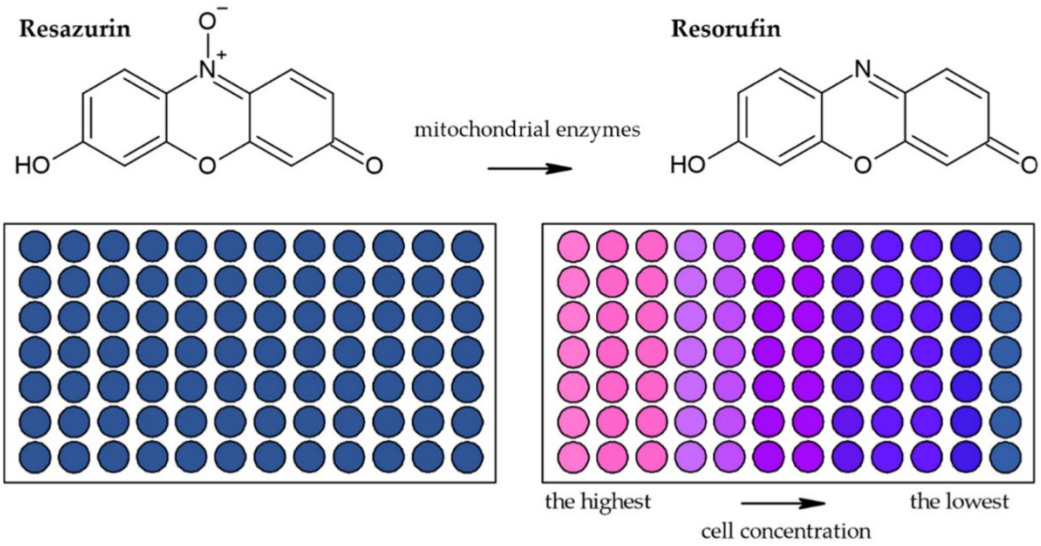

Figure 11. *Graphic representation of Alamar blue assay by Ligasova et al (ref. 83)*

2.10 Cytotoxicity assays

Cytotoxicity tests are performed by seeding out in 96 wells plates 10^5 cells/ml incubated with Doxorubicin and SCI antibodies as a single treatment or in combination. For the evaluation at 24hrs of cytotoxicity induced by antibodies, Doxorubicin as a single treatment or combination treatment we used, as the first step, Trypan blue exclusion assay, which foresaw the utilization of the Trypan blue dye (0,4% PBS solution, ThermoFisher Scientific-Waltham, MA USA) in a ratio 1:1 with the sample. The evaluation of the percentage of mortality is assessed by dropping a few microliters of Trypan blue/sample mixture in a hemacytometer and, after having counted the number of live and dead cells, it is possible to calculate the percentage of viable or dead cells as follows:

Viable cells(%): (total number of viable cells/total number of cells)*100

Dead cells (%): (total number of dead cells/total number of cells)*100

2.11 Immunoprecipitation assay

The protocol used for this assay foresaw the lysis and quantification of the cell lysate, based on the same protocol used for Western blotting. The lysate was incubated for 1 hour with Protein A/G PLUS-Agarose (SantaCruz Biotechnologies-Dallas, TX, USA), followed by overnight incubation with SCI antibodies. the day after we proceeded with a series of washes with PBS in non-stringent condition (3 washes at 1,600 rpm for ten minutes). The pellet was mixed with sample buffer 1X and an SDS-page protocol was performed.

2.12 Human proteome microarray

For this approach, we used collaboration with the company PEPperPRINT (Heidelberg, Germany) that carried out the experiment according to the following protocol: the antibody profiling of the mouse IgM antibody pool was performed on a HuProt™ Human Proteome Microarray v4.0 (CDI Labs, Puerto Rico) containing over 20,000 individual proteins, representing more than 16,000 human genes. The proteins were expressed in yeast (S. cerevisiae) as GST fusions, purified and spotted in duplicate in 20 array blocks. The HuProt™ Human Proteome Microarray was incubated with mouse IgM antibody pool at a concentration of 1 µg/ml, followed by staining with the secondary antibody and read-out with an Innopsys Microarray Scanner. Grid alignment and image quantification was performed using Mapix 9.1.0 (Innopsys). Subsequent data processing was carried out in R 4.1.2. Here below is a schematic representation of proteome microarray analysis (Fig.12).

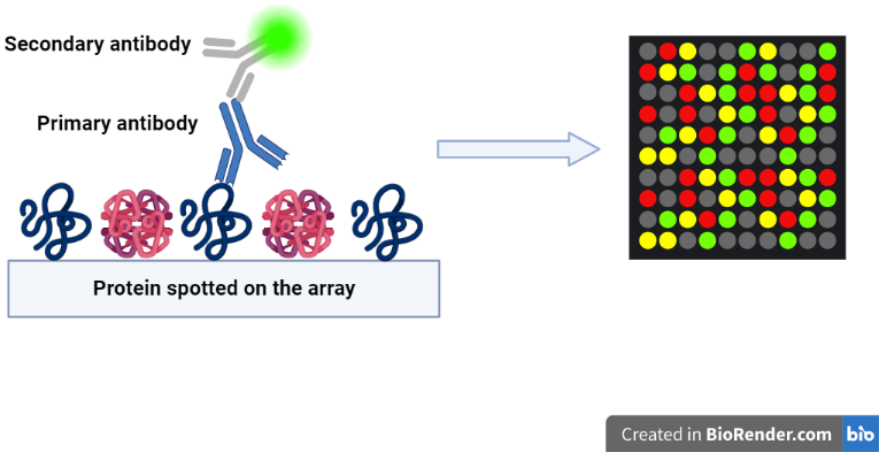

Figure 12. *Schematic overview of proteome microarray approach*

3. RESULTS

3.1 Production and initial screening of mAbs produced against highly glycosylated cell surface components

For the production of mAbs that could specifically react with highly glycosylated cell surface components we arbitrarily chose the follicular lymphoma line Sci-1 (Table 4). Through a specific cell membrane-tagging and enrichment of highly glycosylated cell membrane-associated molecules, conventional immunization of Balb/c mice and spleen fusion, which are at the base of the hybridoma technology, a series of hybridoma clones was generated. These were further screened in ELISA against the cell membrane extract used as immunogen to yield a panel of 25 unique hybridomas clones (hereafter coded anti-Sci mAbs) scoring positively against the immunogen and negatively against streptavidin-biotin complexes used as negative control. The clones were initially cultured in standard serum-containing media, but for effectively pursuing down-stream screens they were in some cases re-conditioned to grow in serum-free culture medium.

Table 4. *Listing of hybridoma clones generated against Sci-1 cell surface components and selected for their reactivity against their original immunogen*

CLONE	ISOTYPES
400A8	IgG_1
400B4	IgG_3, IgM
400D4	IgG_1, IgG_{2a}, IgG_{2b}, IgG_3
400F6	IgG_1, IgM
400G12	IgG_1
401B4	IgG_1, IgM
401E3	IgG_1, IgG_{2a}, IgG_3, IgM
401H11	IgG_1, IgG_{2a}, IgG_{2b}, IgG_3, IgM, IgA
401H2	IgM
402D6	IgG_1, IgM
402F1	IgG_1, IgM
402F12	IgG_{2a}, IgG_{2b}, IgG_3, IgM, IgA
402F6	IgG_1, IgM
402F7	IgG_1, IgM
402F8	IgG_1, IgM
402H6	IgM

403E11	IgG_3, IgM
404H6	IgG_1, IgG_{2a}, IgG_{2b}, IgG_3, IgM
405H6	IgG_1, IgG_{2b}, IgG_3
406A9	IgG_1, IgM
406H2	IgG_3, IgM
406H7	IgG_{2a}, IgG_{2b}, IgM, IgA
408F1	IgG_1, IgG_{2b}, IgM
408F2	IgG_1, IgM
408H7	IgG_{2a}, IgG_{2b}

As expected, a first isotyping of these virgin clones showed a marked heterogeneity in the hybridoma cell populations contained by each clone, with reference to the produced immunoglobulin type (Table 4). As a first step, we then performed flow cytometric analyses of the reactivity patterns of these unseparated clones using the model Sci-1 cells. These assays were initially intended to determine which of the hybridoma clones produced antibodies recognizing surface-exposed antigens, i.e., external membrane components fully accessible to antibody binding in their native form. The tests segregated a subpanel of 14 hybridoma clones that showed a significant surface reactivity with the Sci-1 cells. As the possibility remained that some of the antibodies could recognize antigens that in their natural membrane configuration on Sci-1 cells could be masked and/or poorly accessible to "exogenously added" reagents, antibodies contained by hybridoma clones scoring negatively were further assayed on a selected set of neoplastic cell lines. No surface binding was observed and therefore this screening is still ongoing to ascertain, in a more definitive way, their true lack of reactivity with native membrane-bound components.

We next performed an additional verification of the subset antibodies selected by flow cytometry to determine which of these mAbs could possibly recognize antigens that could be deemed to be highly specific for cancer cells, i.e., not recognize any of the healthy mononucleated cells normally found circulating in peripheral blood (PBMC). The flow cytometric tests disclosed the coincident reactivity of mAbs derived from four of the hybridoma clones with healthy cells (Table 5; Figure 12) and therefore these discrete clones were not further considered for subsequent analyses on neoplastic cells.

Table 5. *Reactivity patterns of anti-Sci mAbs on healthy PBMC as determined by flow cytometry*

mAbs					
	Donor#1	Donor#2	Donor#3	Donor#4	Donor#5
400A8	<10%	<10%	<10%	<10%	<10%
400B4	<10%	<10%	<10%	<10%	<10%
400D4	<10%	<10%	<10%	<10%	<10%
400F6	<10%	<10%	<10%	<10%	<10%
400G12	41,1%	Not Tested	Not Tested	Not Tested	Not Tested
401B4	49,2%	Not Tested	Not Tested	Not Tested	Not Tested
401E 3	<10%	<10%	<10%	<10%	<10%
401H11	<10%	<10%	<10%	<10%	<10%
401H2	<10%	<10%	<10%	<10%	<10%
402D6	<10%	<10%	15.18%	<10%	<10%
402F1	<10%	<10%	<10%	<10%	<10%
402F12	<10%	<10%	<10%	<10%	<10%
402F6	Not Tested	98%	Not Tested	Not Tested	Not Tested
402F7	<10%	<10%	<10%	<10%	<10%
402F8	<10%	<10%	<10%	<10%	<10%
402H6	<10%	<10%	<10%	<10%	<10%
403E 11	<10%	<10%	<10%	<10%	19.21%
404H6	<10%	<10%	<10%	<10%	<10%
405F9	<10%	<10%	<10%	<10%	<10%
405H6	<10%	<10%	<10%	<10%	<10%
406A9	87,1%	Not Tested	Not Tested	Not Tested	Not Tested
406H2	<10%	<10%	<10%	<10%	<10%
406H7	<10%	<10%	<10%	<10%	<10%
408F1	<10%	<10%	<10%	<10%	<10%
408F2	<10%	<10%	<10%	<10%	<10%
408H7	<10%	<10%	<10%	<10%	<10%

Expression of antigens recognized by the antibodies from the selected clones was comprehensively found on a total of 72 cell lines, out of the 100 lines comprehensively tested, and ranged from 10% to over 99% positivity. Cell lines scoring positively for antibody reactivity represented the following hematological malignancies: 33 non-Hodgkin's lymphomas (NHL), 5 Hodgkin's lymphomas (HL), 10 Burkitt's lymphoma (BL), 17 acute lymphoblastic leukemia (B-ALL), 11 acute myeloid leukemia (AML), 5 chronic myeloid leukemia (CML), and 3 chronic B-cell leukemia (B-CLL) cell lines (Figure 15). The cell lines recognized by only one antibody were 12, while 20 antibodies bound to cell surface components on different cell lines, corresponding to different hematologic diseases. A comprehensive representation the disease/cell line distribution of the recognized antigens is depicted

in the heat-map illustrated in Figure 14. Comprehensively, it could be deduced that the antibodies did not specifically recognize antigens proper of one single hematologic malignancy, but that they were shared by different disease entities.

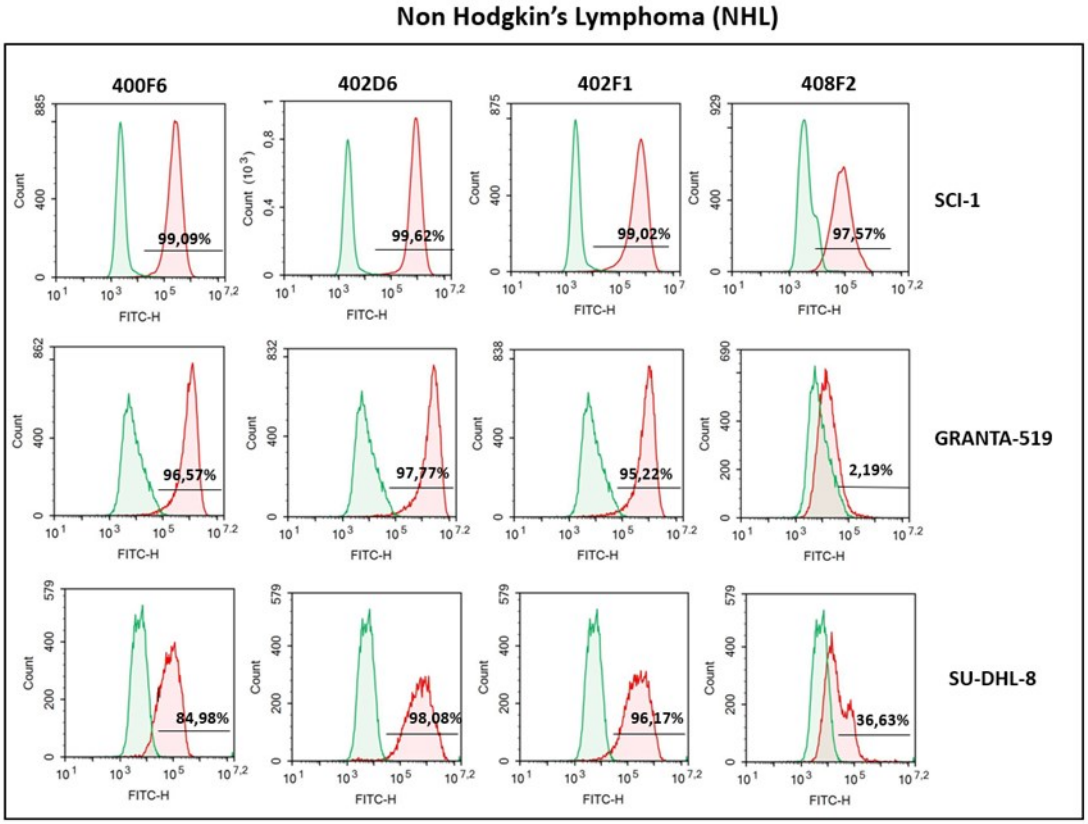

Non Hodgkin's Lymphoma (NHL)

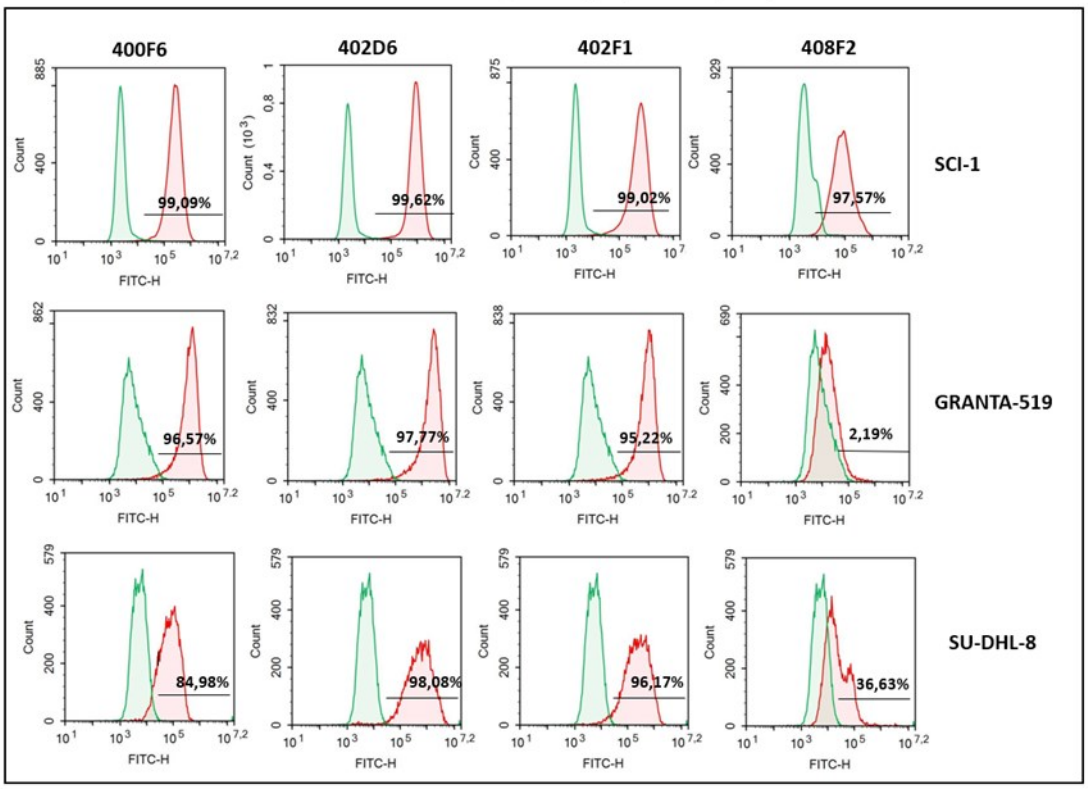

Chronic lymphoblastic leukemia (CLL)

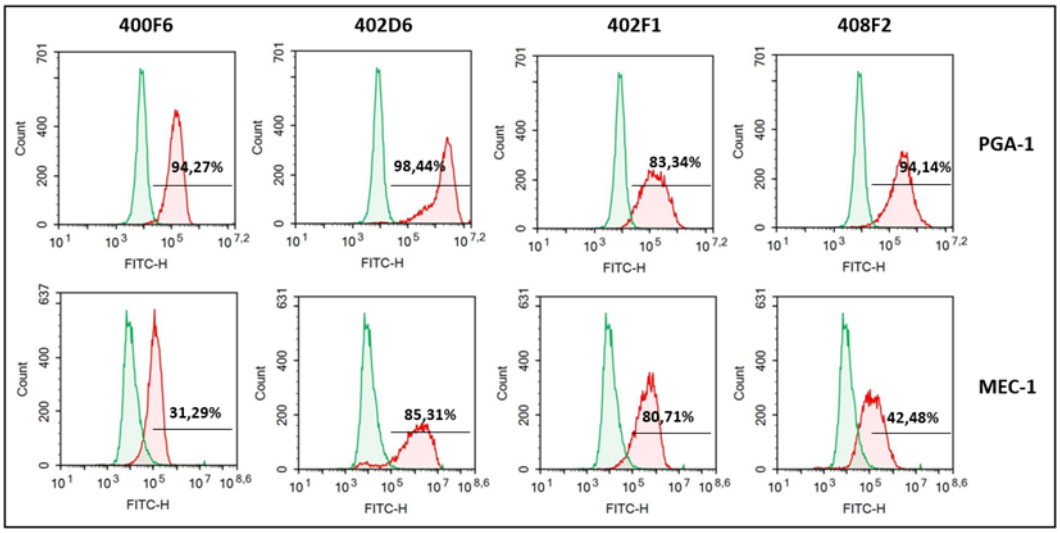

B and T cell acute lymphoblastic leukemia (B-ALL and T-ALL)

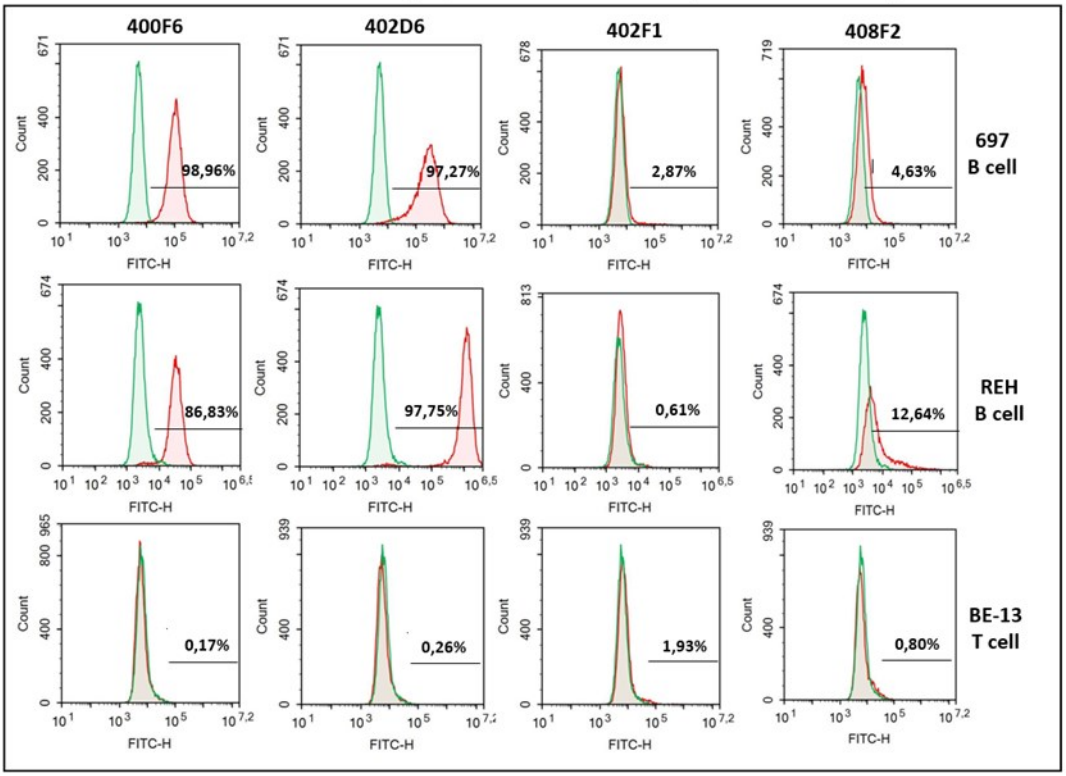

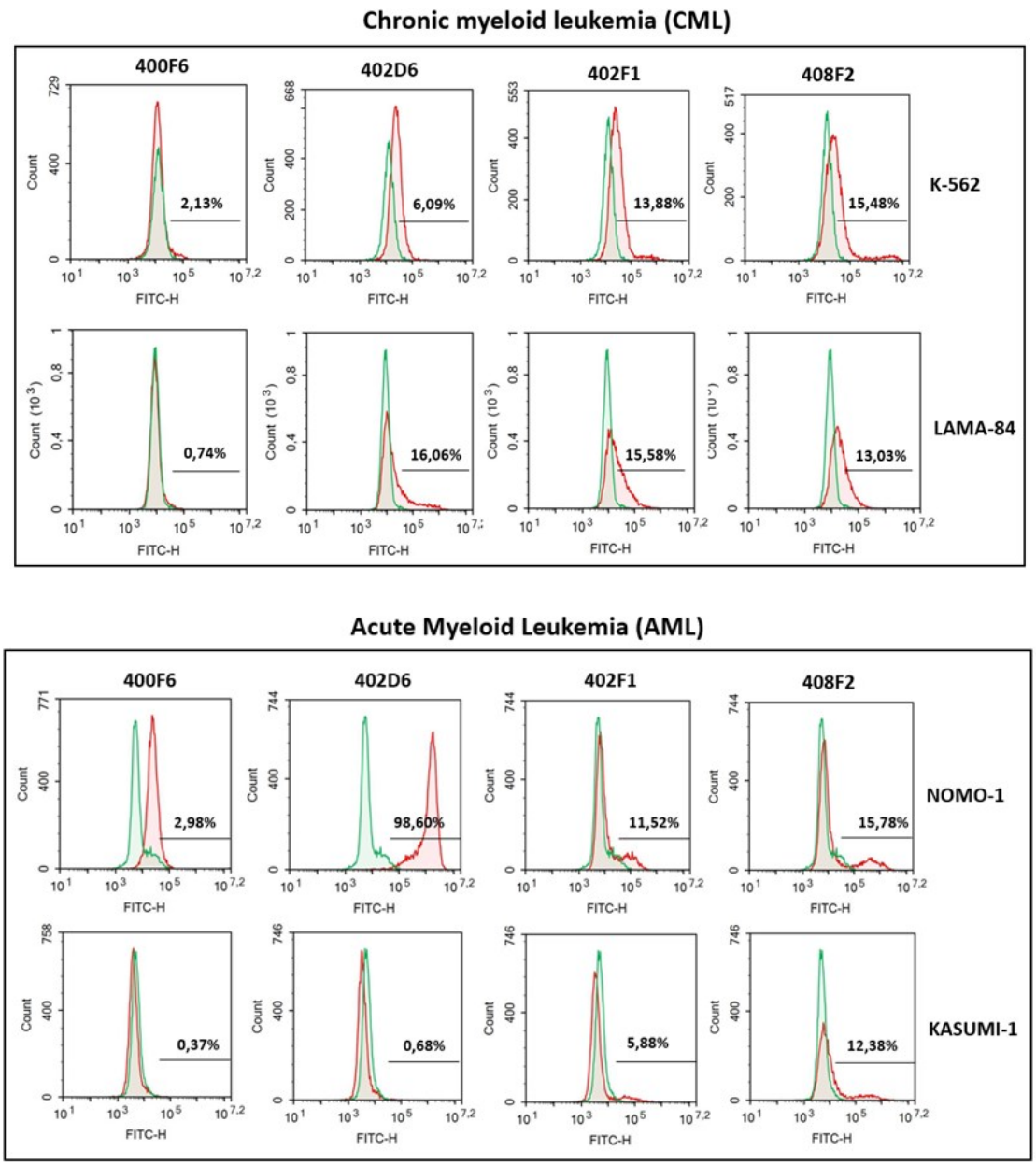

Figure 13. *Representative disease-specific expression profiles of cell surface antigens recognized by the lead anti-Sci-mAbs 400F6, 402D6, 402F1, and 408F2 on the indicated discrete cell lines.*

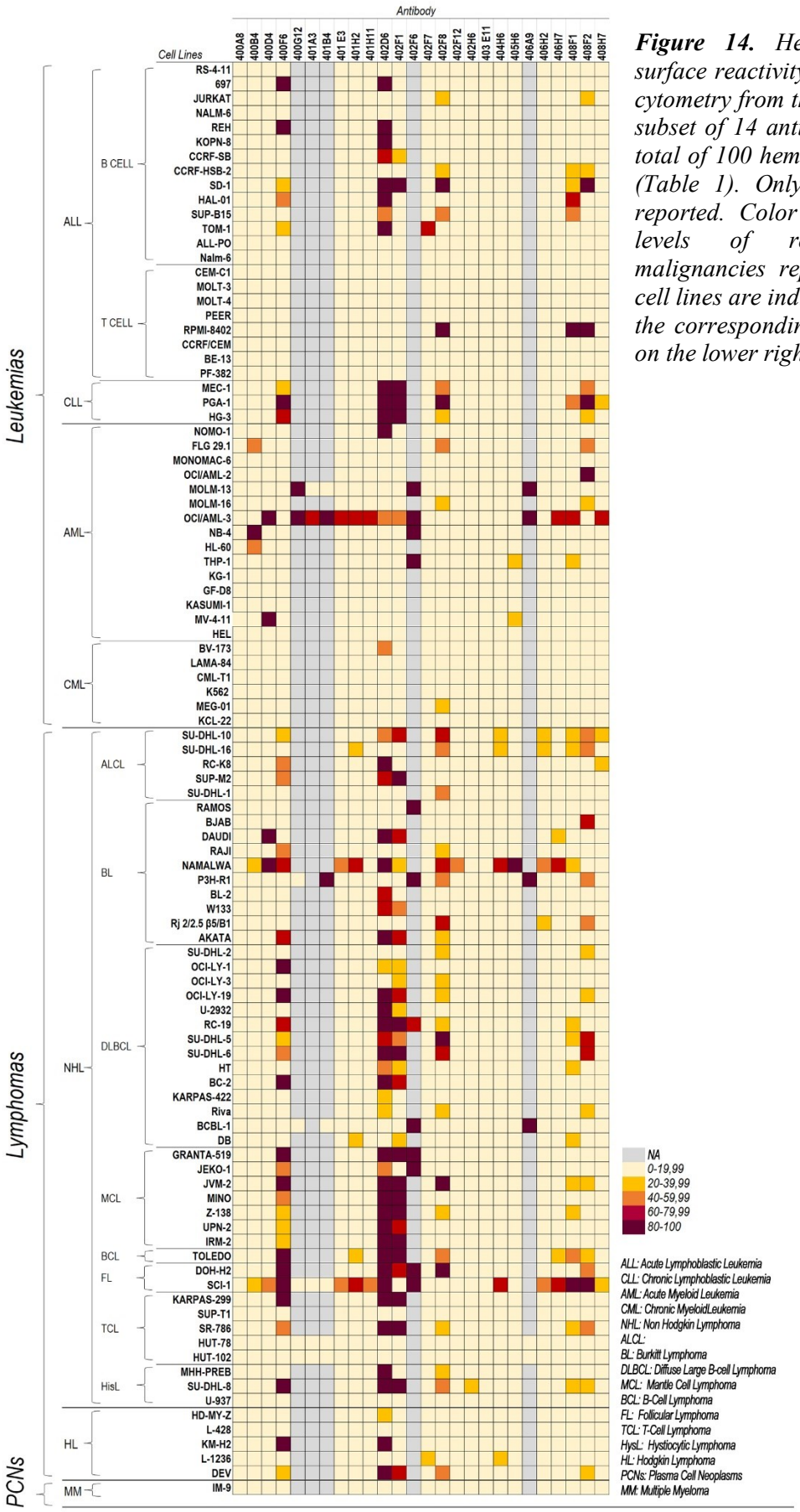

Figure 14. *Heat-map summarizing the surface reactivity patterns obtained by flow cytometry from the screening of the selected subset of 14 anti-Sci mAbs performed on a total of 100 hematopoietic cancer cell lines (Table 1). Only positivity above 10% is reported. Color coding refers to relative levels of reactivities. Hematologic malignancies represented by the different cell lines are indicated on the left, alongside the corresponding abbreviations indicated. on the lower right.*

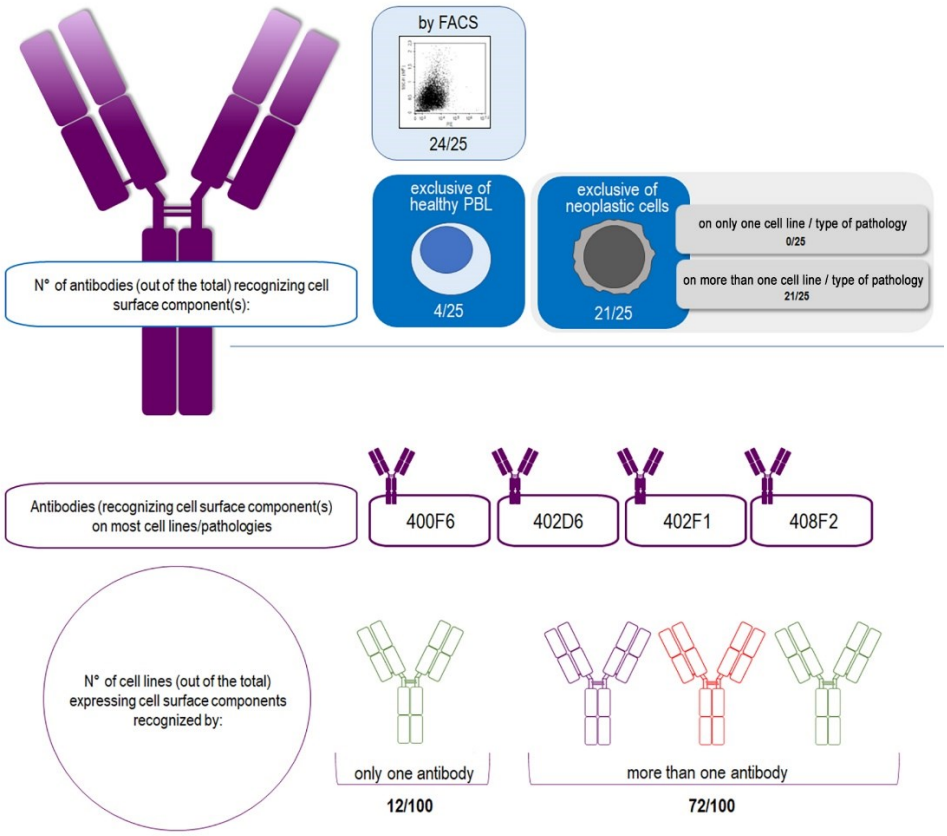

Figure 15. *Overview of the disease/cell line relationships of the reactivity patterns displayed by the anti-SCI mAbs*

3.2 Subcellular membrane localization of antigens recognized by the lead anti-Sci-mAbs

Surface localization of the antigens recognized by the lead anti-Sci-mAbs was asserted by immunolabelling of whole cells. For this purpose, we used a selected number of cell lines which included Sci-1 cells as reference and BE-13 cells as a negative control due to their lack of significant positivity for any of the antibodies in flow cytometry. The overall staining pattern and intensity was aligned with the signals detected by flow cytometry on the same cells, with the labeling appearing strongly circumscribed to the outer cell membrane. However, some primary differences in the subcellular distribution of the antigens recognized by the different antibodies in the different cell types could be noted (Figure 16). For instance, on the leukemic cell line PGA-1, anti-Sci-mAbs 402D6 and 400F6 yielded a homogenous and intense labelling confined to the cell surface, and the same subcellular labeling could be observed for anti-Sci-mAbs 402F1 and 400F6 in the lymphoma cell line GRANTA-519. On Sci-1 and SU-DHL-8 cells, the staining pattern was more heterogenous with focal labeling of certain areas of the cell membrane accompanied by some cytoplasmatic staining. Sparse regular staining was noted with the anti-Sci-mAb 408F2 on the BE-13 control cell line, suggesting that these cells may express low levels of the antigens recognized by this antibody

and that these antigens are heterogeneously distributed within the cell population being present only on subsets of the cells and therefore below the detection levels by flow cytometry.

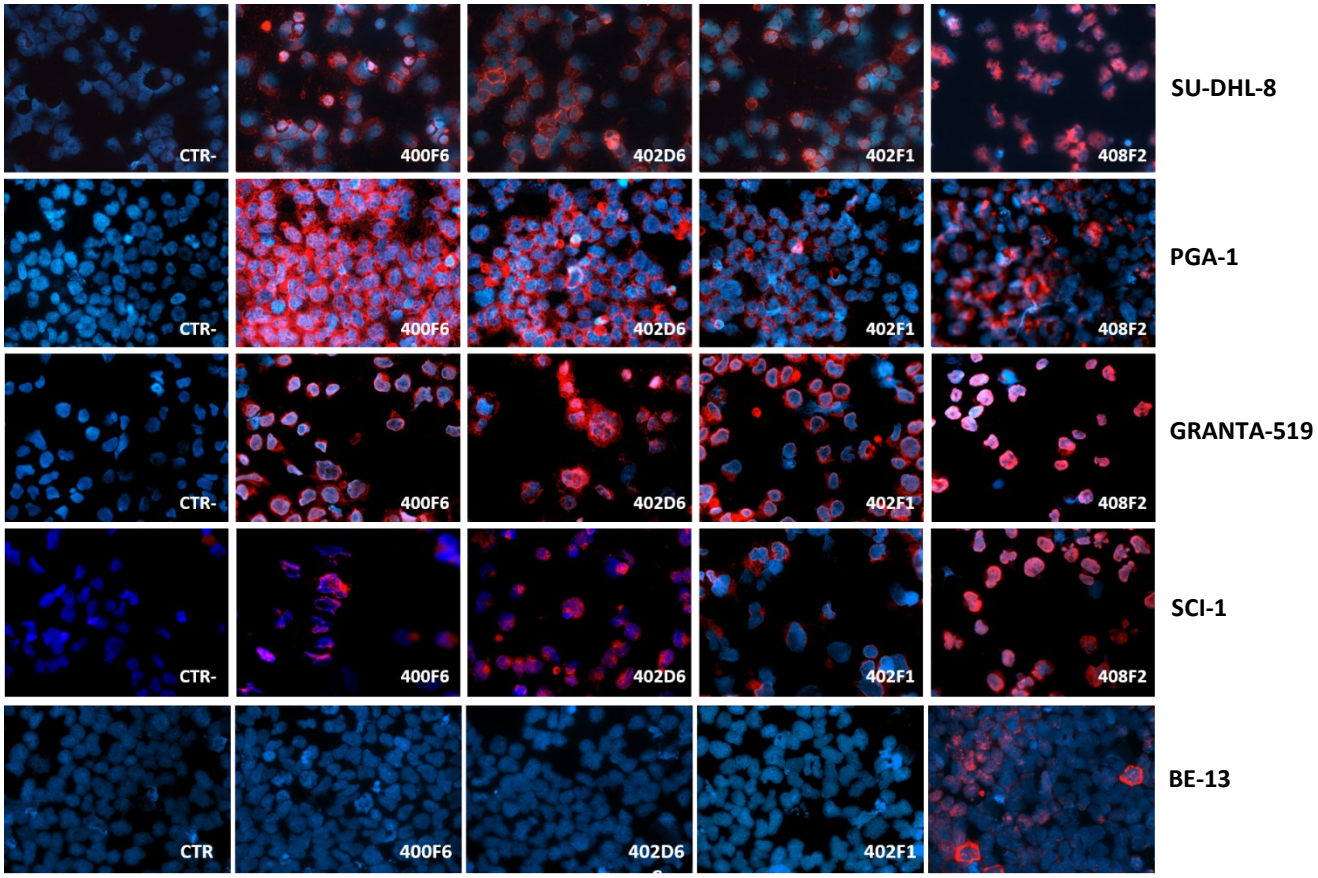

***Figure 16**. Representative immunolabelling on the indicated cell lines observed with the lead anti-Sci-mAbs 400F6, 402D6, 402F1 and 408F2 as revealed by fluorescence microscopy. Nuclei were counterstained with Hoechst. Magnification, 600x.*

3.3 Antibody 402D6 may recognize an antigen(s) expressed by healthy hematopoietic CD34$^+$ stem cells

To investigate whether the lead anti-Sci-mAbs recognized hematopoietic antigen(s) not present or sufficiently abundant in peripheral blood of healthy donor, antibody 402D6 was assayed on an apheresis sample from a multiple myeloma patient mobilized for autologous bone marrow transplantation. Double staining by flow cytometry of this patient sample using antibody 402D6 and an anti-CD34 antibody revealed a binding rate of 24% for antibody 402D6, 11% for the anti-CD34$^+$ antibody and a coincident labelling rate of 6% for the entire cell population contained in the sample (Fig. 17-c). Co-staining for CD34$^+$ and antibody 402D6 indicated that 63% of the former stem cells may have co-expressed the antigen(s) recognized by antibody 402D6 (Fig. 17-d). Verification of the reproducibility of this reactive pattern is in progress.

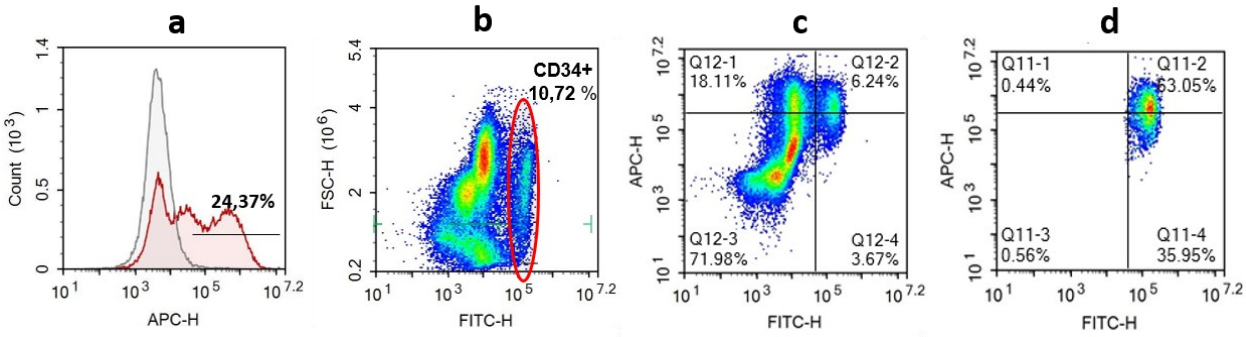

Figure 17. *Double immunolabelling of a peripheral blood sample derived from an immobilized multiple myeloma patient: a) reactivity levels of antibody 402D6 (red, while grey corresponds to the secondary antibody control);* ***b)*** *identification of the CD34$^+$ cell population (red circle) in total cell population of the specimen as permitted by the use of an anti-CD34 antibody (green);* ***c)*** *co-localized staining of antibodies 402D6 and anti-CD34;* ***d)*** *co-localized labeling of antibodies 402D6 and anti-CD34 on the specifically gated CD34$^+$ hematopoietic stem cell population*

3.4 Mabs directed against the cartilage PG aggrecan cross-react with highly glycated components of the malignant hematopoietic cell surface

To assert whether mAbs reacting with the cartilage PG aggrecan could cross-react with highly glycated components of the neoplastic lymphocytes' cell surface, as previously proposed for similar antibodies tested against lymphomas (88), we took advantage of a unique set of mAbs (anti-HAG antibodies) previously produced against this PG (83). Seventeen of the close to 30 mAbs that were originally generated were assayed in this study by flow cytometry on 12 hematopoietic cancer cell lines including 5 lymphoma and 7 leukemic lines. A complex pattern of phenotype and antibody-selective reactivity could be unfolded (Figure 18), which, however, was not further investigated in this study. Thus, the identity of the identified components (which cannot include aggrecan itself as it not transcribed by lymphoma or leukemic cells) remains to be established, alongside the potential of the antibodies to affect vital cellular processes upon binding to their corresponding antigens.

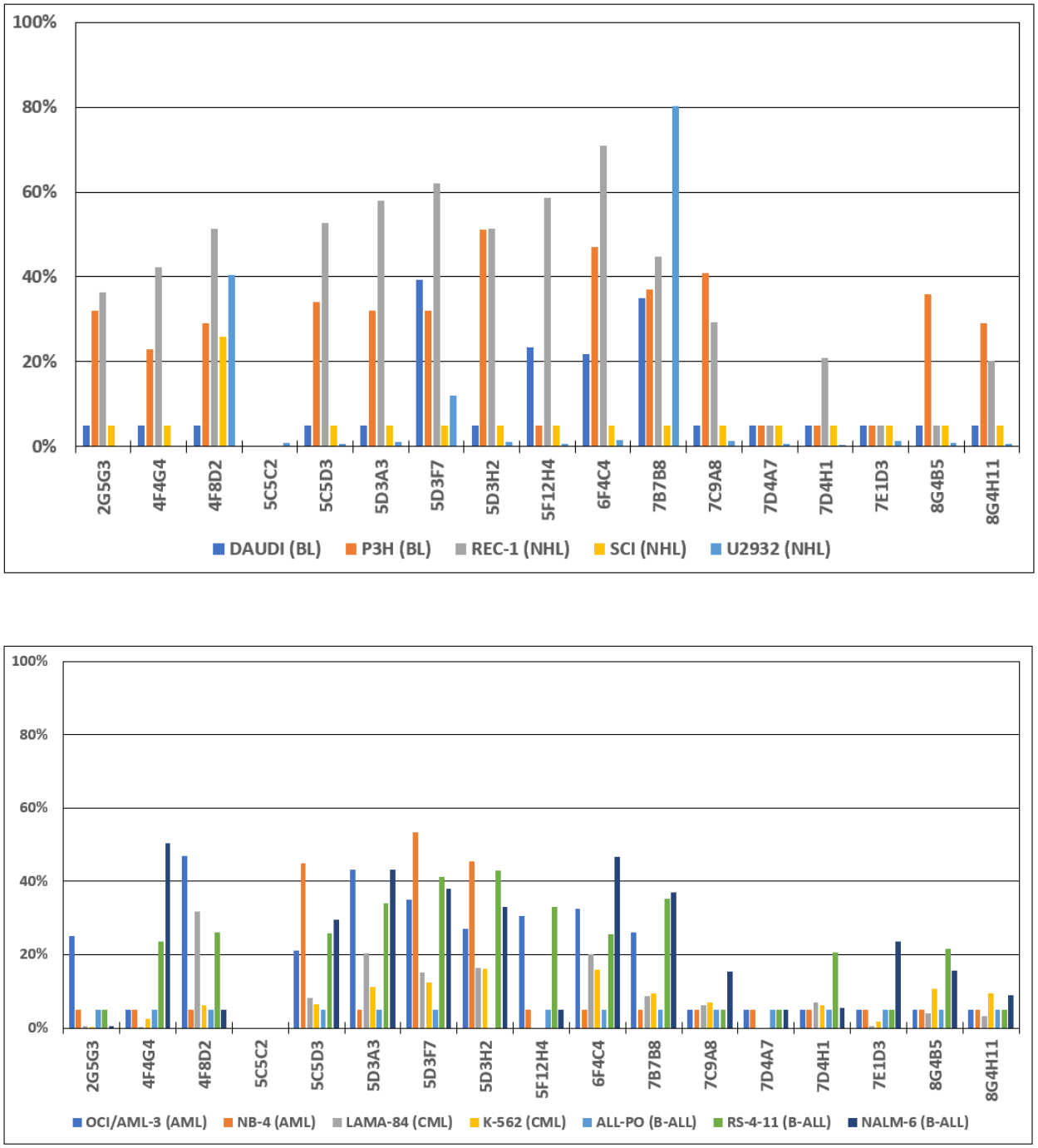

Figure 18. *Binding patterns of anti-aggrecan mAbs (anti-HAG antibodies) on lymphoma and leukemia cell lines as determined by flow cytometry*

3.5 Antibodies Sci-mAbs 402D6, 402F1 and 408F2 recognize high molecular weight and highly glycosylated surface components.

We performed preliminary immunoblotting analyses in the attempt to achieve a first indication on the nature of cell surface components recognized by the Sci mAbs. This was pursued using whole-cell extracts from a set of cell lines scoring highly positively in flow cytometry and using a negative cell line as control. These tests revealed that all three antibodies that were able to react with the cognate

antigens following resolution by SDS-PAGE reacted preferentially with high molecular weight protein complexes harboring a substantial degree of glycosylation (Figure 19). Overall, the banding pattern observed for the different cell lines was rather consistent, with only apparent quantitative differences between the test cell lines and a possible minor variation observed for anti-Sci-mAb 408F2 on Sci-1 cells when compared to GRANTA-519 and SU-DHL-8 cells. The predominant bands were observed at apparent molecular weight superseding 200 kDa and in most cases running significantly above 250 kDa (Figure 19). Accordingly, the same blotting performed on the whole cell extracts run on SDS-PAGE under non-reducing conditions did not yield appreciable banding patterns due to the difficulty of the recognized macromolecular complexes to enter the 4% stacking of them gels (not shown). Single bands running between 90 and 170 kDa were detectable with Sci-mAbs 402D6 and 402F1 and one possibility could be that these lower molecular weight bands may have represented degradation products of larger macromolecules. Based on these preliminary findings, it can be deduced that Sci mAb 402D6 may no be particularly suitable for detection of the cognate antigens in Western blotting.

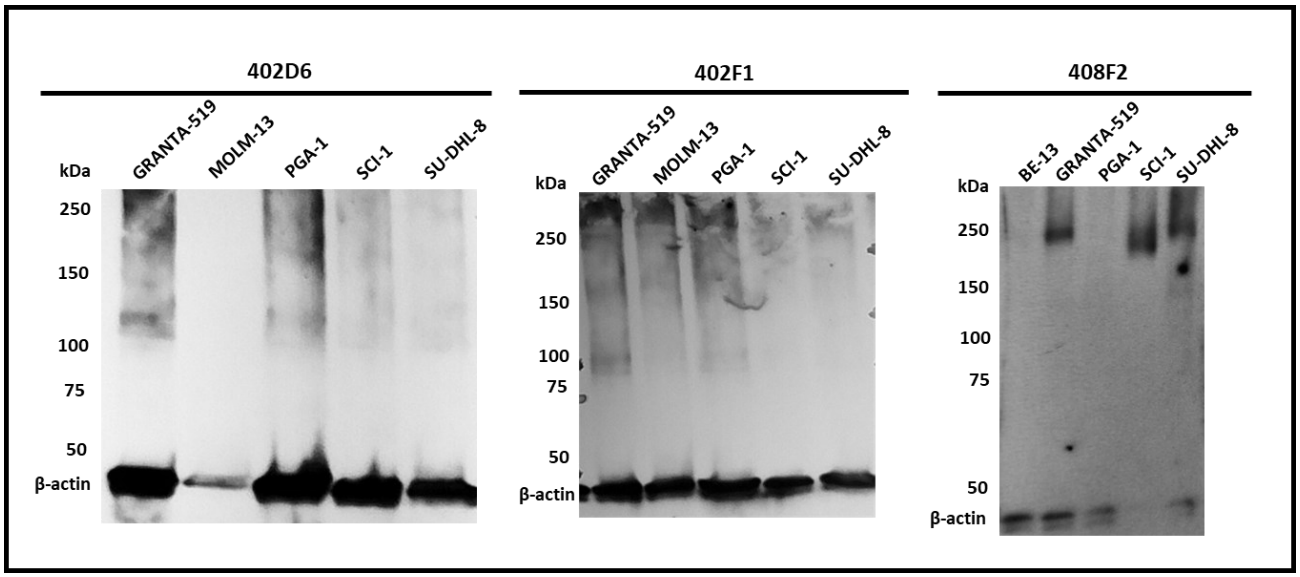

Figure 19. *Immunoblotting analyses performed with antibodies Sci-mAbs 402D6, 402F1 and 408F2 on a set of positively scoring cancer cell lines*

3.6 Antigen identification through screening of protein microarrays

A first attempt made through a canonical approach involving immunoprecipitation of the plasma membrane associated antigens by the lead anti-Sci-mAbs, followed by straightforward shot-gun label-free mass spectrometric peptide identification of the immunoprecipitated molecules did not yield conclusive information about the searched antigens. Therefore, efforts are ongoing to refine the sample preparation procedures and the protocol/strategy for the accomplishing more stringent pull-

downs. Meanwhile, we undertook an alternative approach based on screening of protein microarrays composed of over 20,000 recombinant human proteins using fluorescent detection methods. The screens were outsourced to the German company PEPperPRINT GmbH (Heidelberg) and have thus far been focused on Sci-mAbs 402D6 and 402F1. The two antibodies were simultaneously incubated with the HuProt™ Human Proteome Microarray, followed detection of the spot-bound primary antibody through incubation with a secondary antibody and image analysis through dedicated softwares tools. Surprisingly, top hits were found to correspond to proteins not known to be stably present on the cell surface, with the exception of nectin cell adhesion molecule 3 (Figure 20) and may therefore represent cases of non-specific reactions of the antibodies with glass-spotted recombinant proteins. Intriguingly, however, the most intensely stained protein spot was disclosed to correspond to stress-induced phosphoprotein 1 (STIP1), reported to be an unfavorable prognostic marker for several cancer types and previously found to be associated with the cell membrane. Further investigations are ongoing to assert whether STIP1 is present on cells scoring positively for the antibodies and to confirm the putative recognition of this molecule by the two antibodies.

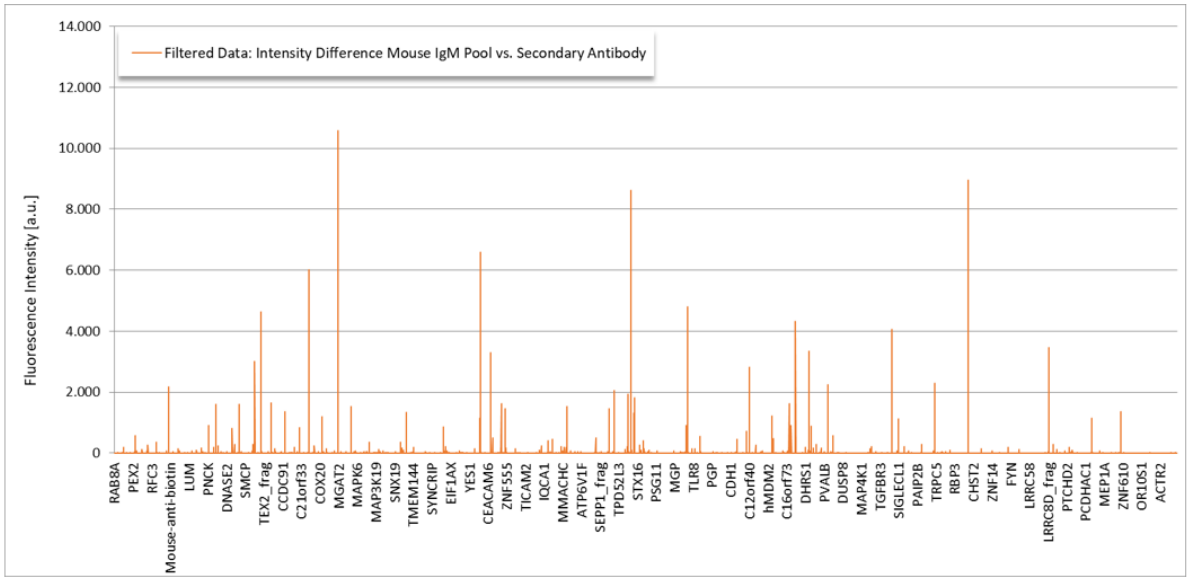

Name	UniProt ID	Ensembl ID	JHU Clone ID	Mouse IgM Pool, 1 µg/ml	Secondary Antibody	Intensity Difference	Corr. Intensity Ratio
STIP1	P31948	ENSP00000443416	JHU05076.B4C3R83	10.600,5	12,5	10.588,0	212,0
HSD17B4	P51659	ENSP00000426272	JHU18191.B15C5R43	9.001,0	49,0	8.952,0	180,0
STIP1	P31948-2	ENSP00000443416	JHU15461.B9C17R65	8.638,0	26,8	8.611,2	172,8
CTNNB1	P35222	ENSP00000401599	JHU07025.B7C17R21	6.620,8	19,8	6.601,0	132,4
GPBP1_frag			JHU02535.B4C6R37	6.016,5	8,2	6.008,3	120,3
RPSA	P08865	ENSP00000396716	JHU15365.B10C5R61	4.815,2	9,5	4.805,7	96,3
PVRL3_frag			JHU03238.B3C8R53	4.649,2	15,0	4.634,2	93,0
CRNN	Q9UBG3	ENSP00000271835	JHU13904.B12C8R41	4.339,0	14,5	4.324,5	86,8
RPSA	P08865	ENSP00000396716	JHU02089.B14C5R13	4.069,8	13,5	4.056,3	81,4
NUDT22	Q9BRQ3	ENSP00000443127	JHU02170.B16C5R73	3.471,2	5,5	3.465,7	69,4
RPSA	P08865	ENSP00000396716	JHU15365.B12C14R61	3.361,2	16,5	3.344,7	67,2
ATCAY	Q86WG3	ENSP00000470842	JHU08359.B7C31R37	3.302,0	14,0	3.288,0	66,0
CRNN	Q9UBG3	ENSP00000271835	JHU03003.B3C13R43	3.006,0	9,0	2.997,0	60,1
RPSA	P08865	ENSP00000396716	JHU15455.B11C22R61	2.816,2	12,0	2.804,2	56,3
ANXA10	Q9UJ72	ENSP00000483710	JHU04900.B12C29R89	2.262,0	11,0	2.251,0	45,2
FAM131C	Q96AQ9	ENSP00000364814	JHU05680.B1C7R89	2.188,5	14,5	2.174,0	43,8
STUB1	Q9UNE7	ENSP00000476751	JHU14160.B9C7R39	2.069,0	14,5	2.054,5	41,4
PAIP2	Q9BPZ3	ENSP00000422508	JHU15547.B9C16R61	1.951,0	17,2	1.933,8	39,0
TXN	P10599	ENSP00000363641	JHU04603.B3C7R69	1.652,0	10,5	1.641,5	33,0
ARFGAP1	Q8N6T3	ENSP00000443716	JHU13507.B12C14R31	1.647,5	20,0	1.627,5	33,0
APBB1	O00213	ENSP00000374556	JHU09027.B7C19R53	1.639,0	11,5	1.627,5	32,8
UBE2Q2	Q8WVN8	ENSP00000454742	JHU04793.B2C22R73	1.620,0	13,5	1.606,5	32,4
FAM131C	Q96AQ9	ENSP00000364814	JHU00996.B3C6R17	1.608,0	10,5	1.597,5	32,2
TNS1	Q9HBL0-2	ENSP00000480559	JHU06229.B5C5R9	1.540,0	14,0	1.526,0	30,8
PACSIN1	Q9BY11	ENSP00000439639	JHU09374.B8C29R59	1.533,8	14,0	1.519,8	30,7
LBHD1	Q9BQE6-2	ENSP00000437582	JHU09320.B7C8R59	1.484,5	26,0	1.458,5	29,7
AAMP	Q13685	ENSP00000393818	JHU13499.B9C17R31	1.467,8	10,0	1.457,8	29,4
COL23A1	Q86Y22-2		JHU09332.B7C14R59	1.458,0	27,2	1.430,8	29,2
ARFGAP1	Q8N6T3-2	ENSP00000443716	JHU05382.B3C23R89	1.363,5	15,0	1.348,5	27,3
PANK1	Q8TE04	ENSP00000302108	JHU24640.B19C13R3	1.356,0	6,5	1.349,5	27,1
RPSA	P08865	ENSP00000396716	JHU05929.B6C17R1	1.355,0	10,8	1.344,2	27,1
ING3	Q9NXR8-3	ENSP00000388506	JHU11705.B12C17R5	1.227,0	11,8	1.215,2	24,5
KCNRG	Q8N5I3	ENSP00000324191	JHU03698.B4C16R57	1.191,2	8,8	1.182,4	23,8
UBE2O			JHU07002.B7C2R21	1.165,8	11,5	1.154,3	23,3
UBE2Q1	Q7Z7E8	ENSP00000292211	JHU25696.B18C24R1	1.164,5	11,5	1.153,0	23,3

Figure 20. *Fluorescence intensity ranking of the microarray molecules recognized by anti-Sci-mAbs 402D6 and 402F1*

3.7 Anti-Sci-mAbs 400F6 and 402D6 induce cell-cell aggregation

As the primary aim of this work was to generate antibodies exhibiting an anti-neoplastic effect on cancer cells, we approached a first assaying of such potential by incubating cells in the presence of the antibodies. This screening was initiated with the anti-Sci-mAbs. When we incubated the positively scoring cell lines PGA-1 and SU-DHL-8 and the largely negative NALM-6 and BE-13 cells with the anti-Sci-mAbs, we observed that antibodies 400F6 and 402D6 (but not the other two lead anti-Sci-mAbs) induced aggregation of the PGA-1 and SU-DHL-8 cells, which tended to cluster in spheroid-like configurations. Conversely, the NALM-6 and BE-1 cells failing to be recognized by these

antibodies remained as single cells (Figure 21). Induction of cell aggregation was observed within 24 hrs in continuous presence of the antibodies, added directly to the culture medium, increased by 48 hrs and remained constant thereafter.

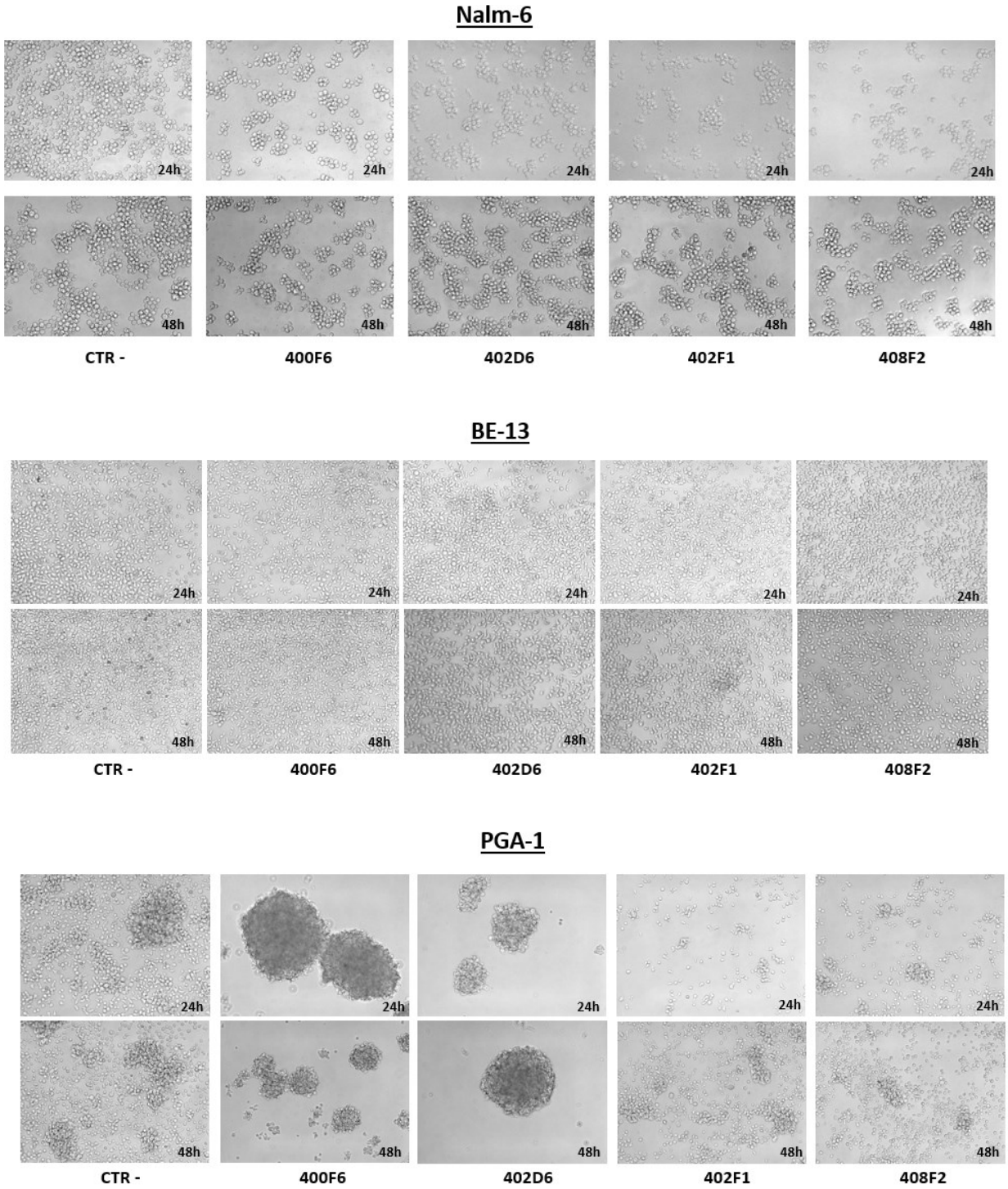

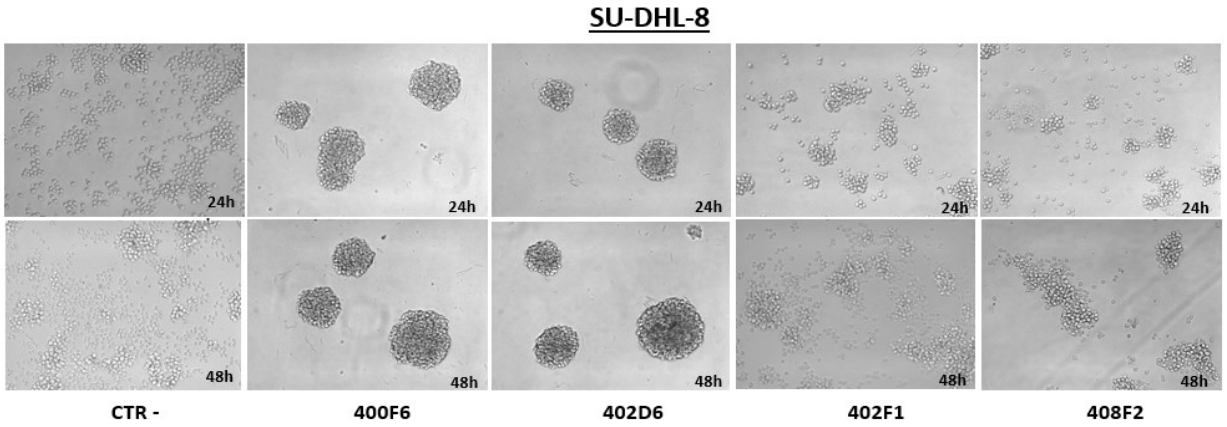

Figure 21. *Phase-contrast images showing induction of the cell-cell aggregation induced by anti-Sci-mAbs 400F6 and 402D6 in cell lines PGA-1 and SU-DHL-8 presenting the cognate antigens, but not in NALM-6 and BE-13 cells used as reference/control*

3.8 Effects of anti-Sci-mAbs on cell proliferation and cell survival

We next assayed whether the antibodies affected some of the more vital processes of the cells and therefore evaluated the effects of the antibodies on the proliferation rates of non-synchronized cells at three-time points, i.e., 24, 48, and 72 hrs, when initially exposed to the antibodies. For this type of experiment, we chose four test cell lines (and a control one), each corresponding to a different hematological disease, but having in common the exhibition of a strong surface reactivity for the antibodies. The first pilot tests highlighted a marked inhibitory effect on the proliferation of SU-DHL-8 cells exerted by all four antibodies and a specific effect of the anti-Sci-mAb 402D6 on the proliferation of the other cell lines (albeit to apparently different extents; Figure 22). Further time-dependent analysis of this effect by precise cell counting confirmed the temporal blockade of cell proliferation by the lead antibodies anti-Sci-mAbs 402D6 and 400F6, and to a certain extent mAb 402F1 (but not mAb 408F2) on several of the cell lines (Figure 23). Time-dependency tests demonstrated the strongest overall effect of the antibodies on Sci-1 cells.

Since the utilization of the Alamar Blue kit for assessment of cell proliferation may also be used for monitoring cell survival, we observed that antibody 402D6 also affected survival in all test cell lines, but not in the control/reference ones, while antibody 400F6 induced significant cell toxicity in SU-DHL-8 cells (Figure 22). The maximum cytotoxic effect of the antibodies was observed already after 24 hrs of antibody treatment and remained constant for the subsequent 48 hrs.

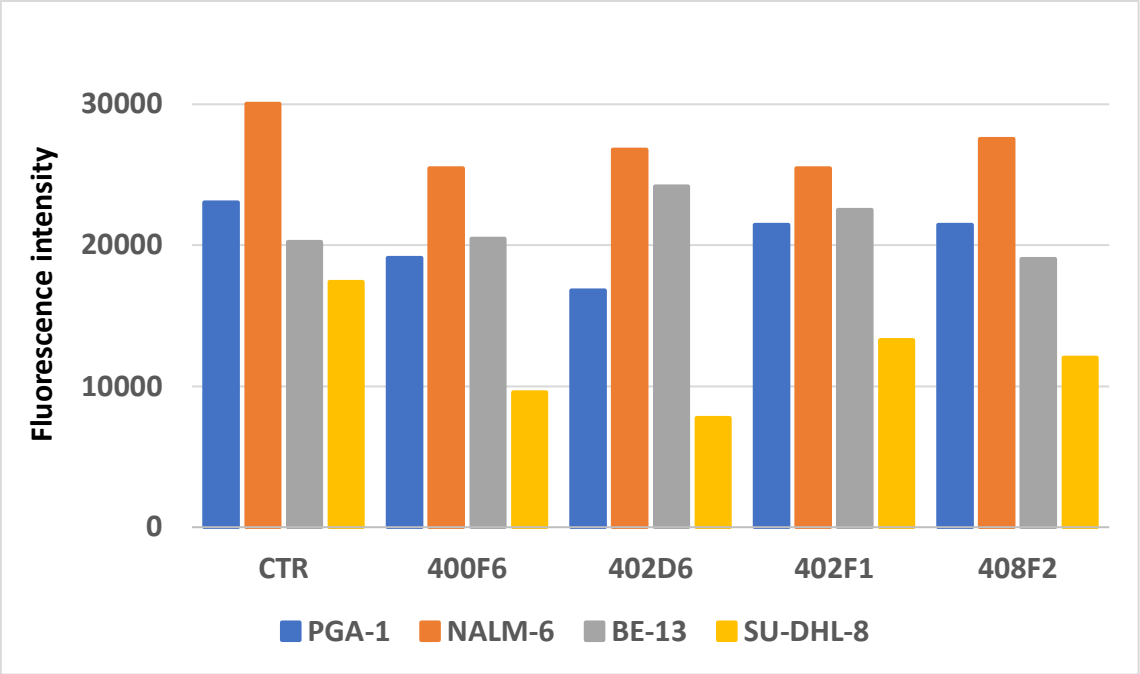

Figure 22. *Effects on cell proliferation induced by lead anti-Sci-mAb antibodies on four model cell lines expressing high surface levels of the cognate antigens*

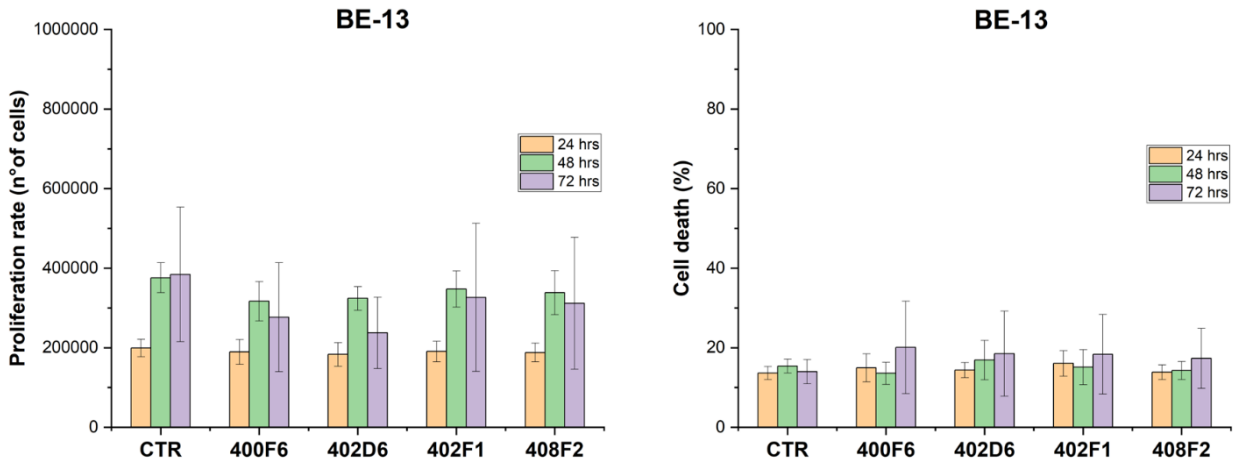

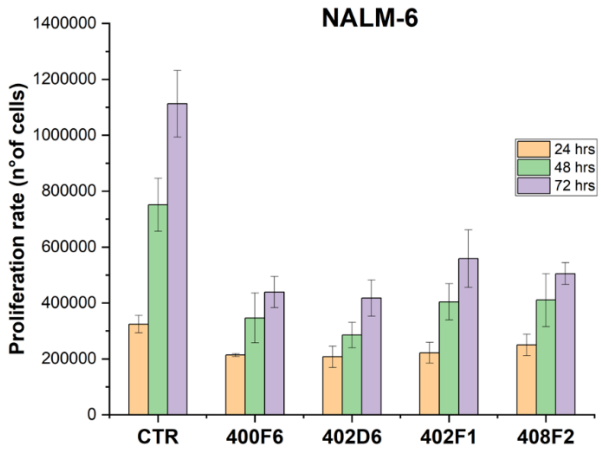
NALM-6
Proliferation rate (n°of cells)
1400000
1200000
1000000
800000
600000
400000
200000
0
24 hrs
48 hrs
72 hrs
CTR
400F6
402D6
402F1
408F2

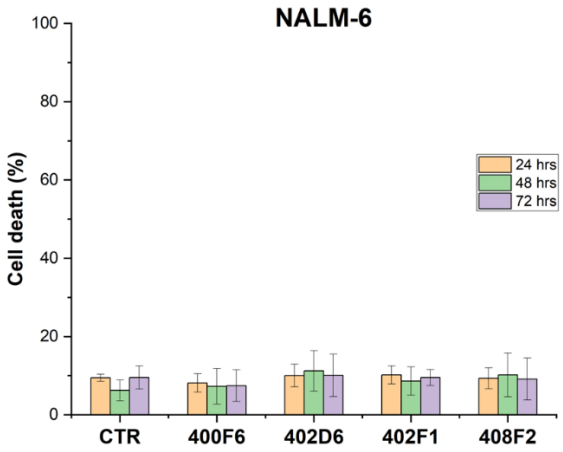
NALM-6
Cell death (%)
100
80
60
40
20
0
24 hrs
48 hrs
72 hrs
CTR
400F6
402D6
402F1
408F2

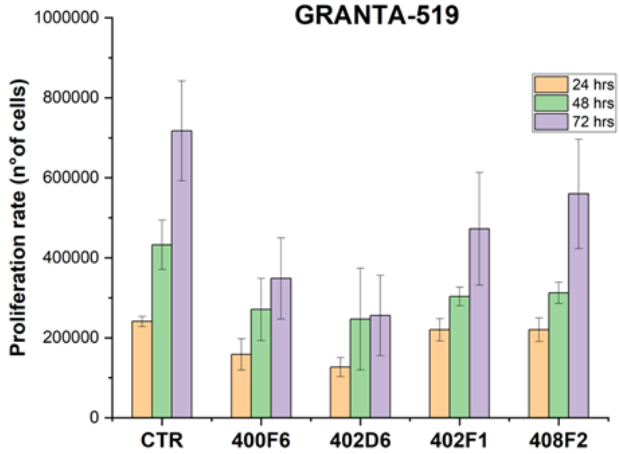
GRANTA-519
Proliferation rate (n°of cells)
1000000
800000
600000
400000
200000
0
24 hrs
48 hrs
72 hrs
CTR
400F6
402D6
402F1
408F2

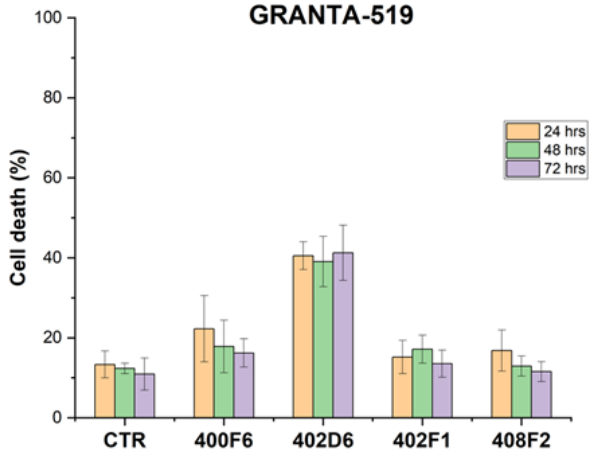
GRANTA-519
Cell death (%)
100
80
60
40
20
0
24 hrs
48 hrs
72 hrs
CTR
400F6
402D6
402F1
408F2

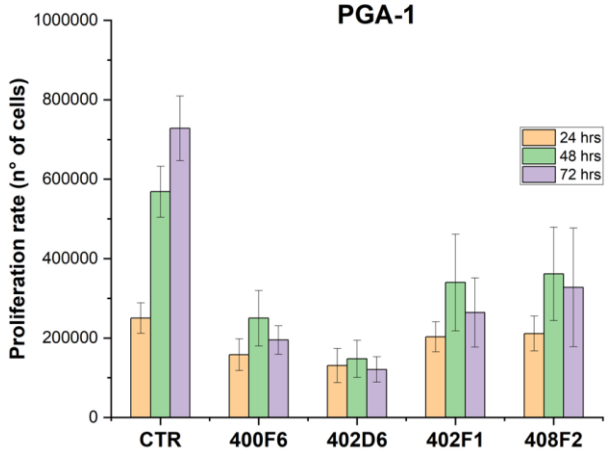
PGA-1
Proliferation rate (n° of cells)
1000000
800000
600000
400000
200000
0
24 hrs
48 hrs
72 hrs
CTR
400F6
402D6
402F1
408F2

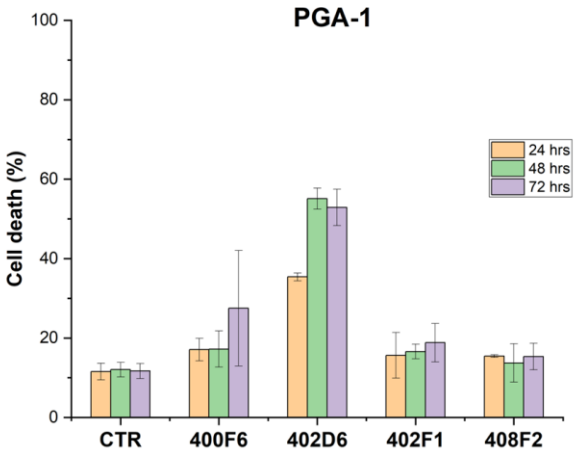
PGA-1
Cell death (%)
100
80
60
40
20
0
24 hrs
48 hrs
72 hrs
CTR
400F6
402D6
402F1
408F2

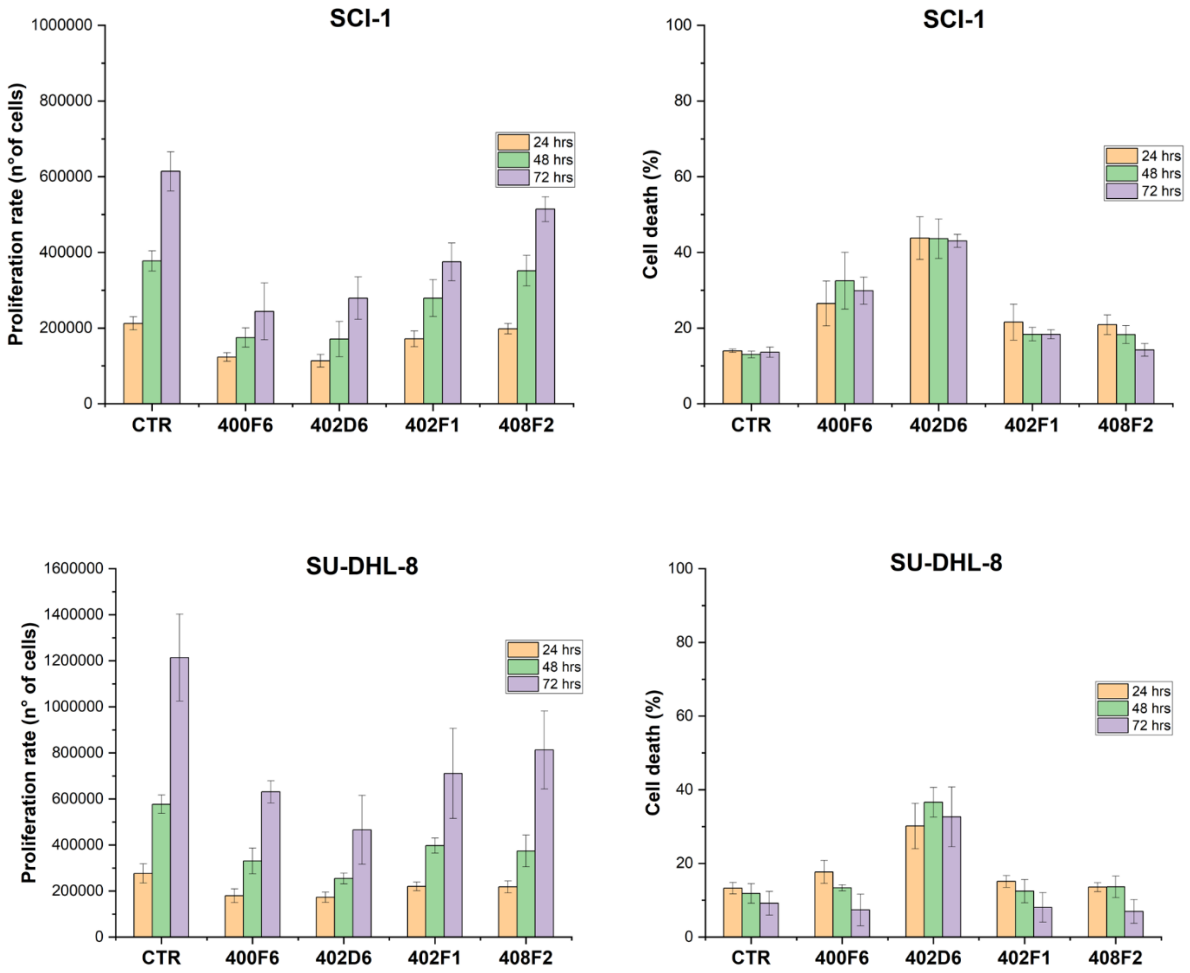

Figure 23. *Time-dependent effects of the lead anti-Sci-mAbs on cell proliferation and survival on four model cell lines expressing high surface levels of the cognate antigens*

To then confirm the potential cytotoxic effect of antibodies 400F6 and 402D6, we performed a first evaluation of the upregulation of the standard putative markers for regulated cell death and cell membrane permeabilization (i.e., annexin V-surface binding/propidium iodide – PI - intracellular accumulation) in asynchronized cells exposed to the antibodies. After 48 hrs of treatment with anti-Sci-mAb 402D6 a substantial level of cell death was noted in SU-DHL-8 and PGA-1 cells, but not in the reference cell line Nalm-6 failing to be recognized by the antibodies in flow cytometry (Figure 24). Although the cellular and molecular mechanisms underlying the antibody-induced effect on cell survival remains to be established, preliminary evidence suggests that the induced cell death may not be fully caspase-dependent.

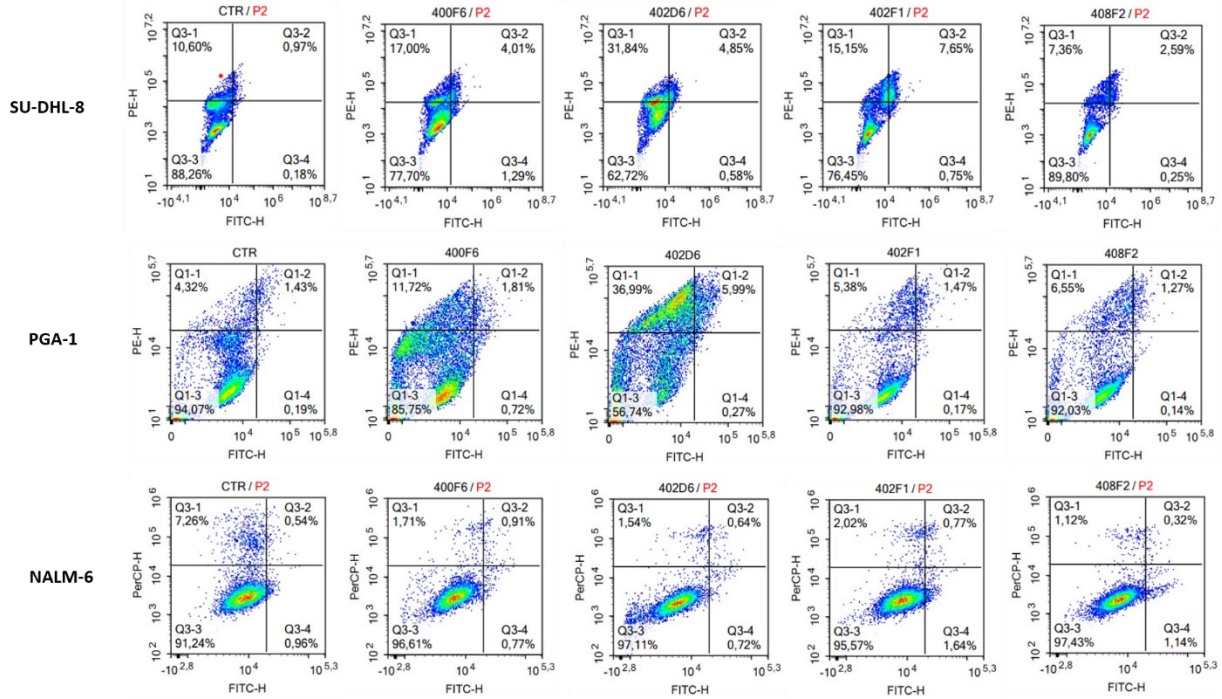

Figure. 24. *Representative annexin V-surface binding/PI incorporation in SU-DHL-8 and PGA-1 cells showing a putative apoptotic/necrotic cell death after 48 hrs of continuous incubation with antibody 402D6. No surface display/incorporation was observed in the control NALM-6 cells*

3.9 Antibody Sci-mAb 402D6 increases drug sensitivity in several leukemia and lymphoma cell lines

The cell death-inducing effect of the anti-Sci-mAbs led us to hypothesize that treatment of the cells with the antibodies could potentiate the cytotoxic effect of chemotherapeutic drugs used for standard-of-care treatment of lymphomas and leukemia. We therefore approached this possibility by initially assessing the cytotoxic effect of doxorubicin in presence and absence of antibody Sci-mAb 402D6. In the first round of experiments, we tested Sci-mAb 402D6 at the dose previously established to yield maximum cytotoxic effects in combination with increasing doses of doxorubicin. As reported in Figure 26, co-treatment of the test cell lines with both doxorubicin and Sci-mAb 402D6 significantly increased cell mortality, with the most dramatic additive/synergistic effect seen at lower doses of the cytotoxic drug. In these experiments, the MOLM-13 leukemia cell line, failing to show positive staining for the antibody in flow cytometry, was used as a control.

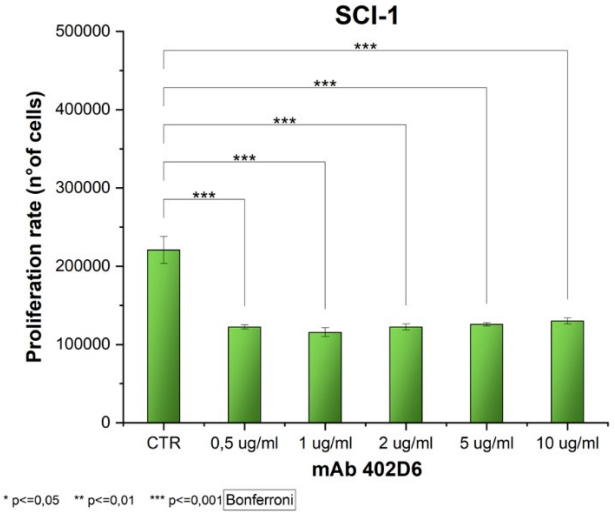
SCI-1
Proliferation rate (n°of cells)
500000
400000
300000
200000
100000
0
***
***
***
***
***
CTR
0,5 ug/ml
1 ug/ml
2 ug/ml
5 ug/ml
10 ug/ml
mAb 402D6
* p<=0,05 ** p<=0,01 *** p<=0,001 Bonferroni

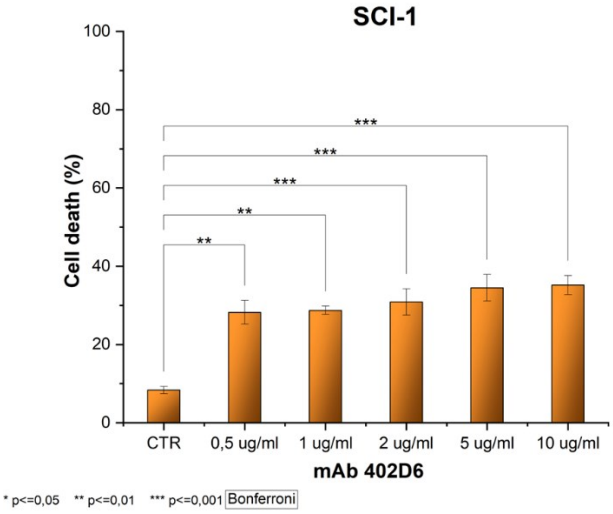
SCI-1
Cell death (%)
100
80
60
40
20
0
***
***
***
**
**
CTR
0,5 ug/ml
1 ug/ml
2 ug/ml
5 ug/ml
10 ug/ml
mAb 402D6
* p<=0,05 ** p<=0,01 *** p<=0,001 Bonferroni

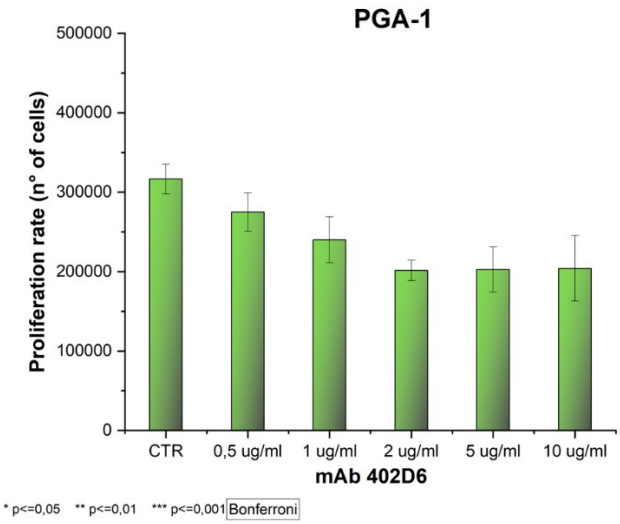
PGA-1
Proliferation rate (n° of cells)
500000
400000
300000
200000
100000
0
CTR
0,5 ug/ml
1 ug/ml
2 ug/ml
5 ug/ml
10 ug/ml
mAb 402D6
* p<=0,05 ** p<=0,01 *** p<=0,001 Bonferroni

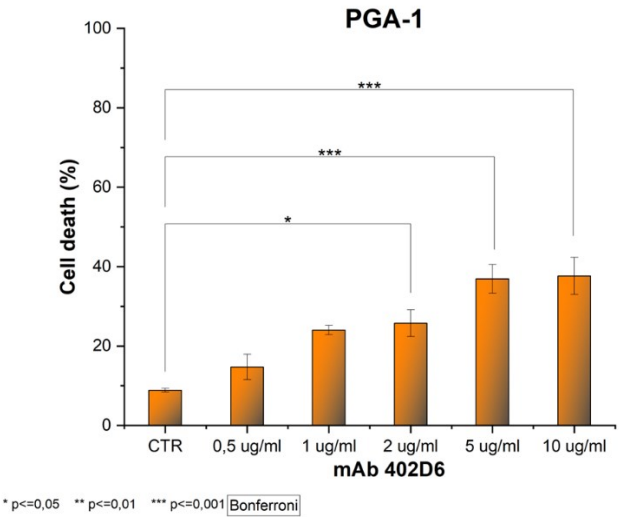
PGA-1
Cell death (%)
100
80
60
40
20
0
***
***
*
CTR
0,5 ug/ml
1 ug/ml
2 ug/ml
5 ug/ml
10 ug/ml
mAb 402D6
* p<=0,05 ** p<=0,01 *** p<=0,001 Bonferroni

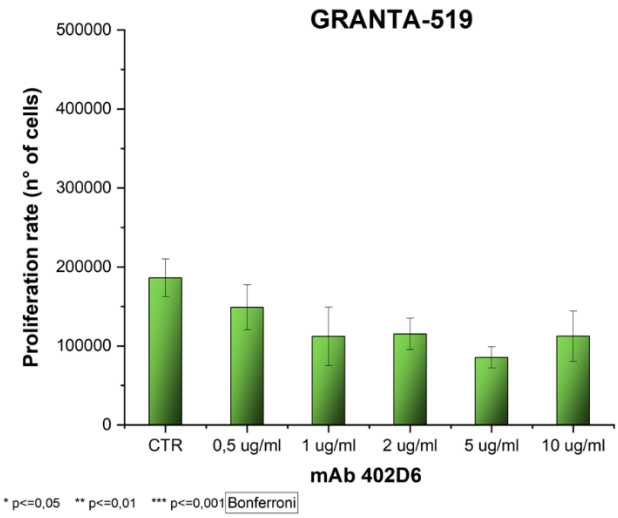
GRANTA-519
Proliferation rate (n° of cells)
500000
400000
300000
200000
100000
0
CTR
0,5 ug/ml
1 ug/ml
2 ug/ml
5 ug/ml
10 ug/ml
mAb 402D6
* p<=0,05 ** p<=0,01 *** p<=0,001 Bonferroni

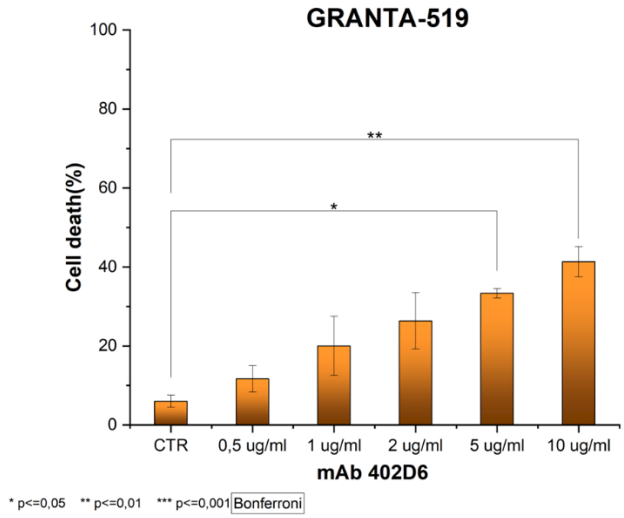
GRANTA-519
Cell death(%)
100
80
60
40
20
0
**
*
CTR
0,5 ug/ml
1 ug/ml
2 ug/ml
5 ug/ml
10 ug/ml
mAb 402D6
* p<=0,05 ** p<=0,01 *** p<=0,001 Bonferroni

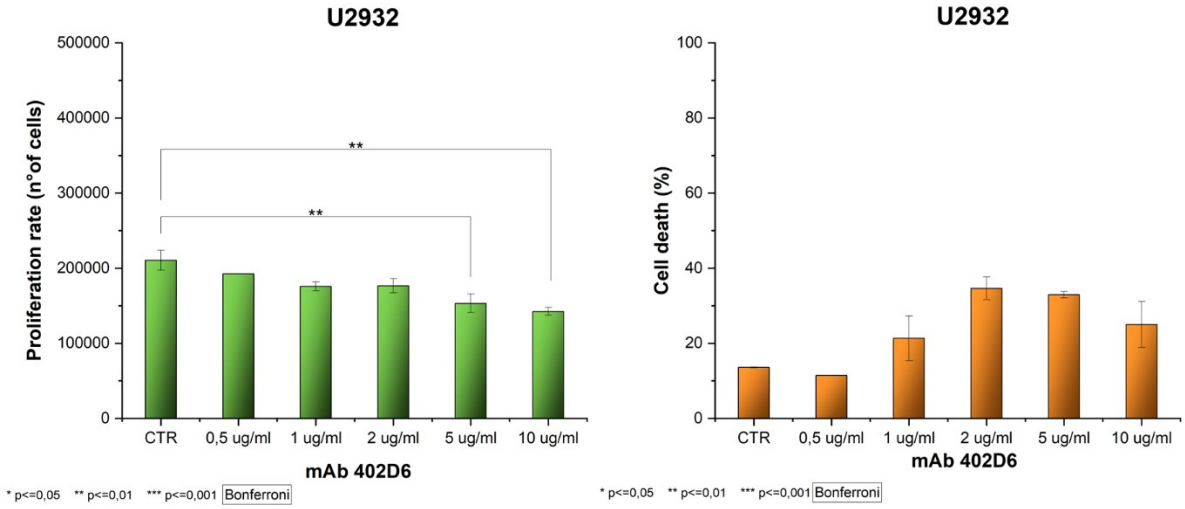

Figure. 25. *Levels of cell proliferation and mortality in the indicated cell lines treated for 24 hrs with dose-escalating amounts of anti-Sci-mAb 402D6*

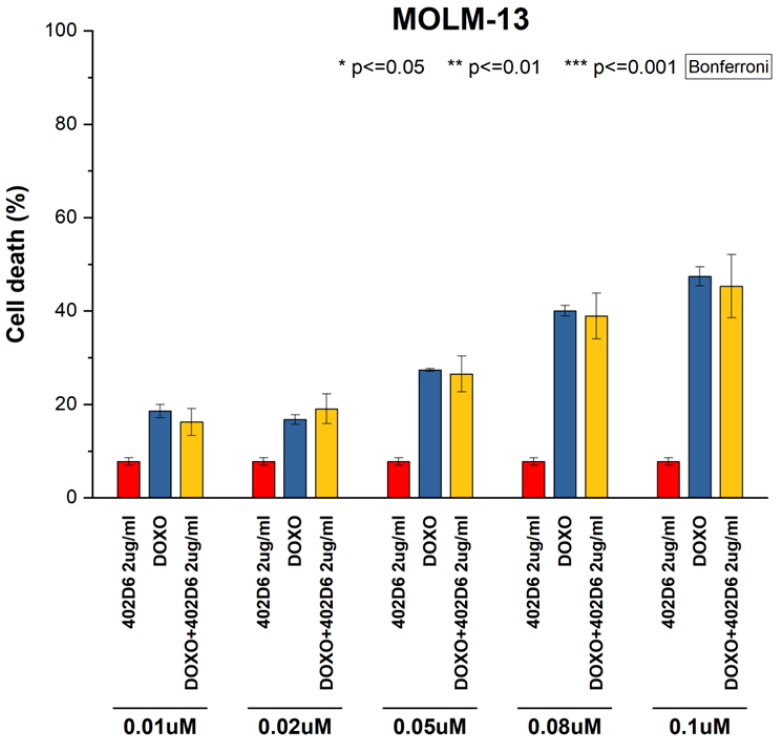

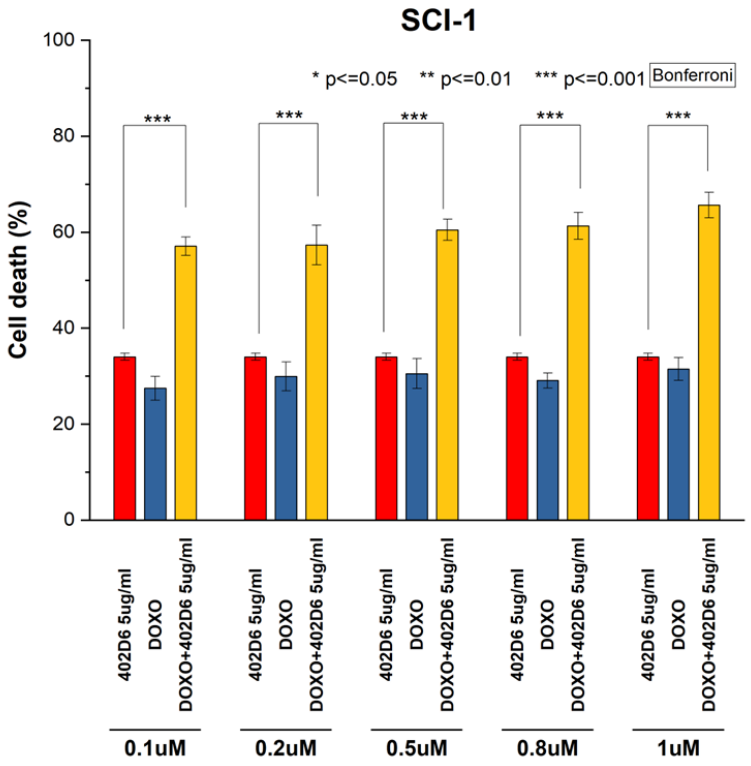
SCI-1
* p<=0.05 ** p<=0.01 *** p<=0.001 Bonferroni
Cell death (%)
100
80
60
40
20
0
***
402D6 5ug/ml
DOXO
DOXO+402D6 5ug/ml
0.1uM
0.2uM
0.5uM
0.8uM
1uM

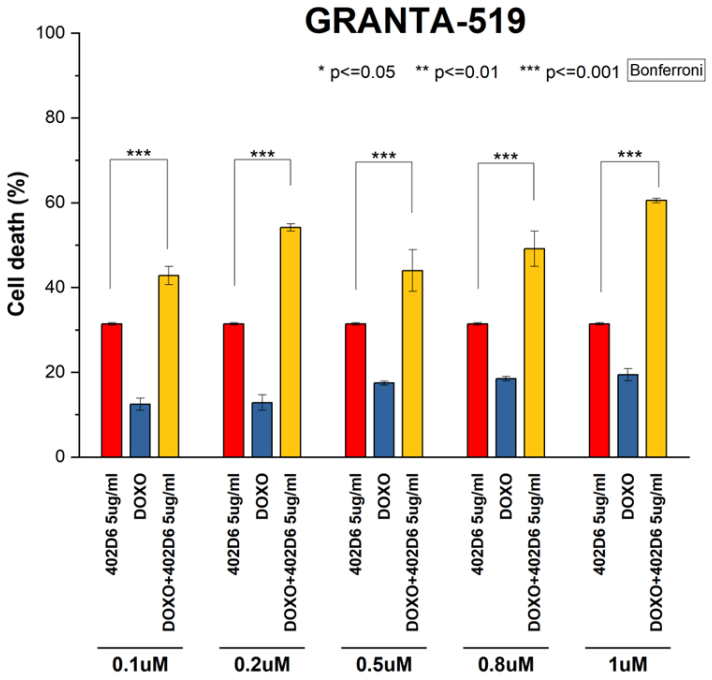
GRANTA-519
* p<=0.05 ** p<=0.01 *** p<=0.001 Bonferroni
Cell death (%)
100
80
60
40
20
0
***
402D6 5ug/ml
DOXO
DOXO+402D6 5ug/ml
0.1uM
0.2uM
0.5uM
0.8uM
1uM

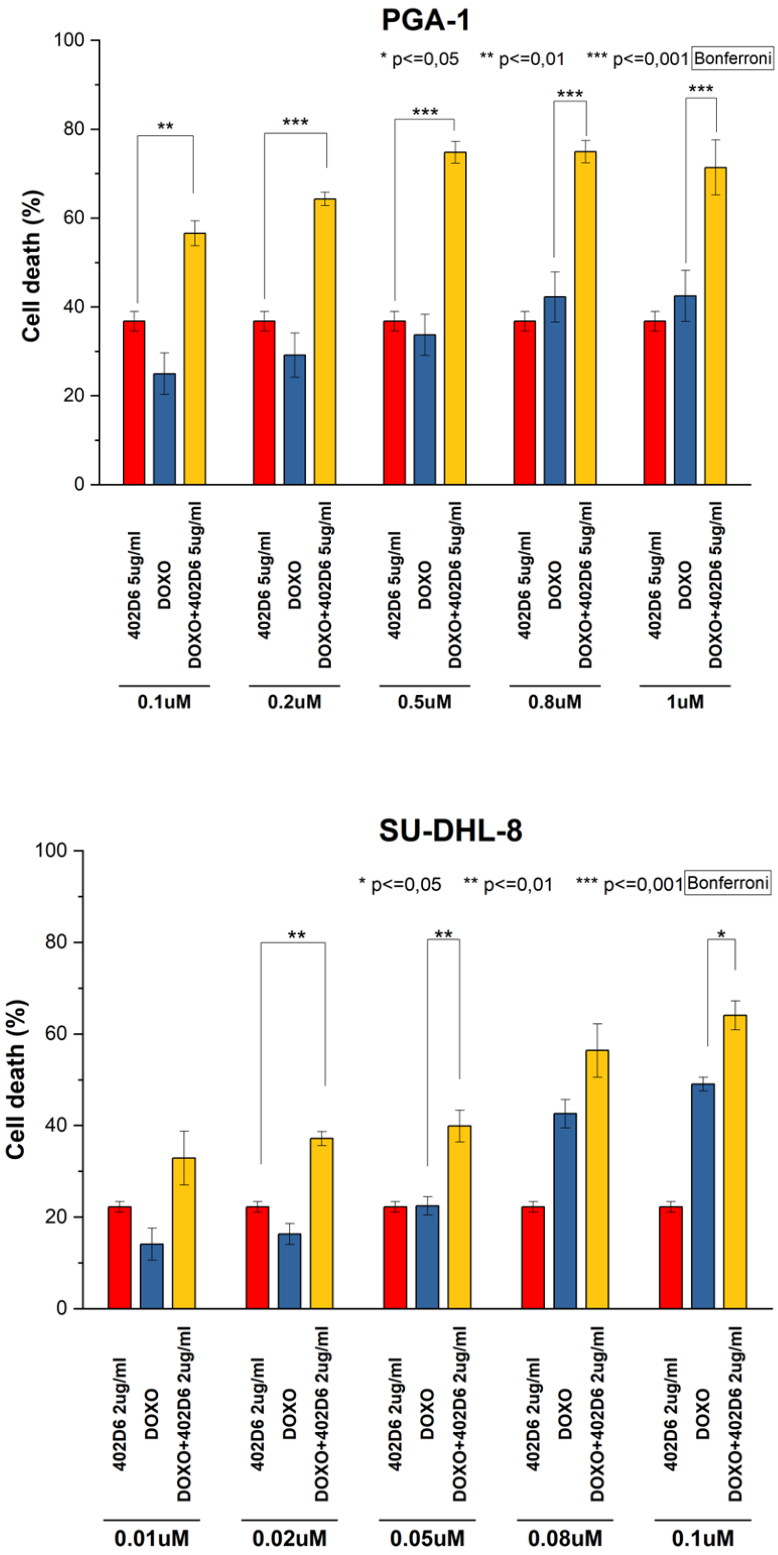

Figure. 26. *Levels of cell death in the indicated cell lines treated for 24 hrs with increasing doses of doxorubicin in the presence of a fixed dose of mAb 402D6. The effect of either agent is shown for reference.*

We also evaluated the combinatorial effect of the chemotherapeutics-antibody treatment using the drug at a fixed IC_{50} dose. In this case, the additive/synergistic effect was less evident (Figure 26).

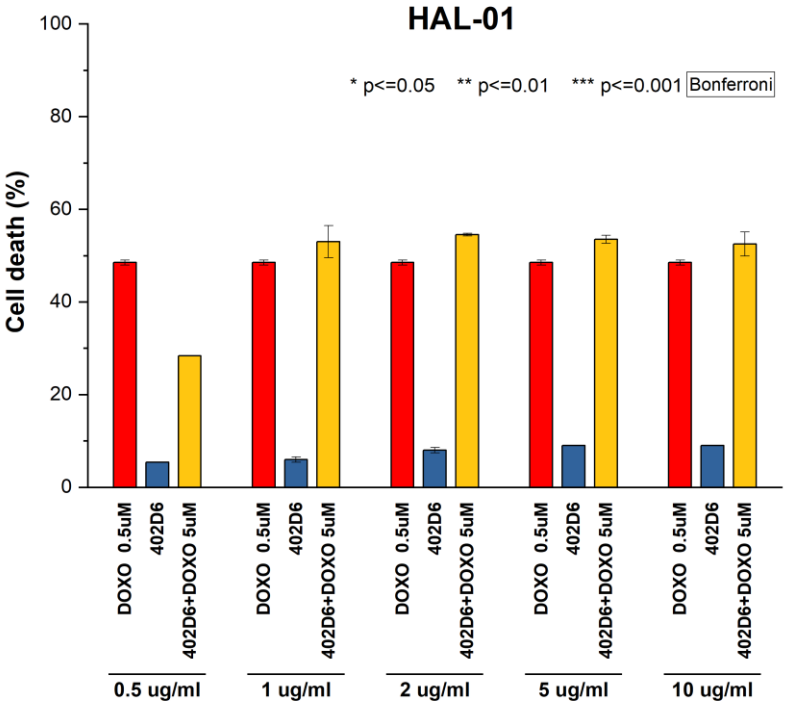

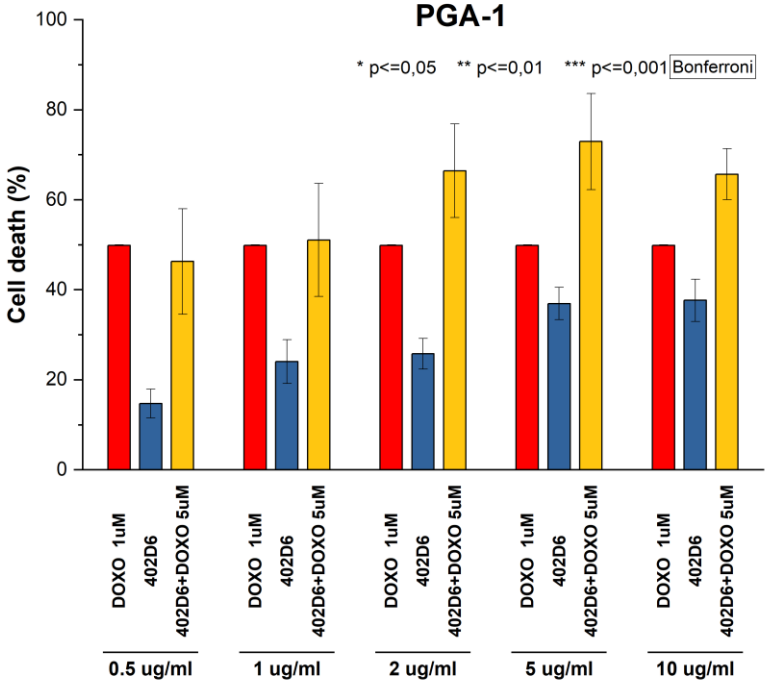

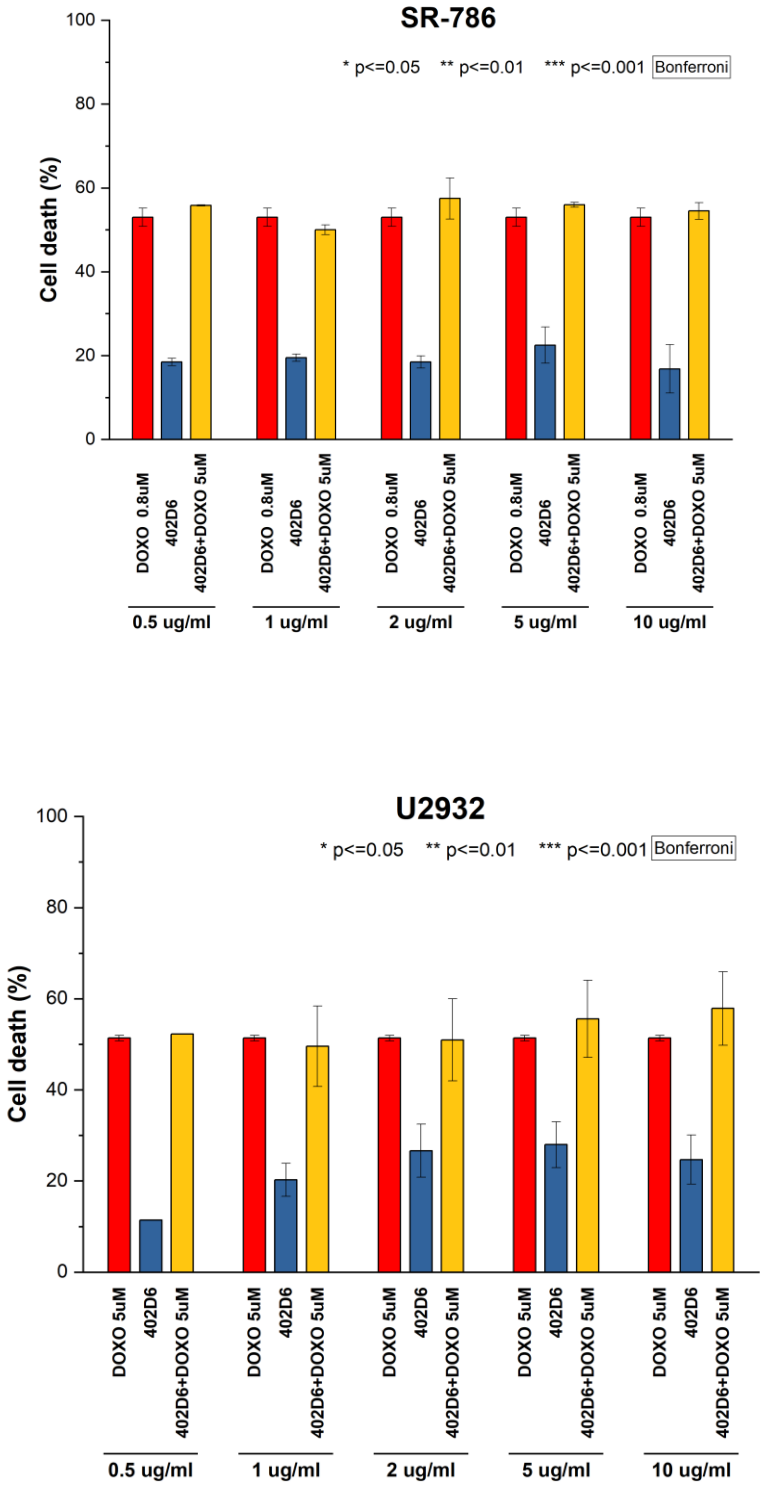

Figure. 26. *Combinatorial effects of doxorubicin treatment of the cells using an IC_{50} dose of the drug and increasing doses of antibody.*

DISCUSSION

The study has been focused on the identification of novel antibody-antigen pairs that would be highly specific and selective for hematologic malignancies and thereby provide attractive immunotherapeutic platforms to be further developed preclinically. This objective is along the line of thoughts that immunotherapeutic targeting of hematologic neoplasia is a critical step forward towards the circumvention of the limited effectiveness of the currently used chemotherapeutic agents. The work was therefore devoted to a first functional characterization of some of the generated antibodies and was further centred upon the pursuing of alternative immune-proteomic approaches in the attempt to disclose the nature of the recognized antigens.

To generate novel monoclonal antibodies directed against unique tumor targets, the attention was directed towards protein targets harbouring putative tumor-specific post-translational modifications, not expected to be detectable on healthy hematopoietic cells. Raising antibodies against glycoforms of cell surface-associated components is naturally not a trivial task and this challenge was addressed using two independent strategies. In one case, we took advantage of a panel of previously generated and partially characterized mAbs raised against different isoforms of the proteoglycan aggrecan (79). The rational for this approach was given by the fact that some studies conducted in the 90s with similar antibodies had reported cross-reactivity with unidentified cell membrane components of non-Hodgkin's lymphomas (84). In another approach we exploited specific protocols for enrichment of highly glycosylated molecules associated with the membrane of a model lymphoma cell line and used such glycoprotein mixtures to immunize mice and produce hybridomas. Enrichment of highly glycosylated cell surface molecules is a strategy widely used in the context of glyco-proteomic analyses of the "surfaceome" but, to our knowledge, has not been employed for generating specific monoclonal antibodies against membrane-bound, cancer-specific glycoproteins serving as putative immunotherapeutic targets for treatment of hematologic neoplasia. We have denominated the approach "reversed immune-glycoproteomics" and have conducted a first characterization of antibodies generated through such approach.

A starting point of this project was therefore to determine the patterns of cell surface reactivity and specificity of a panel 25 mAbs produced using cell membrane preparations of the follicular lymphoma cell line Sci-1. Since for immunotherapeutic approaches the antibody drug has to be preferentially directed against continuously exposed and/or highly accessible cell surface antigens, we approached the first screening of the mAbs by flow cytometry using a limited set of model cell lines. This led to the identification of a sub-panel of fourteen antibodies that displayed an intense surface reactivity. As protein mixtures used as immunogen should have been derived from the cell surface, it could be

envisioned that the remainder of the antibodies that failed to bind to cells may recognize membrane-associated components that are transiently exposed on the surface, or antigens that in their natural configuration could be masked or not fully accessible for the antibodies. These antibodies were not further characterized nor used for the subsequent phases of the study.

Since the aim of the approach was to select out antibodies reacting specifically with neoplastic cells, we differentially screened the antibodies against PBMCs from healthy donors and were able to disclose four antibodies which reacted apparently equally well with healthy cells. These were not further investigated in this study, although they could still bind to cell surface components that could be of potential interest for cancer therapy, as in the case of many of the antigens currently targeted by immunotherapeutics in clinical use, e.g., CD19, CD20, CD38, CD52, etc. To then establish a comprehensive map of the hematologic diseases expressing the recognized surface antigens, we made use of a panel of 100 characterized hematologic cancer cell lines (85). This extended screening led to the identification of four lead antibodies that could be prioritized for further studies based on their effective binding to several of the cell lines assayed. Intriguingly, the mAbs were found to recognize cell lines representing hematologic diseases different than the follicular lymphoma model, suggesting that the recognized antigens are shared by neoplastic cells of various pathologies. The precise subcellular localization of these antigens was examined by immunocytochemistry, which confirmed an intense and homogenous cell membrane labelling in most cells, which in some cases showed concentration in focal spots. Whether these local accumulations of the antigens along the cell membrane correspond to transient clustering of the recognized antigens in lipid rafts, or whether it represents more permanent focal concentrations of certain membrane components, remains to be established.

An intriguing finding, still to be fully corroborated, was the putative reactivity of the antibodies with CD34+ hematopoietic stem cells mobilized in the peripheral blood of a multiple myeloma patient referred to autologous bone-marrow transplantation. Coincident staining of one of the antibodies with an anti-CD34 antibody suggested that in this specific patient, more than 60% of the total CD34+ cell population co-expressed the stem cell marker and the antigens. Analyses of additional patient samples are ongoing to determine the reproducibility of this co-localization and to further understand its significance.

A first attempt to employ a canonical approach for the identification of the recognized cell surface antigens, involving immunoprecipitation and subsequent mass spectrometry analyses of the precipitated protein complexes, did not yield conclusive data. Efforts are therefore undertaken to refine the starting immunoprecipitation protocol, such as to yield more suitable samples to process

by mass spectrometric analyses. As a second attempt, we evaluated an alternative method entailing a custom-outsourced fluorescence-based screening of protein microarrays, with a representation of more 20,000 human recombinant proteins. Unexpectedly, the combination of antibodies 402D6 and 402F1 the top hits turned out to be proteins unknown to be localized at the cell surface, with the exception of nectin cell adhesion molecule-3 and the stress-induced phosphoprotein-1 (STIP-1), which was the top scoring molecule in terms signal intensity of binding. The rather challenging corollary finding is that this protein has been shown to represent an unfavourable prognostic marker for several cancers and it is known to be transiently associated with the cell membrane (86-88). Although these proteins were not the expected ones, both because of the predicted low abundance on the cell surface and the lack of significant post-translational modifications to create neoepitopes, they still could be relevant and therefore further studies are ongoing to verify their actual distribution pattern in lymphomas and leukemia. However, to note, they do not seem to be discernible within the banding patterns highlighted by the antibodies in immunoblotting. The possibility remains that this may be due to the fact that these molecules are only recognized by the antibodies in their native state, and or that they were not sufficiently represented on the blotted membranes.

When we approached the potential of a direct biological effect of the antibodies when administered to the cells in their naked form, we were surprised to find that the antibodies 400F6 and 402D6 seemed to induce cell-cell aggregation and formation of cell spheroids in time-dependent manner. Preliminary experimental evidence suggests that the phenomenon was not cation- or cell cycle-dependent, while the cellular and molecular mechanisms deserve to be further investigated. In the presence of the antibodies, time- and dose-dependent effects on cell proliferation were also observed on four model cell lines, each one representative of a different pathology, that had as a common denominator high binding rates in flow cytometry. On the asynchronized cells the four lead antibodies inhibited proliferation in a variable and differentiated manner between the test cell lines, suggesting that the recognized antigens were discretely associated with the proliferation machinery of the cells. More importantly, the blockade of cell proliferation seemed to be associated with survival impairment in the affected cells that did not appear to be associated with the canonical caspase-regulated extrinsic pathway of regulated cell death. Thus, the cytotoxic effect of the antibodies seemed to be connected with an alternative induction of regulated cell death which may involve the activation of caspase-10/14.

The ancillary implication of cell death-inducing activity of the antibodies incited the formulation of the idea that treatment of the cells with the antibodies could impact on their drug resistance. The hypothesis was addressed by combinatorial treatments of model cells with the antibodies and

standard-of-care chemiotherapeutic drugs currently used for the treatment of each single variant of lymphomas and leukemia. This line of investigation was initiated combining the anti-Sci mAb 402D6 and doxorubicin, using inversely an IC50 dose of the chemotherapeutic drug and dose-escalating administration of the antibody and an optimal dose of the antibody and increasing doses of the drug. Thus far, the most striking additive/synergistic effect was seen at a lower dose of doxorubicin, i.e., a higher mortality rate that that seen with the combination of the antibody and the drug at IC50. This observation would suggest that a combinatorial treatment with the antibody may be exploited to strongly reduce the therapeutic dose of doxorubicin and the existence of a similar relationship is now explored with other chemiotherapeutic drugs.

In conclusion, we find that two sets of antibodies, obtained through the classical hybridoma technology and made unique by the choice of immunogen and immunization protocol, embody novel potential immunotherapeutic agents to be further developed preclinically for monotherapy and combinatorial treatment strategies on lymphomas and leukemia. Meanwhile, the post-translationally modified macromolecular complexes that seem to correspond to the recognized antigens may represent novel biomarkers and/or cell surface components directly involved in the survival and growth of the neoplastic leukocytes/lymphocytes. To determine whether their mode of regulation of key tumorigenic cellular processes affords a future challenge to be pursued alongside investigations aimed at transferring these reagents to clinical settings.

BIBLIOGRAPHY

1) Newell LF, Cook RJ. Advances in acute myeloid leukemia. BMJ. (2021); 375(2026).

2) Centers for Disease Control and Prevention. Hematologic Cancer Incidence, Survival, and Prevalence. USCS Data Brief, no. 30. Atlanta, GA: Centers for Disease Control and Prevention, US Department of Health and Human Services; 2022.

3) Kantarjian HM, Kadia TM, DiNardo CD, et al. Acute myeloid leukemia: Treatment and research outlook for 2021 and the MD Anderson approach. Cancer. 2021;127(8):1186-1207.

4) Farkona S, Diamandis EP, Blasutig IM. Cancer immunotherapy: the beginning of the end of cancer?. BMC Med. 2016; 14: 73.

5) Jabbour E, Kantarijan H. Chronic myeloid leukemia: 2020 update on diagnosis, therapy and monitoring. Am J Hematol. 2020; 95: 691–709.

6) Malard F, Mothy M. Acute lymphoblastic leukemia. Lancet. 2020; 395: 1146-1162.

7) Hallek M, Al-Sawaf O. Chronic lymphocytic leukemia: 2022 update on diagnostic and therapeutic procedures. Am J Hematol. 2021; 96(12): 1679-1705.

8) Patel K, Pagel JM. Current and future treatment strategies in chronic lymphocytic leukemia. J Hematol Oncol. 2021; 14, 69.

9) Bowzyk Al-Naeeb A, Ajithkumar T, Behan S et al. Non-Hodgkin lymphoma. BMJ. 2018; 362.

10) Singh R, Shaik S, Negi BS. Non-Hodgkin's lymphoma: A review. J Family Med Prim Care. 2020; 9(4): 1834-1840.

11) Momotow J, Borchmann S, Eichenauer DA, et al. Hodgkin Lymphoma-Review on Pathogenesis, Diagnosis, Current and Future Treatment Approaches for Adult Patients. J Clin Med. 2021; 10(5): 1125.

12) Sahu M, Suryawanshi H. Immunotherapy: The future of cancer treatment. J Oral Maxillofac Pathol 2021;25:371.

13) Lu RM, Hwang YC, Liu IJ et al. Development of therapeutic antibodies for the treatment of diseases. J Biomed Sciences. 2020; 27:1.

14) The Antibody Society. Therapeutic monoclonal antibodies approved or in regulatory review. (date accessed); www.antibodysociety.org/antibody-therapeutics-product-data.

15) Jin S, Sun Y, Liang X, et al. Emerging new therapeutic antibody derivatives for cancer treatment. Sig Transduct Target Ther. 2022; 7: 39 (2022).

16) Kaplon H, Chenoweth A, Crescioli S, et al. Antibodies to watch in 2022. MABS. 2022; 14(1).

17) Kennedy PJ, Oliveira C, Granja PL, et al. Monoclonal antibodies: technologies for early discovery and engineering. Critical reviews in Biotechnologies. 2017.

18) Huse WD, Sastry L, Iverson SA, et al. Generation of a large combinatorial library of the immunoglobulin repertoire in phage lambda. Science. 1989; 246: 1275–1281.

19) Zhao A, Tohidkia MR, Siegel DL, et al. Phage antibody display libraries: a powerful antibody discovery platform for immunotherapy. Crit Rev Biotechnol. 2016; 36: 276–289.

20) Burton DR, Barbas CF III, Persson MA, et al. A large array of human monoclonal antibodies to type 1 human immunodeficiency virus from combinatorial libraries of asymptomatic seropositive individuals. Proc Natl Acad Sci USA. 1991; 88: 10134–10137.

21) Boder ET, Wittrup KD. Yeast surface display for screening combinatorial polypeptide libraries. Nat Biotechnol. 1997; 15: 553–557.

22) Chao G, Lau WL, Hackel BJ, et al. Isolating and engineering human antibodies using yeast surface display. Nat Protoc. 2006; 1:755–768.

23) Sun Y, Ban B, Bradbury A, et al. Combining yeast display and competitive FACS to select rare hapten-specific clones from recombinant antibody libraries. Anal Chem. 2016; 88: 9181–9189.

24) Boder ET, Raeeszadeh-Sarmazdeh M, Price JV. Engineering antibodies by yeast display. Arch Biochem Biophys. 2012; 526:99–106.

25) Li H, Sethuraman N, Stadheim TA, et al. Optimization of humanized IgGs in glycoengineered Pichia pastoris. Nat Biotechnol. 2006; 24:210–215.

26) Beerli RR, Bauer M, Buser RB, et al. Isolation of human monoclonal antibodies by mammalian cell display. Proc Natl Acad Sci USA. 2008; 105: 14336–14341.

27) Zhou C, Jacobsen FW, Cai L, et al. Development of a novel mammalian cell surface antibody display platform. mAbs. 2010; 2:508–518.

28) Smith ES, Mandokhot A, Evans EE, et al. Lethality-based selection of recombinant genes in mammalian cells: application to identifying tumor antigens. Nat Med. 2001; 7:967–972.

29) Ho M, Pastan I. Mammalian cell display for antibody engineering. Methods Mol Biol. 2009;525:337-52,

30) Ernest SS, Maurice Z. Antibody library display on a mammalian virus vector: combining the advantages of both phage and yeast display into one technology. Curr Drug Discov Technol. 2014; 11:48–55.

31) Stech M, Kubick S. Cell-free synthesis meets antibody production: a review. Antibodies (Basel). 2015; 4:12.

32) Hanes J, Pluckthun A. In vitro selection and evolution of functional proteins by using ribosome display. Proc Natl Acad Sci USA. 1997; 94: 4937–4942.

33) Fukuda I, Kojoh K, Tabata N, et al. In vitro evolution of single-chain antibodies using mRNA display. Nucleic Acids Res. 2006; 34: e127.

34) He M, Taussig MJ. Antibody–ribosome–mRNA (ARM) complexes as efficient selection particles for in vitro display and evolution of antibody combining sites. Nucleic Acids Res. 1997; 25: 5132–5134.

35) Stafford RL, Matsumoto ML, Yin G, et al. In vitro Fab display: a cell-free system for IgG discovery. Protein Eng Des Sel. 2014; 27: 97–109.

36) Cai Q, Hanson JA, Steiner AR, et al. A simplified and robust protocol for immunoglobulin expression in Escherichia coli cell-free protein synthesis systems. Biotechnol Prog. 2015; 31:823–831.

37) Zemella A, Thoring L, Hoffmeister C, et al. Cell-free protein synthesis: pros and cons of prokaryotic and eukaryotic systems. Chembiochem. 2015;16: 2420–2431.

38) Bannas P, Hambach J, Koch-Nolte F. Nanobodies and Nanobody-Based human heavy chain antibodies as Antitumor therapeutics. Frontiers in Immunology. 2017; 8(1603).

39) Kijanka M, Dorresteijn B, Oliveira S et al. Nanobody-based cancer therapy of solid tumors. Nanomedicine. 2015; 10(1): 161-174.

40) Sun S, Ding Z, Yang X, et al. Nanobody: A Small Antibody with Big Implications for Tumor Therapeutic Strategy. Int J Nanomed. 2021; 16: 2337-2356.

41) Wu Y, Yi M, Zhu S et al. Recent advances and challenges of bispecific antibodies in solid tumors. Exp Haematol Onc. 2021; 10: 56.

42) Wang S, Chen K, Lei Q et al. The state of the art of bispecific antibodies for treating human malignancies. EMBO Mol Med. 2021; 13(9).

43) Ma J, Mo Y, tang M et al. Bispecific antibodies: from research to clinical application. Front Immunol. 2021; 12.

44) Gashaw I, Ellinghaus P, Sommer A, et al. What makes a good drug target? Drug Discov Today. 2012;17 Suppl:S24-30.

45) Terstappen GC, Schlüpen C, Raggiaschi R et al. Target deconvolution strategies in drug discovery. Nature Reviews. 2007; 7: 891-903.

46) Lansdowne LE. Target identification and validation in drug discovery. Technology Network. 2018.

47) Croston GE. The utility of target-based discovery. Expert Opin Drug Discov. 2017;12(5):427-429.

48) Lindsay M. Target discovery. Nat Rev Drug Discov. 2003; 2: 831–838.

49) Jain, KK. RNAi and siRNA in target validation. Drug Discov Today. 2004; 9(7):307-309.

50) Keenan EK, Zachman DK, Hirschey MD. Discovering the landscape of protein modifications. Mol Cell. 2021; 81(9): 1868-1878.

51) Dunphy K, Dowling P, Bazou D, O'Gorman P. Current Methods of Post-Translational Modification Analysis and Their Applications in Blood Cancers. Cancers (Basel). 2021; 13(8): 1930.

52) Li W, Li F, Zhang X, Lin HK, Xu C. Insights into the post-translational modification and its emerging role in shaping the tumor microenvironment. Signal Transduct Target Ther. 2021; 6(1): 422.

53) Iozzo RV, Schaefer L. Proteoglycan form and function: A comprehensive nomenclature of proteoglycans. Matrix Biol. (2015); 42:11-55.

54) Drzeniek Z, Stöcker G, Siebertz B, et al. Heparan sulfate proteoglycan expression is induced during early erythroid differentiation of multipotent hematopoietic stem cells. Blood. 1999; 93(9): 2884-2897.

55) Fadnes B, Husebekk A, Svineng G, et al. The proteoglycan repertoire of lymphoid cells. Glycoconj J. 2012; 29(7): 513-523.

56) Tsidulko AY, Matskova L, Astakhova LA, et al. Proteoglycan expression correlates with the phenotype of malignant and non-malignant EBV-positive B-cell lines. Oncotarget. 2015; 6(41): 43529-43539.

57) Wegrowski Y, Milard AL, Bernard J et al. Cell surface proteoglycan expression during maturation of human monocytes-derived dendritic cells and macrophages. Clin Exp Immunol. 2006; 144(3): 485-493.

58) Melo CM, Nader HB, Justo GZ, et al. Heparanase modulation by Wingless/INT. Mol Biol Rep. 2021; 48:3117–3125.

59) Rothemberg ME, Pomerantz JL, Owen WF, et al. Characterization of human eosinophil proteoglycans, and augmentation of its biosynthesis and size by interleukin 3, interleukin 5 and granulocyte/macrophage colony stimulating factor. J. Biol. Chem. 1988; 263(27): 13901-13908.

60) Schick BP. Regulation of expression of megakaryocyte and platelet proteoglycans. Stem cells. 1996; 14 (1):220-231.

61) Schick BP, Senkowski-Richardson S. Proteoglycan synthesis in human erythroleukaemia (HEL) cells. Biochem. J. 1992; 282: 651-658.

62) Bendall LJ, Nilsson SK, Khan NI et al. Role of CD44 variant exon 6 in acute lymphoblastic leukaemia: association with altered bone marrow localisation and increased tumour burden. Leukemia. 2004; 18(7): 1308-1311.

63) Jin L, Hope KJ, Zhai Q, et al. Targeting of CD44 eradicates human acute myeloid leukemic stem cells. Nat Med. 2006: 12(10): 1167-1174.

64) Attarbaschi A, Mann G, Schumich A, et al. CD44 deficiency is a consistent finding in childhood Burkitt's lymphoma and leukemia. Leukemia. 2007; 21: 1110-1113.

65) Kamazani FM, Bahoush GR, Aghaeipour M et al. CD44 and CD27 expression pattern in B cell precursor acute lymphoblastic leukemia and its clinical significance. Med Oncol. 2013; 1: 359.

66) Casucci M, Nicolis di Robilant B, Falcone L et al. CD44v6-targeted T cells mediate potent antitumor effects against acute myeloid leukemia and multiple myeloma. Blood 2013; 122 (20): 3461–3472.

67) Singh V, Erb U, Zöller M. Cooperativity of CD44 and CD49d in leukemia cell homing, migration, and survival offers a means for therapeutic attack. J Immunol. 2013;191(10): 5304-5316.

68) García-Peydró M, Fuentes P, Mosquera M, et al. The NOTCH1/CD44 axis drives pathogenesis in a T cell acute lymphoblastic leukemia model. J Clin Invest. 2018; 128(7): 2802-2818.

69) Orentas RJ, Yang JJ, Wen X, et al. Identification of cell surface proteins as potential immunotherapy targets in 12 pediatric cancers. Front Oncol. 2012; 2 (194).

70) Seftalioglu A, Kerakus S. Syndecan-1/CD138 expression in normal myeloid, acute lymphoblastic and myeloblastic leukemia cells. Acta Histochem. 2003; 105(3): 213-221.

71) Sun L, Sun C, Sun J, et al. Downregulation of endocan in myeloid leukemia cells inhibits proliferation and promotes apoptosis by suppressing nuclear factor-kB activity. Molec. Med. Rep. 2019; 19:3247-3254.

72) Behm FG, Smith FO, Raimondi SC, et al. Human homologue of the rat chondroitin sulfate proteoglycan, NG2, detected by monoclonal antibody 7.1, identifies childhood acute lymphoblastic leukemias with t(4;11)(q21;q23) or t(11;19)(q23;p13) and MLL gene rearrangements. Blood. 1996; 87(3): 1134-1139.

73) Gleissner B, Goekbuget N, Rieder H, et al. CD10- pre-B acute lymphoblastic leukemia (ALL) is a distinct high-risk subgroup of adult ALL associated with high frequency of MLL aberrations: result of the German Multicenter Trials for Adult ALL (GMALL). Blood. 2005; 106: 4054-4056.

74) Bueno C, Montes R, Catalina P, et al. Insights into the cellular origini and etiology of the infant pro-B acute lymphoblastic leukemia with MLL-AF4 rearrangement. Leukemia. 2011; 25: 400-410.

75) Prieto C, Lopez-Millán B, Roca-Ho H, et al. NG2 antigen is involved in leukemia invasiveness and central nervous ststem infiltration in MLL-rearranged infant B-ALL. Leukemia. 2018; 32: 633-644.

76) Driessen EMC, Mimoso Pinhanços SS, de Lorenzo P, et al. Versican expression is an adverse prognostic factor in MLL-rearranged infant acute lymphoblastic leukemia. E J Cancer. 2016; 57: 87-90.

77) Zhou X, Liang S, Zhan Q, et al. HSPG2 overexpression independently predicts poor survival in patients with acute myeloid leukemia. Cell Death Dis. 2020;11(6):492.

78) Jelinek DF, Tschumper RC, Stolovitzky GA, et al. Identification of a global gene expression signature of B chronic lymphocytic leukemia. Mol. Canc. Res. 2003; 1: 346-361.

79) Virgintino D, Perissinotto D, Girolamo F, et al. Differential distribution of aggrecan isoforms in perineuronal nets of the human cerebral cortex. J Cell Mol Med. 2009; 13: 3151-3173.

80) Kirkemo LL, Elledge SK, Yang J, Byrnes JR, Glasgow JE, Blelloch R, Wells JA. Cell-surface tethered promiscuous biotinylators enable comparative small-scale surface proteomic analysis of human extracellular vesicles and cells. Elife. 2022; 11:e73982.

81) Grün CH, van Vliet SJ, Schiphorst WE, Bank CM, Meyer S, van Die I, van Kooyk Y. One-step biotinylation procedure for carbohydrates to study carbohydrate-protein interactions. Anal Biochem. 2006; 354(1): 54-63.

82) Cheah JS, Yamada S. A simple elution strategy for biotinylated proteins bound to streptavidin conjugated beads using excess biotin and heat. Biochem Biophys Res Commun. 2017; 493(4): 1522-1527.

83) Ligasová A, and Koberna K. DNA Dyes—Highly Sensitive Reporters of Cell Quantification: Comparison with Other Cell Quantification Methods. Molecules. 2021; 26: 5515.

84) Quentmeier, H., Pommerenke, C., Dirks, W.G. et al. The LL-100 panel: 100 cell lines for blood cancer studies. Sci Rep. 2019; 9: 8218.

85) Hollander N, and Haimovic J. Altered N-Linked glycosylation in follicular lymphoma and chronic lymphocytic leukemia: involvement in pathogenesis and potential therapeutic targeting. Front. Immunol. 2017; 912.

86) Chao A, Lai CH, Tsai CL, Hsueh S, Hsueh C, Lin CY, Chou HH, Lin YJ, Chen HW, Chang TC, Wang TH. Tumor stress-induced phosphoprotein1 (STIP1) as a prognostic biomarker in ovarian cancer. PLoS One. 2013;8(2):e57084.

87) Erlich RB, Kahn SA, Lima FR, Muras AG, Martins RA, et al. (2007) STI1 promotes glioma proliferation through MAPK and PI3K pathways. Glia 55: 1690–1698.

88) Lin CY, Chen SH, Tsai CL, Tang YH, Wu KY, Chao A. Intracellular targeting of STIP1 inhibits human cancer cell line growth. Transl Cancer Res. 2021 Mar;10(3):1313-1323.